

RECEIVED
DOE/PETC

97 FEB 14 AM 10:04

DOE/PC/92543--716

ADJUSTANCE DIV.

**MICRO-AGGLOMERATE FLOTATION FOR
DEEP CLEANING OF COAL***

Final Report for
DOE Grant No. DE-FG22-92PC92543

Submitted to

The U.S. Department of Energy
Pittsburgh Energy Technology Center
P. O. Box 10904
Pittsburgh, PA 15236

by

S. Chander and R. Hogg

The Pennsylvania State University
115 Hosler Building
University Park, PA 16802

January 15, 1997

*US/DOE Patent Clearance is not required prior to the publication of this document."

DISTRIBUTION OF THIS DOCUMENT IS UNLIMITED

MASTER

**CLEARED BY
PATENT COUNSEL**

DISCLAIMER

This report was prepared as an account of work sponsored by an agency of the United States Government. Neither the United States Government nor any agency thereof, nor any of their employees, make any warranty, express or implied, or assumes any legal liability or responsibility for the accuracy, completeness, or usefulness of any information, apparatus, product, or process disclosed, or represents that its use would not infringe privately owned rights. Reference herein to any specific commercial product, process, or service by trade name, trademark, manufacturer, or otherwise does not necessarily constitute or imply its endorsement, recommendation, or favoring by the United States Government or any agency thereof. The views and opinions of authors expressed herein do not necessarily state or reflect those of the United States Government or any agency thereof.

DISCLAIMER

Portions of this document may be illegible in electronic image products. Images are produced from the best available original document.

TABLE OF CONTENTS

	Page
COVER SHEET	i
TABLE OF CONTENTS	ii
LIST OF FIGURES	iv
LIST OF TABLES	ix
ACKNOWLEDGEMENTS	x
EXECUTIVE SUMMARY	xi
CHAPTER 1. INTRODUCTION	1
1.1 The Problems of Deep Cleaning Fine Coal	2
1.2 Selective Agglomeration	2
1.3 Flotation of Ultrafine Coal	3
1.4 Wetting Phenomena	3
1.5 Emulsion Phenomena	6
1.6 Agglomerate Formation and Growth	8
1.7 Agglomerate Flotation	8
CHAPTER 2. ADSORPTION OF PEO/PPO TRIBLOCK CO-POLYMERS AT AIR/WATER INTERFACE	10
2.1 Introduction	10
2.2 Surface Tension as a Function of Time	13
2.3 Effect of Surfactant Concentration	15
2.4 Effect of Molecular Weight	16
2.5 Effect of Ethylene Oxide Groups	27
2.6 Conclusions	27
CHAPTER 3. KINETICS OF EMULSIFICATION IN THE ABSENCE AND PRESENCE OF PEO/PPO TRI-BLOCK CO-POLYMERS	30
3.1 Introduction	30
3.2 Experimental Set-up	33
3.3 A Phenological Dispersion Model	36
3.4 Effect of Dodecane Concentration	47
3.5 Effect of Block Co-polymer Concentration and Type	47
3.5.1 Water soluble PEO/PPO/PEO	47
3.5.2 Oil soluble PPO/PEO/PPO	53
3.5.3 Effect of Time of Reagent Addition	55
3.6 Conclusions	55

	Page
CHAPTER 4. WETTING CHARACTERISTICS OF PEO/PPO/PEO BLOCK CO-POLYMERS IN COAL/AIR/WATER AND COAL/ DODECANE/WATER SYSTEMS	58
4.1 Introduction	58
4.2 Contact Angle Studies in the Presence of Block Co-polymers	58
4.2.1 Coal/Air/Water/System	58
4.2.2 Coal/Dodecane/Water System	71
4.3 Adsorption of Block Co-polymers on Solid/Liquid Interface	71
4.3.1 Pure Hydrophobic and Hydrophilic Surfaces	71
4.3.2 A Hypothesis for Block Co-polymers Adsorption on Coal ..	73
4.4 Conclusions	79
CHAPTER 5. AGGLOMERATE GROWTH AND STRUCTURE	81
5.1 Introduction	81
5.2 Collision Processes	81
5.3 Disruption/Breakage Processes	83
5.4 Agglomerate Formation and Growth	84
5.5 Experimental	87
5.5.1 Materials	87
5.5.2 Procedure	90
5.5.3 Results	90
5.6 Conclusions	103
CHAPTER 6. AGGLOMERATE FLOTATION	105
6.1 Introduction	105
6.2 Background Discussion	106
6.3 Agglomerate Flotation Studies	109
6.3.1 Flotation of P40 Coal Sample	109
6.3.2 Flotation of P20 Coal	117
6.4 Conclusions	123
REFERENCES	125

LIST OF FIGURES

	Page
Figure 2.1. The effect of conditioning time elapsed between the placement of the solution in the measurement cell and the measurement of surface tension of Pluronic L-64	12
Figure 2.2. The γ/γ_{∞} versus time plot for various concentrations of Pluronic L-64	14
Figure 2.3. The variation in the surface tension of Pluronic L-64 as a function of concentration for the gently stirred and non-stirred solutions ...	18
Figure 2.4. A comparison of two sets of surface tension data of P-104 in the presence of gentle stirring from this study and literature (Alexandridis et al., 1994), respectively	19
Figure 2.5. The surface tension versus concentration curves for L-44, L-64 and P-104 which demonstrate effect of the molecular weight	20
Figure 2.6. A schematic diagram of the surface tension behavior PEO/PPO triblock co-polymers as a function of block co-polymer concentration	21
Figure 2.7. The effect of conditioning time on the surface tension of Pluronic L-44, L-64 and P-104 surfactants	23
Figure 2.8. The CMC values reported in literature by light scattering and surface tension methods as a function of temperature	26
Figure 2.9. The surface tension versus concentration curves for L-62, L-64 and P-65 which demonstrate the effect of the fraction of EO groups	28
Figure 3.1. Experimental set-up used in the study	34
Figure 3.2. A schematic representation of the agitation vessel and the turbine type stirrer used in this study	35
Figure 3.3. The size distribution of oil droplets measured in-situ in the flow through vessel and after encapsulation using piperazine and terephthaloyl chloride	37

	Page
Figure 3.4. a) Size distribution of dodecane droplets in water at various times; b) Normal size distribution of dodecane droplets in water	38
Figure 3.5. Change in the median droplet size, X_{50} , as a function of time of agitation for 0.1% dodecane	39
Figure 3.6. A plot of the fraction of droplets that are smaller than λ_0 (Kolmogorov's microscale of turbulence) as a function of agitation time. Dodecane concentration 0.1% by volume	43
Figure 3.7. The median droplet sizes as a function of agitation time; symbols: experimentally determined; solid line: predicted by Equation 8	45
Figure 3.8. The mean droplet sizes as a function of agitation time (data obtained by Narsimhan et al., 1980)	46
Figure 3.9. Change in the median droplet size as a function of time at dodecane concentrations of 0.1% and 1.1% by volume	48
Figure 3.10. Effect of the concentration of Pluronic L-64 on the kinetics for emulsification of dodecane. Amount of dodecane: 0.1% by volume	49
Figure 3.11. Effect of the concentration of Pluronic P-104 on the kinetics for emulsification of dodecane. Amount of dodecane: 0.1% by volume	51
Figure 3.12. A schematic figure to explain the effect of surfactant on the kinetics of emulsification of dodecane	52
Figure 3.13. Effect of the concentration of Pluronic P-25R1 on the kinetics emulsification of 0.1% dodecane	54
Figure 3.14. Effect of the time of surfactant addition on emulsification of 0.1% by volume dodecane	56
Figure 4.1. Contact angle of Pittsburgh Seam sample in distilled water. Test #1, Test #2, Test #3 and Test #4 are replicate measurements	60

	Page
Figure 4.2. Change in the contact angle distribution of Pittsburgh Seam sample (PIT) as a function of L-64 concentration	61
Figure 4.3. Effect of ethylene oxide fraction of PEO/PPO/PEO triblock co-polymer on the mean contact angle of Pittsburgh Seam sample as a function of Pluronic-60 series	63
Figure 4.4. Effect of ethylene oxide fraction of PEO/PPO/PEO triblock co-polymer on the mean contact angle of Pittsburgh Seam sample as a function of Pluronic-100 series	64
Figure 4.5. Effect of molecular weight of PEO/PPO/PEO triblock co-polymers on the mean contact angle of Pittsburgh Seam sample	65
Figure 4.6. Effect of HLB value of the PEO/PPO/PEO triblock co-polymers on contact angle of Pittsburgh Seam sample for two series of Pluronic surfactants; • : 60-series; o: 100-series	66
Figure 4.7. Change in the contact angle distribution of Pittsburgh (PIT) and Upper Freeport (UF) coal samples as a function of L-64 concentration	68
Figure 4.8. Change in the contact angle distribution of Lower Kittanning (LK) and Illinois No. 6 (IL6) coal samples as a function of L-64 concentration	69
Figure 4.9. A comparison between the mean contact angles of Pittsburgh Seam sample as a function of L-64 and Triton X-100 concentration	70
Figure 4.10. Contact angle distribution of Pittsburgh Seam sample in the absence and presence of L-64 (10^{-6} M) in both the coal/air/water and the coal-dodecane/water systems	72
Figure 4.11. A schematic illustration of PEO/PPO/PEO type block co-polymer adsorption on hydrophobic and hydrophilic sites of coal surface	74
Figure 4.12. The proposed surface types present on the surface of Pittsburgh Seam sample	77

	Page
Figure 5.1. Agglomerate growth in simple flocculation systems showing the effect of enhanced adhesion efficiency (as determined by the rate of flocculant addition R) on settling rate (a measure of floc size. (After Maffei, 1989)	86
Figure 5.2. Size distribution of P40 coal sample showing comparison of results obtained using wetting and dispersing agents with those using the standard reagent-free procedure	88
Figure 5.3. Particle size distribution for P20 coal	89
Figure 5.4. Typical agglomerate size distributions observed following oil addition to P20 coal	91
Figure 5.5. Typical agglomerate growth curve	93
Figure 5.6. Development of the agglomerate size distribution for 5% oil (dodecane) addition to P40 coal at 1500 rpm	96
Figure 5.7. Effect of agitation speed and oil addition level on agglomerate formation and growth (P40 coal)	98
Figure 5.8. Effect of surfactant concentration (Pluronic L-64) on agglomerate formation and growth for P40 coal with pre-emulsified oil. (Surfactant added prior to pre-emulsified oil)	100
Figure 5.9. Effect of agitation speed on agglomerate development for P20 coal	101
Figure 5.10. Effect of surfactant addition on agglomeration of P20 coal at 3600 rpm	102
Figure 6.1. Recovery vs. cumulative ash for flotation for P40 coal preagglomerated at various times. Agitator speed during agglomeration was 2500 rpm	110
Figure 6.2. Recovery vs. cumulative ash for flotation for P40 coal preagglomerated at various times. Agitator speed during agglomeration was 3500 rpm	111

	Page
Figure 6.3. Effects of agglomeration time and agitation speed on cumulative ash percent A_{80} recovery by flotation in the absence of frother. (P40 coal)	112
Figure 6.4. Effects of agglomeration time and agitation speed on cumulative ash percent A_{80} at 80% recovery by flotation with 50 μm MIBD as frother (P40 coal)	113
Figure 6.5. Effect of surfactant addition (Pluronic L-64) on ash rejection in coal flotation following preagglomeration for different times and agitation speeds. (P40 coal)	115
Figure 6.6. Effect of surfactant addition (10^{-6} M Pluronic 64) on the selectivity of flotation after preagglomeration at different speeds	116
Figure 6.7. Recovery-residual ash content curves for flotation of P20 coal after agglomeration with wt % dodecane at 3600 rpm	119
Figure 6.8. Recovery-residual ash content curves for flotation of P20 coal after agglomeration with wt % dodecane at 7200 rpm	120
Figure 6.9. Recovery-residual ash content curves for flotation of P20 coal after agglomeration at 3600 rpm with wt % dodecane pre-emulsified in the presence of L-64 surfactant	121
Figure 6.10. Recovery-residual ash content curves for flotation of P20 coal after agglomeration at 3600 rpm with wt % dodecane. L-64 added to the coal slurry, prior to the addition of (mechanically) pre-emulsified oil	122

LIST OF TABLES

	Page
Table 2.1. Critical micelle concentration of Pluronic L-64 surfactant reported in the literature	11
Table 3.1. The calculated surface area of droplets in the system and the number of molecules at monolayer coverage (Γ_m) as a function of time (assuming a parking area of 1.04 nm^2)	53
Table 4.1. HLB values for selected functional groups (after Davis and Lin, 1972)	75
Table 4.2. The estimated fractions of hydrophobicity of coal	76
Table 6.1. Effect of agglomeration conditions on flotation selectivity expressed as product ash content at 85% coal recovery	117

ACKNOWLEDGEMENTS

The contributions of the students, staff and faculty of the Mineral Processing Section, Department of Mineral Engineering at The Pennsylvania State University are gratefully acknowledged. Special thanks are due to H. Polat, M. Polat, M. Lutsky, D. Wei, D. Mahajan, U. Pendyala, J. Sarkar, H. Sis, J. Kovalchick, D. DeCapria, D. Baney, K. Gummo, S. Rockey and Prof. M. T. Ityokumbul. The work was supported primarily through the U. S. Department of Energy under Grant No. DE-F22-92PC92543.

EXECUTIVE SUMMARY

Coal is the most abundant domestic energy source in the U.S. Its long-term viability, however, will require appropriate measures to minimize detrimental environmental impact. Deep cleaning of the raw coal together with modernized combustion technologies and post-combustion treatment of effluents represent the most practical approach to the problem. The development of practical technologies for the deep cleaning of coal has been seriously hampered, especially by the problems of carrying out efficient coal/mineral separations at the very fine sizes (often finer than 10 μm) needed to achieve adequate liberation of the mineral matter from the coal matrix. It is generally recognized that surface-based separation processes such as froth flotation or selective agglomeration offer considerable potential for such applications. Both of these processes, however, suffer from an inability to achieve high selectivity together with an acceptable yield of combustibles.

In froth flotation, selectivity is substantially reduced at fine sizes due, primarily, to overloading of the froth phase which leads to excessive carryover of water and entrained mineral matter. Oil agglomeration, on the other hand, can provide good selectivity at low levels of oil addition but the agglomerates tend to be too fragile for separation by the screening methods normally used. The addition of larger amounts of oil can yield large, strong agglomerates which are easily separated but the selectivity is reduced and reagent costs can become excessive.

In this investigation a hybrid process - Micro-agglomerate flotation - which is a combination of oil-agglomeration and froth flotation was studied. The basic concept is to use small quantities of oil to promote the formation of dense micro-agglomerates with minimal entrapment of water and mineral particles and to use froth flotation to separate these micro-agglomerates from the water/dispersed-mineral phase.

Micro-agglomerate is a complex process which involves at least five phases: two or more solids (coal and mineral), two liquids (oil and water) and one gas (air). It is demonstrated in this study that the process is very sensitive to fluctuations in operating parameters. It is necessary to maintain precise control over the chemistry of the liquid

phases as well as the agitation conditions in order to promote selectivity. Both kinetics as well as thermodynamic factors play a critical role in determining overall system response. To establish design and operation criteria for application of the process, systematic investigations were conducted in the following general areas:

- Adsorption
- Emulsification
- Wetting
- Agglomerate Growth and Structure
- Agglomerate Flotation

Adsorption studies were conducted to evaluate the role of ethylene and propylene oxide block co-polymers, used in this study to enhance selectivity of separation. The adsorption behavior was complex and depended on reagent concentration, hydrophilic-lipophilic balance (HLB), molecular weight, and configuration of the hydrophobic and hydrophilic components in the molecule. The effects of these variables are discussed.

Since reagents are known to act as both emulsifiers and wetting control reagents and the two processes might act in synergistic or antagonistic modes, both emulsification and wetting studies were performed to delineate the mechanisms by which these reagents affect coal cleaning by micro-agglomerate flotation. The kinetics of emulsification was determined in the presence of selected reagents and the results show that the block co-polymers affected both the dispersion and coalescence sub-processes. The size distribution of the emulsion droplets could be normalized, on the basis of which the emulsification kinetics could be described by an average droplet diameter. A phenomenological model was developed to describe the kinetics of emulsification in the dispersion stage. In subsequent studies on agglomerate growth it was discovered that the oil droplets are almost instantaneously covered with hydrophobic coal particles, affecting coalescence to a large extent. The reagents that were tested increased the dispersion rate in most cases although the effect was reagent specific.

The block co-polymers also affected the wetting of coals in a complex manner. The effect was a function of reagent concentration, molecular weight and configuration of hydrophobic and hydrophilic blocks in the molecule. All these effects make the reagent type and concentration a very sensitive parameter in the choice of the reagent. Because of the competition between the emulsification and wetting sub-processes, the order of reagent addition and conditioning stages were also important.

The agglomerate growth process is characterized by an initial period of rapid growth to a maximum size followed by a slow decrease. We believe the growth pattern is determined by the balance between simultaneous agglomerate growth and breakage processes whose relative rates vary as oil is redistributed among the agglomerates. Changes in the effects of process variables for different coal particle sizes are attributed to differences in the oil redistribution mechanisms. Surfactant additions influence agglomerate growth through their effects on oil emulsification and coal hydrophobicity. Increasing hydrophobicity generally favors agglomerate growth while changes in oil droplet size through emulsification control affects oil distribution in the agglomerates.

Agglomeration is the critical stage of the separation process investigated in this project. The efficiency of separation, that is the ability to clean coal depends on preferential agglomeration of coal during the growth period. Although some degree of emulsification is essential to promote selective formation of agglomerates, too much emulsification, that is formation of very small droplets, could be detrimental. Although the issue of phase inversion was not specifically investigated in this study, sufficient evidence exists to suggest that the phase inversion from oil/water to water/oil emulsion, which is favored by the presence of hydrophobic coal particles at the interface, promotes rejection of mineral matter and enhances the overall flotation separation. If conditions exist that favor the formation of large and strong agglomerates, the entrapped mineral matter cannot be rejected by continued agitation. Such a condition is analogous to flotation of partially liberated particles and the selectivity is generally poor.

Chapter 1

INTRODUCTION

The development of practical technologies for the deep cleaning of coal has been seriously hampered by the problems of carrying out efficient coal/mineral separations at the very fine sizes (often finer than 10 μm) needed to achieve adequate liberation of the mineral matter from the coal matrix. It is generally recognized that surface-based separation processes such as froth flotation or selective agglomeration offer considerable potential for such applications but many problems in obtaining the required selectivity with acceptable recovery of combustible remain. In froth flotation, selectivity is substantially reduced at fine sizes due, primarily, to overloading of the froth phase which leads to excessive carryover of water and entrained mineral matter. Oil agglomeration, on the other hand, can provide good selectivity at low levels of oil addition but the agglomerates tend to be too fragile for separation by the screening methods normally used. The addition of larger amounts of oil can yield large, strong agglomerates which are easily separated but the selectivity is reduced and reagent costs can become excessive.

In this investigation a hybrid process - Micro-agglomerate flotation - which is a combination of oil-agglomeration and froth flotation was studied. The basic concept is to use small quantities of oil to promote the formation of dense micro-agglomerates with minimal entrapment of water and mineral particles and to use froth flotation to separate these micro-agglomerates from the water/dispersed-mineral phase. Since the floating units will be relatively large agglomerates (30-50 μm in size) rather than fine coal particles (1-10 μm) the problems of froth overload and water/mineral carryover should be significantly alleviated.

Micro-agglomerate flotation has considerable potential for the practical deep cleaning of coal on a commercial scale. We believe it should be possible to achieve both high selectivity and high yield at reasonable cost. The process requires only conventional, off-the-shelf equipment and reagent usage (oil, surfactants, etc.) should be small. There are, however, complications. The process involves at least five phases: two

or more solids (coal and mineral), two liquids (oil and water) and one gas (air). It is demonstrated in this study that the process is very sensitive to fluctuations in operating parameters. It is necessary to maintain precise control over the chemistry of the liquid phases as well as the agitation conditions in order to promote selectivity. Both kinetics as well as thermodynamic factors play a critical role in determining overall system response.

1.1. The Problems of Deep Cleaning Fine Coal

Of the many possible approaches to the deep cleaning of coal, surface-based processes (particularly selective agglomeration and froth flotation) appear to offer the greatest potential. Both of these processes, however, suffer from an inability to achieve high selectivity together with an acceptable yield of combustible matter.

1.2. Selective Agglomeration

Spherical or oil agglomeration has been used commercially to clean coal for many years. The so-called Trent process was used at several commercial installations in the early decades of this century, and was found to work better than flotation for -300 mesh coal (Ralston, 1922). However, its use had to be discontinued due to high process costs (Mehrotra et al., 1983). A reduction in the oil consumption from about 30% (oil:coal) in the Trent process was achieved in the Convertol process which used only ~3 to 10% oil (Lemke, 1954; Brisse and McMorris, 1958). Further developments in oil agglomeration occurred in the early 1960's at the National Research Council of Canada where the emphasis was on the use of a combination of agitator cells for the production of compact, spherical pellets (Capes and Darcovich, 1984). A similar pelletizing separator which combines the effect of several agitating vessels into a single unit was developed by Shell (Zuiderweg, et al., 1968). Relatively high ash and moisture contents of the pellets together with high oil requirements have prevented this process from becoming a success. Conventional applications of oil agglomeration have generally been based on the separation, by size, of agglomerated coal from dispersed mineral particles. This approach requires large, strong agglomerates which infers high oil usage and consequent loss of selectivity and high reagent costs. An additional problem is that the agglomerates tend to

have high moisture content and, because of their integrity, are not amenable to simple, mechanical dewatering. Agglomeration at low levels of oil addition can give excellent selectivity but the agglomerates tend to be small and not strong enough to withstand separation by size.

1.3. Flotation of Ultrafine Coal

Froth flotation is commercially practiced to clean approximately - 28 mesh coal using fuel oil as the collector. The quantity of oil usually increases as the rank decreases; ranging from about 1 lb/ton for high rank coals to about 5-35 lb/ton for sub-bituminous coals (Aplan et al., 1986). Grinding to fine sizes is needed to achieve the desired liberation for deep cleaning of coal, but the efficiency of flotation separation decreases as the particle size becomes small, especially for particles $< 10 \mu\text{m}$. In the past, different approaches have been used to float fine particles. Yoon and Luttrell (1986), employed fine bubbles to increase the rate of flotation of fine particles. Although the recovery is higher when fine bubbles are used, the grade is often poor because of the large amount of water carryover into the froth phase. This is the reason for the necessity to use wash water in column flotation cells. An alternative approach to increase the rate of flotation is to aggregate the fine particle as was discussed by Fuerstenau, Chander and Abouzeid (1979).

1.4. Wetting Phenomena

The basis for coal cleaning by flotation of micro-aggregates is controlled wetting of particle surfaces by air or oil. It is often considered that oil should spontaneously displace water at the coal surface while water displaces oil at the surfaces of mineral particles. In this study it is shown that while the latter is essential for selectivity, only spontaneous adhesion of oil to coal is necessary for agglomerate formations. Complete spreading may, in fact, be detrimental to the process by serving primarily to increase oil usage. That is, complete spreading might not directly contribute to agglomerate growth, even though it will have some benefit through increased hydrophobicity.

Wetting is the process of displacement of one fluid by another at a solid surface. In the context of micro-agglomeration the fluids are both liquids: oil and water. Two kinds of wetting need to be considered here:

- adhesional wetting which is the formation of a stable three-phase (solid-oil-water) contact and
- spreading wetting which refers to the displacement of one liquid by the other (water by oil at a coal surface, oil by water at a mineral surface).

Thermodynamically, the processes can be described by free energy changes expressed in terms of interfacial tensions. Thus, for adhesion of a solid particle to an oil droplet,

$$\Delta G_A = \gamma_{SO} - \gamma_{SW} - \gamma_{OW} \quad 1.1$$

where γ_A , γ_{SO} , γ_{OW} are, respectively the solid/oil, solid-water and oil-water interfacial tensions. For selective agglomeration, ΔG_A should be positive for the mineral particles but negative for coal particles.

For the displacement of water by oil at a solid surface

$$\Delta G_S = \gamma_{SO} - \gamma_{SW} - \gamma_{OW} \quad 1.2$$

Spontaneous displacement of water by oil at a solid surface will occur if ΔG_S is negative. If ΔG_A is negative but ΔG_S is positive, oil will adhere to the surface, in the form of drops, but will not spread spontaneously over the surface. There is reason to believe that this may represent an optimum condition for selective aggregation of coal particles through oil bridging.

The wetting criteria expressed by Equations 1.1 and 1.2 are of limited value as written since the solid/fluid interfacial tensions, γ_{SO} , γ_{SW} are not known and are not generally amenable to measurement. By introducing Young's equation (Adamson, 1990), these relationships can be expressed in terms of contact angles, i.e.

$$\Delta G_A = \gamma_w \cos \theta_w - \gamma_o \cos \theta_o - \gamma_{ow} \quad 1.3$$

and

$$\Delta G_S = \gamma_w \cos \theta_w - \gamma_o \cos \theta_o + \gamma_{ow} \quad 1.4$$

where γ_w and γ_o are the surface tensions of water and oil, respectively and θ_w and θ_o are the contact angles for water and oil on the solid.

Equations 1.3 and 1.4 can be used in the selection of the hydrocarbon phase for selective agglomeration of coal. Thus, to minimize the inclusion of mineral particles in the agglomerates:

$$\gamma_w \cos\theta_{MW} - \gamma_o \cos\theta_{MO} - \gamma_{ow} > 0 \quad 1.5$$

where θ_{MO} and θ_{MW} are the respective contact angles (against air) of oil and water on the mineral surface. Similarly, to ensure adhesion of the oil to the coal particles,

$$\gamma_w \cos\theta_{CW} - \gamma_o \cos\theta_{CO} - \gamma_{ow} < 0 \quad 1.6$$

To minimize the spreading of oil on the coal surface, thereby leaving it in the form of adhering droplets, appropriate for bridging-type aggregation,

$$\gamma_w \cos\theta_{CW} - \gamma_o \cos\theta_{CO} + \gamma_{ow} > 0 \quad 1.7$$

The use of Young's equation is strictly valid only for finite (i.e. non-zero) contact angles and, of course, this constraint is often violated, especially at mineral surfaces where both θ_{MW} and θ_{MO} are often zero. Under such conditions, Inequalities 1.5, 1.6 and 1.7, represent sufficient but not necessary conditions; systems which appear to violate one or other of the conditions may, nevertheless, be appropriate.

Each of the quantities in Inequalities 1.5, 1.6 and 1.7 can be measured experimentally, and an extensive body of such data is already available in the literature for reagent free systems. The addition of surfactants leads to changes (generally reduction) in interfacial tensions. In principle, appropriate surfactant additions could be used to satisfy the wetting criteria defined above. However, the results of surfactant addition can be complex and very difficult to predict. Measurement of interfacial tensions and contact angles will be required if surfactants are used to control the wetting properties. The net effect of a surfactant addition will also depend on its distribution between the bulk liquid phases, which is a function of the relative solubility, and on subsequent adsorption at the various interfaces which, in turn, depends on the bulk concentrations. The thermodynamic criteria defined by Inequalities 1.5, 1.6 and 1.7 were useful in selection of appropriate surfactants.

1.5. Emulsion Phenomena

In emulsion flotation, the quantity of oil used is intermediate between froth flotation (say 1-35 lb/ton) and selective agglomeration (160-400 lb/ton). The effectiveness of this process has been demonstrated in previous studies in our laboratories (Olson and Aplan, 1987; Bonner and Aplan, 1993), who observed that for high rank coals emulsion inversion occurs using only a few lb/ton of oil. In this case the continuous emulsion phase in the flotation cell is water and the continuous phase in the froth is oil and air. The nature of the froth is totally different from the loose, watery froths typically of froth flotation. Under emulsion flotation conditions, when the air is turned on during flotation, the highly hydrophobic coal instantly agglomerates and floats to the top of the cell as a slug. This is perhaps the reason for high entrainment of mineral matter in the froth product which decreases process efficiency. Further work has shown that, under proper conditions, careful control of the amount of oil and time of flotation can lead to a substantial rejection of pyritic sulfur and ash (Olson and Aplan, 1987; Bonner and Aplan, 1993) but the physico-chemical phenomena involving the oil remain to be fully understood.

Emulsification of oil depends on

- The concentration and type of surfactant
- the hydrophobicity of particles
- hydrodynamics

The type of emulsion produced in the presence of a surfactant can be readily predicted based on a knowledge of the hydrophilic-hydrophobic balance (HLB) number. Similarly, the type of emulsion can be related to the hydrophobicity of fine particles. But, for both the cases the droplet size distribution is much more difficult to predict. Furthermore, when both surfactants and particles are present, properties of emulsions cannot be adequately predicted. Investigations were carried out to determine the size distribution of emulsions in presence of surfactants.

Although the importance of phase inversion was recognized in the Convertol process with the incorporation of a phase inversion mill, the significance of phase

inversion in oil-based coal cleaning process is not fully recognized. Only recently, Aplan and his associates (Bonner and Aplan, 1993; Olson and Aplan, 1987) observed a decrease in the recovery and flotation rate constant for ash and "liberated pyritic sulfur" when the addition of fuel oil was above a certain critical value. The rejection of ash and pyrite was suggested to occur as a result of changes in the flotation mechanism possibly accompanied by phase inversion.

The incipient conditions of phase inversion also gave maximum rejection of ash-forming minerals in the liquid-liquid separation of ultrafine coal ($-10\ \mu\text{m}$) (Hsu and Chander, 1988). Our recent studies at the Pennsylvania State University show that the conditions of phase inversion depend strongly on the hydrophobicity of the coal used. Since particles stabilize oil-in-water or water-in-oil emulsions, depending upon their hydrophobicity, the process of liquid-liquid separation involves transfer of coal from aqueous to an emulsion phase at the oil/water boundary. Liquid-liquid separation has been shown to be especially effective for recovery of particles in the ultrafine sizes (Mellegren and Shergold, 1966; Lai and Fuerstenau, 1968; Raghavan and Fuerstenau, 1975; Zambrana et al., 1974). The so-called Otisca-T and LICARDO processes are also based on partitioning of hydrophobic coal particles between two immiscible liquids. In a study at the Pennsylvania State University, Hsu and Chander (1988) carried out a detailed investigation of the mechanisms involved in liquid-liquid separation of ultrafine coal ($-10\ \mu\text{m}$). In the initial stages of mixing, an oil-in-water emulsion forms, which captures both weakly and strongly hydrophobic particles. This results in a poor selectivity for the process during its initial stages. The oil-in-water emulsion inverts to water-in-oil emulsion in the presence of strongly hydrophobic particles. The rejection of pyrite and mineral matter was observed to be maximum under incipient conditions of phase inversion. On prolonged agitation a water-in-oil-in-water complex emulsion forms which increases mineral matter pick-up through entrainment. Intense agitation results in bridged emulsions with oil acting as the bridging liquid. These findings on the effect of hydrocarbons in the presence of ultra fine coal particles on emulsification was discussed by Polat and Chander (1994).

1.6. Agglomerate Formation and Growth

A general requirement for the use of selective agglomeration for the deep cleaning of fine coal is the production of agglomerates which are sufficiently large for effective separation from the dispersed phases (refuse) and have high density - to minimize the inclusion of water and dispersed mineral particles. In recent years, there has been extensive research into the size and structure of agglomerates formed by coagulation/flocculation of fine particles from liquid dispersion. Theoretical analyses and simulations (Vold 1963; Sutherland 1967; Weitz and Huang 1984) and experimental studies (Medalia 1967; Koglin 1977; Klimpel, Dirican and Hogg, 1986) consistently indicate that there is an inverse relationship between agglomerate size and agglomerate density. Studies in our laboratories (Klimpel and Hogg, 1986; 1991) have shown that the relationship is essentially independent of the mechanisms of agglomerate formation, the binding forces in the agglomerates and the conditions of agglomerate growth. As a general rule, the density of an agglomerate is determined primarily by its size relative to that of the particles from which it is formed. In the agglomeration of particles in the 1 to 10 μm size range, however, we have shown (Klimpel and Hogg, 1986; 1991) that agitation of the suspension during agglomerate growth promotes the development of dense micro-agglomerates of size up to about 50 μm . Further agglomeration leads to more open structures which follow the general size-density relationships but are built up from the dense micro-agglomerates rather than from primary particles. To our knowledge, such studies have not been carried out on oil-agglomerated coal, but the consistency of the results obtained for a very broad variety of systems (carbon black in air, minerals in water with polymer flocculants, etc.,) strongly support the proposition that such relationships should indeed be valid for coal-water-oil systems.

1.7. Agglomerate Flotation

The key problem in previous attempts to use this approach has been the difficulty of producing agglomerates relatively free of ash. The polymeric reagents often used in efforts to selectively flocculate coal (Venkatadri, et al., 1989; Attia and Yu, 1988) tend to

produce large, low density flocs which generally entrain large quantities of mineral matter. A substantial increase in ash and sulfur with agglomerate size was observed by Lai, et. al. 1989). In this investigation an attempt was made to use small amounts of oil and surfactants to produce dense, micro-agglomerates of high grade. Such aggregates will have a higher rate of flotation because of their larger size (30-50 μm) and enhanced hydrophobicity. The latter can be readily attained by proper use of oil with and without reagents. The increased rate of flotation of such aggregates will minimize water carryover with a resultant increase in selectivity. The results of this study should be applicable to flotation in conventional cells or in columns because the aggregate size will never be large enough to have an adverse effect.

Chapter 2

ADSORPTION OF PEO/PPO TRIBLOCK CO-POLYMERS AT AIR/WATER INTERFACE

2.1. Introduction

Even though some studies employing light scattering and ultra-centrifugation techniques have indicated that triblock co-polymers do not form micelles (Mankowich, 1954; Bell, 1959; Dwiggins et al., 1960; Anderson, 1972), other studies confirmed micelle formation in the form of a PPO core surrounded by hydrated PEO shell (Ross and Oliver, 1959; Nevolin et al., 1963; Sasaki and Shah, 1965; Schmolka and Reymond, 1965; Schick, 1967; Zhou and Chu, 1988; Reddy et al., 1990; Almgren et al., 1992; Pandya et al., 1993). These studies show large differences in CMC, aggregation number (N_{agg}) and polydispersibility, with the results depending on the measurement techniques. A summary of various CMC values is given in Table 2.1 for Pluronic L-64 at different temperatures. Although the CMC varied by three orders of magnitude from one method to another, the differences were small when a given method was used. The light scattering method usually gave larger values (0.97×10^{-3} to 6.9×10^{-3}) compared to the surface tension method (4.2×10^{-6} to 1.7×10^{-4}).

Surface tension is one of the most common techniques for investigating the adsorption and association behavior of surfactants at air/water interfaces. The micellization behavior of block co-polymers, however, is more complex than that of conventional, low molecular weight surfactants. Surface tension data reported recently by several investigators for various aqueous PEO/PPO/PEO block co-polymer solutions show unusual characteristics¹. A change was observed in the slope of the surface tension versus concentration curves at a characteristic concentration, after which the surface tension values continued to decrease until a constant value was reached. There was a

¹Wanka et al. (1990) for P-104, P-123 and F-127; Hecht and Hoffmann (1994) for F127; Alexandridis et al. (1994) for several co-polymers such as P-104, P-103, P-105, P-85, F-108 and P-65.

general agreement in attributing the second break in the curve to the formation of micelles in the solution. However, conflicting suggestions were made by various investigators to Table 2.1. Critical micelle concentrations and aggregation numbers for Pluronic L-64 determined by different techniques at various temperatures.

Table 2.1. Critical micelle concentration of Pluronic L-64 surfactant reported in the literature.

Method	Temp. °C	CMC, M	N _{agg}	Reference	
Light scattering	27	2.4×10^{-3}	-	<i>Reddy et al., 1990</i>	
	34.5	9.7×10^{-4}	-		
	40	3.1×10^{-4}	-		
		40		19	<i>Almgren et al., 1992</i>
		60		85	
		28	6.9×10^{-3}	-	<i>Pandya et al., 1993</i>
		30	3.4×10^{-3}	-	
33		1.7×10^{-3}	-		
Sedimentation velocity	40		54	<i>Zhou & Chu, 1988</i>	
	42		88		
Differential dye adsorption	25	6.8×10^{-6}	-	<i>Schmolka & Raymond, 1965</i>	
Surface tension	20	1.7×10^{-4}	-	<i>Nevolin et al., 1963</i>	
	25	6.9×10^{-5}	-	<i>Saski & Shah, 1965</i>	
	25	4.2×10^{-6}	-	<i>Schmolka & Raymond, 1965</i>	
	25	7.0×10^{-6}	-	<i>Schick, 1967</i>	

explain the first break. For example, Gao and Eisenberg (1993) argued that the first break in the curve was due to the wide molecular weight distribution of the co-polymers while Hecht and Hoffmann (1994) proposed that hydrophobic impurities were responsible for this behavior. Alexandridis et al. (1994 and 1995) suggested yet another hypothesis in which the break was attributed to reconfiguration of molecules at the surface. These authors considered that the molecules reconfigured when the interface was covered with a

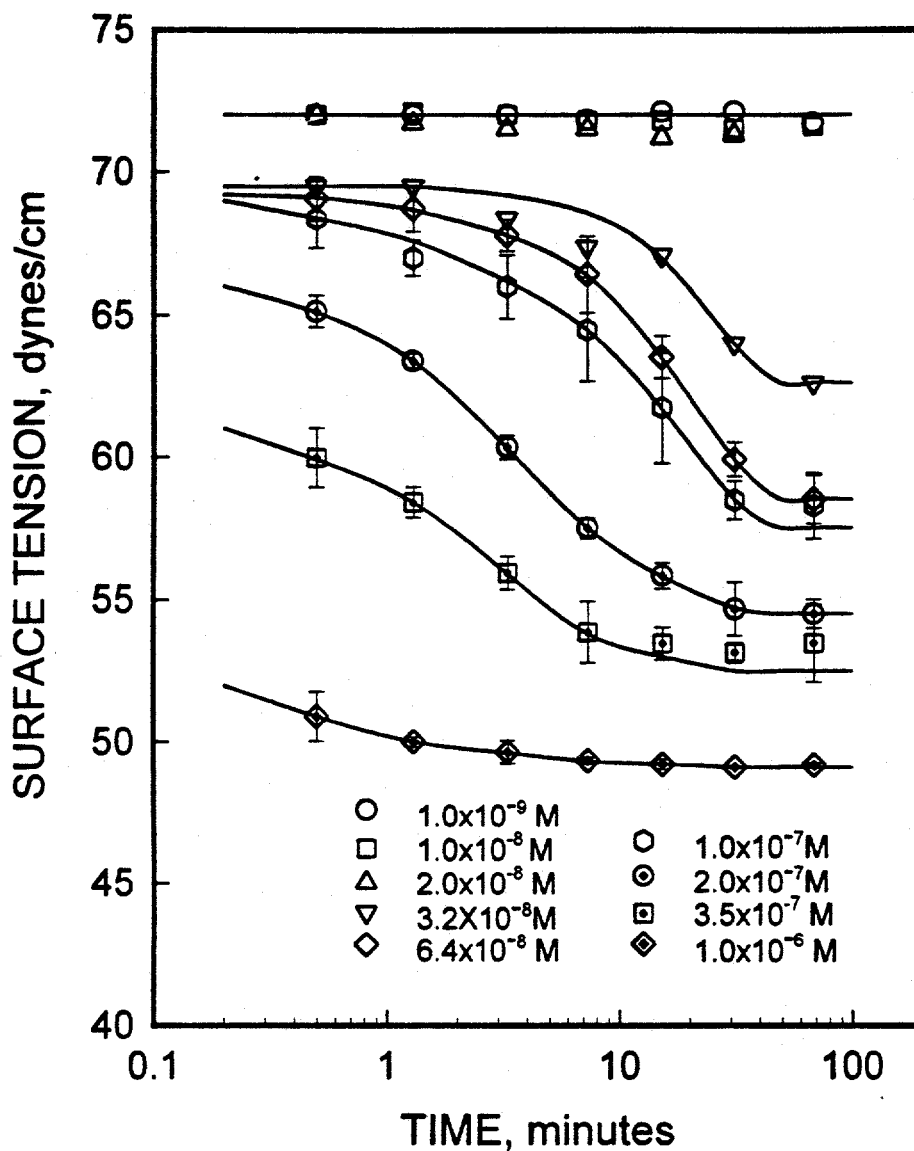


Figure 2.1. The effect of conditioning time elapsed between the placement of the solution in the measurement cell and the measurement of surface tension of Pluronic L-64.

monolayer of the co-polymer to produce a more compact layer at the interface. The decrease in the surface tension after the first break was due to the fact that this compact layer could accommodate more polymer molecules. The decrease in the slope was postulated to be due to slower rate of adsorption after reconfiguration (Alexandridis et al., 1994).

In this part of the study, surface tension measurements were carried out to elucidate the adsorption and association behavior of selected PEO/PPO/PEO triblock copolymers at the air/water interface. The effect of diffusion time on the surface tension was also studied. The effect of different surfactant characteristics, such as molecular weight and ethylene/propylene oxide fraction was investigated and the results are discussed in the following sections.

2.2. Surface Tension as a Function of Time

During initial phases of this study, it was observed that surface tension measurements were affected by the time elapsed between the placement of the solution in the measurement cell and the actual measurement. Therefore, tests were carried out as a function of time and surfactant concentration using a fixed volume of solution (50 ml) in a cylindrical glass cell 4.5 cm in diameter. The solutions were gently stirred after being placed in the cell to enhance diffusion of surfactant molecules without causing significant surface turbulence. Surface tension measurements were taken at preset time intervals for a period of about an hour. The measurements were repeated four times to ensure reproducibility. The averages of these readings and the corresponding 95% confidence intervals are presented in Figure 2.1. At the lowest concentrations tested, 10^{-9} , 10^{-8} M and 2×10^{-8} M, no variation in the surface tension was observed with time. At higher concentrations the surface tension decreased as a function of time and reached a constant value which was taken as the equilibrium value. The time needed to reach the equilibrium decreased with increase in concentration. Figure 2.2 gives the γ/γ_{∞} versus time curves to show the significance of the difference between the surface tension values obtained after 1 hour of conditioning and the equilibrium values. For lower

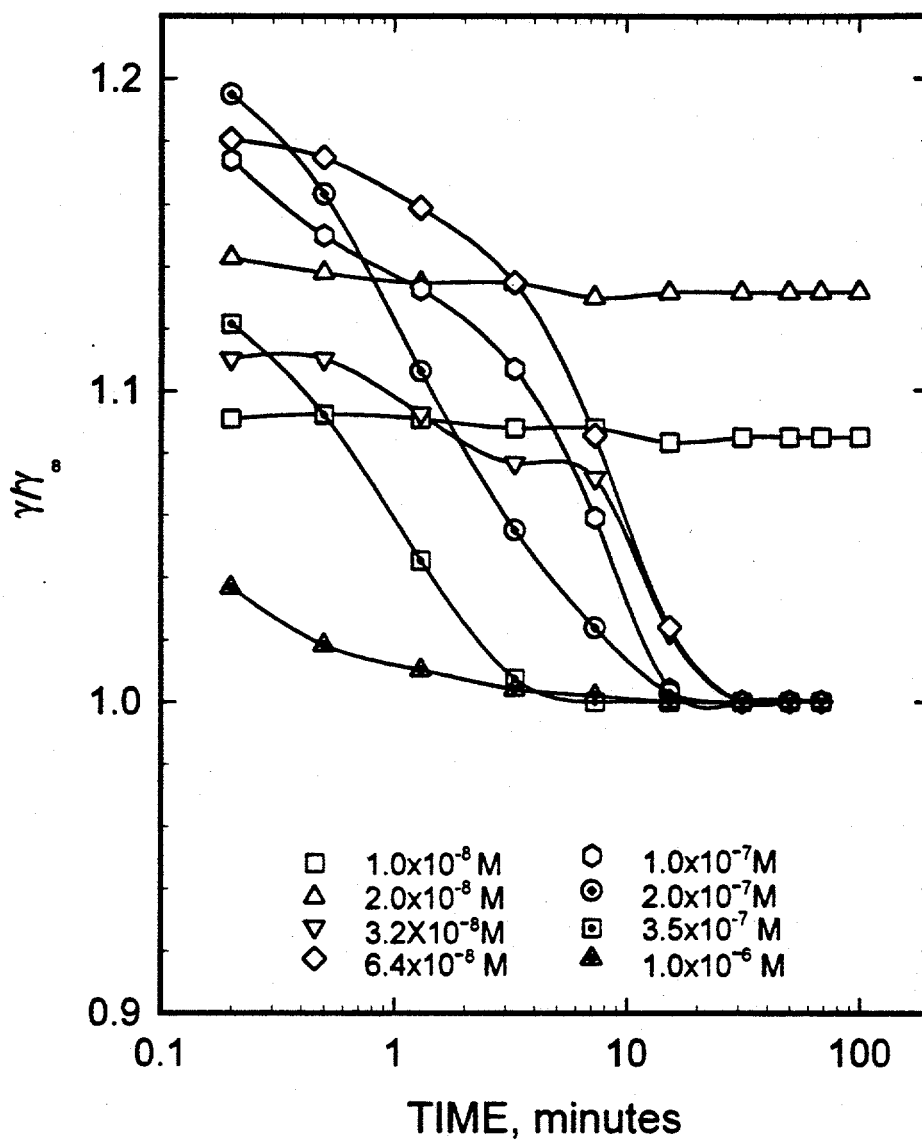


Figure 2.2. The γ/γ_∞ versus time plot for various concentrations of Pluronic L-64.

concentrations (10^{-8} and 2×10^{-8} M) the γ_{∞} was estimated from the extrapolation of the surface tension versus concentration curve obtained for higher concentrations ($<10^{-6}$ M). For low concentrations of 10^{-8} and 2×10^{-8} M it can be seen that the ratio is higher than one and does not change with time, suggesting that one hour was not enough for diffusion of sufficient number of surfactant molecules to the surface to attain equilibrium. The effect of stirring on surface tension is shown in Figure 2.3. It could be seen that the two data sets differ significantly at concentrations below 10^{-6} M.

In the literature, no attention has been paid to the effect of time on surface tension measurements. For example, in a recent detailed study, Alexandridis et al. (1994) did not specify the times for which the solutions were equilibrated prior to the surface tension measurement. In this study it is shown that time for which the solution is kept in the measurement cell is an important variable affecting surface tension. Hence, the slope of the surface tension curves at low concentrations could not be used to calculate the parking area of the molecules since they would vary under non-equilibrium conditions. The area estimated will be smaller in the case of slowly diffusing co-polymer molecules. The results obtained in this study by enhancing the diffusion and the results taken from literature (Alexandridis et al., 1994) are given in Figure 2.4 for P-104. The method used to measure surface tension was the same for these two cases. The only difference was the temperature which was 21°C in this study while it was 25°C in their study. It can be seen that the data taken from Alexandridis et al. (1994) resemble that in Figure 2.3 where the surface tension was measured without stirring.

Taking the time effect into account in carrying out surface tension measurements is important for an accurate interpretation of the complex surface tension versus concentration profiles of these surfactants. Hence, the procedure of gentle stirring of the solutions prior to the surface tension measurement was used throughout the test work.

2.3. Effect of Surfactant Concentration

The surface tension decreased from an initial value of 72 dynes/cm for the no surfactant case to a value of about 33 dynes/cm at a surfactant concentration of 5×10^{-1} M

(Figures 2.3 and 2.4). Unlike the surface tension profiles for the ethoxylated nonyl and octyl phenols which consist of two regions corresponding to the presence of monomers and micelles, there are several regions where the slope of the surface tension curve shows distinct breaks. At concentrations greater than 7×10^{-2} M, surface tension did not change.

2.4. Effect of Molecular Weight

To determine the effect of molecular weight, surface tensions of L-44, L-64 and P-104 series block co-polymers were measured and the results are presented in Figure 2.5. The molecular weights were, respectively, 2200, 2900, and 5900).

Based on the results given above, a schematic representation of the changes in surface tension as a function of surfactant concentration is given in Figure 2.6. The surface tension behavior for Pluronics could be divided into three concentration regions marked as Regions I, II and III. Region I is believed to consist principally of monomers whereas Region III involves fully developed micelles. Region II is a transition region between the two. Region II may be further divided into three sub-sections. A detailed interpretation of these regions is given in the following paragraphs:

Region I. All the molecules are considered to be in their monomer form and are expected to adsorb at the air/water interface. The adsorption density may be calculated from surface tension data by using the Gibbs equation. It is well known that the Pluronic series of reagents have a broad molecular weight distribution² (Gao and Eisenberg, 1993), and a distribution of EO and PO groups (Zhou and Chu, 1988; Hecht and Hoffmann, 1994). One could assume that they are made up of 3 discrete molecular weight and 3 discrete PO fraction intervals (high, intermediate and low) such that any molecule would fall into one of the 9 molecular weight-PO fraction intervals. Then, the Gibbs adsorption isotherm can be written as follows:

²Polydispersibility index, PI, which is a measure of the width of the distribution of molecular weights for a given surfactant, is 1.34 for Pluronic P104 (Fears and Lucham, 1994). The polydispersibility index, takes values between 1, narrow distributions, and 2, broad distribution. It is defined as the ratio of weight-average molecular weight to number-average molecular weight of the surfactant molecules.

$$d\gamma = -RT \sum_{i=1}^3 \sum_{j=1}^3 \Gamma_{ij} d \log C_{ij} \quad 2.1$$

Where γ is the surface tension in dynes/cm and Γ_{ij} and C_{ij} are the adsorption density and the bulk concentration of the component which falls into i th molecular weight and j th PO fraction interval, in moles/cm² and moles/liter, respectively. It is reasonable to assume that low molecular weight component possesses a larger diffusivity and constitutes the main portion of the adsorbing molecules, especially at early stage of adsorption. Surface tension at low surfactant concentrations is therefore likely to be dominated by smaller molecular weight more surface active components in the reagent. Then, the adsorption isotherm for Region I can be written as follows:

$$d\gamma = -RT \sum_{j=1}^3 \Gamma_{1j} d \log C_{1j} \quad 2.2$$

where Γ_{1j} and C_{1j} are the surface excess and the bulk concentration of the low molecular weight component which falls into j th PO fraction interval, respectively. The area per molecule at the interface, A_m , can be calculated as:

$$A_m = \frac{1}{\Gamma_m N_{av}} \quad 2.3$$

where Γ_m is the surface excess concentration at monolayer coverage and N_{av} is the Avagadro's number. The area calculated provides information on the degree of packing and the orientation of the adsorbed molecule.

From the surface tension measurements given in the above paragraphs, the adsorption density was calculated to be 1.59×10^{-10} moles/cm² for Pluronic L-64. This corresponds to a parking area of about 1.04 nm² per molecule. If one compares this area with the parking area of a single PO group (0.11 nm²), it is obvious that L-64, which

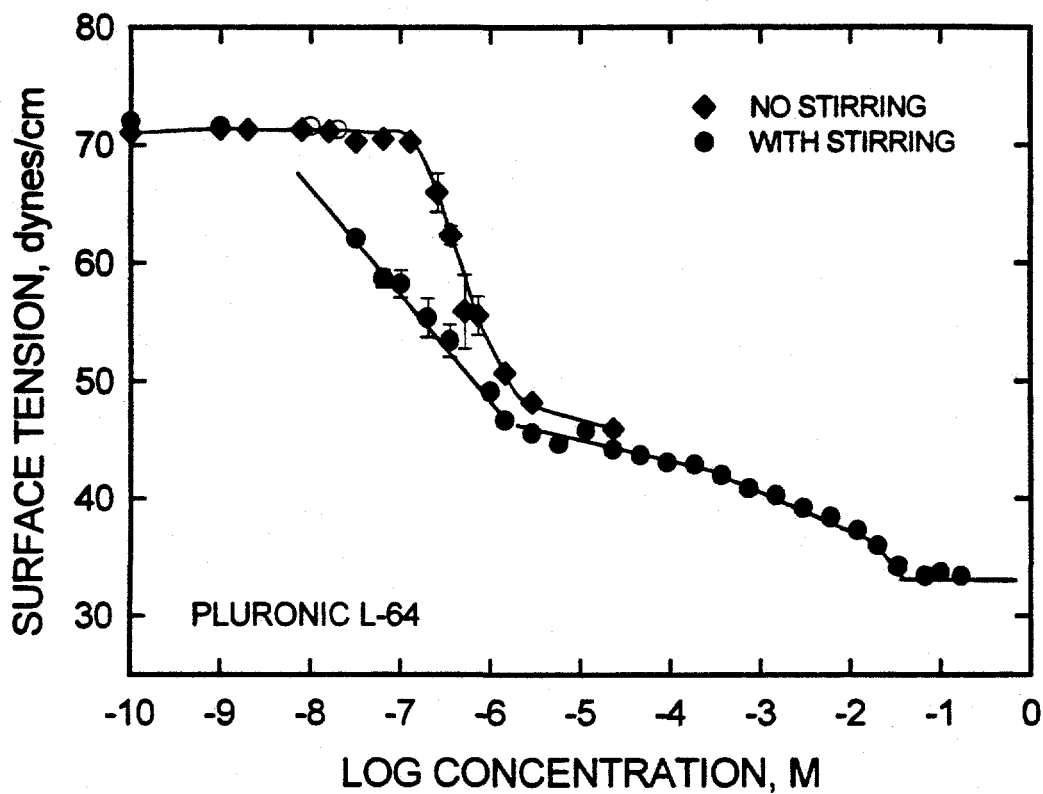


Figure 2.3. The variation in the surface tension of Pluronic L-64 as a function of concentration for the gently stirred and non-stirred solutions.

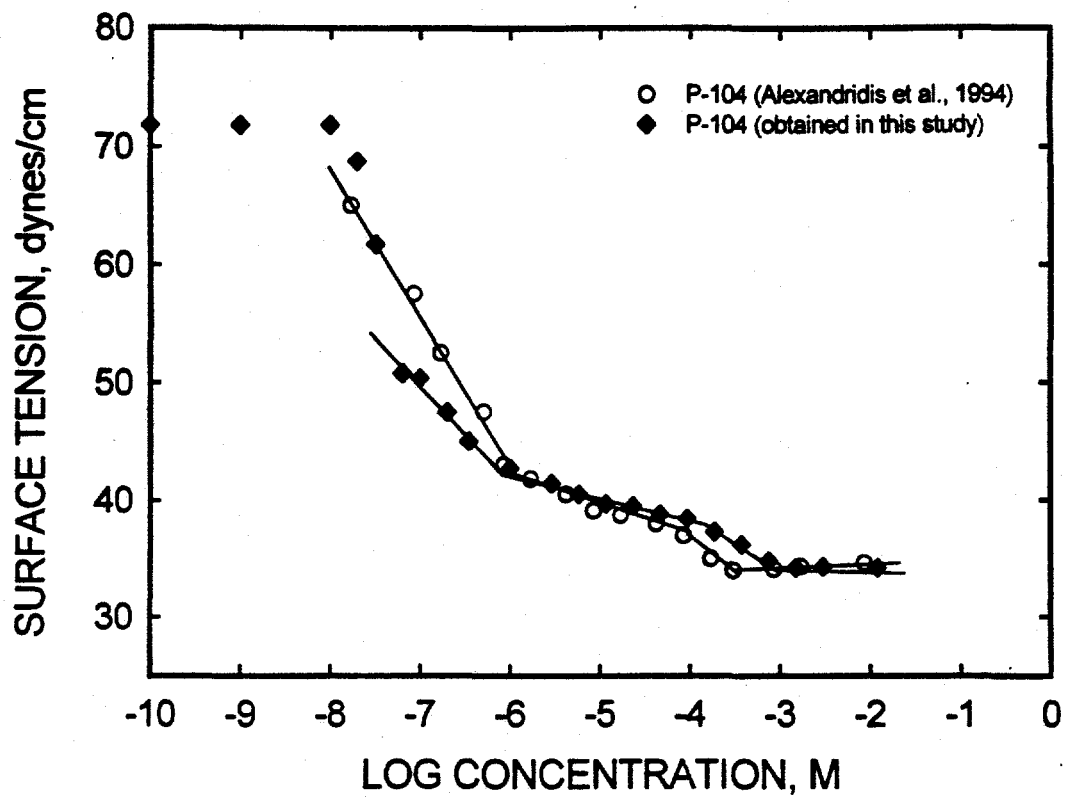


Figure 2.4. A comparison of two sets of surface tension data of P-104 in the presence of gentle stirring from this study and literature (Alexandridis et al., 1994), respectively.

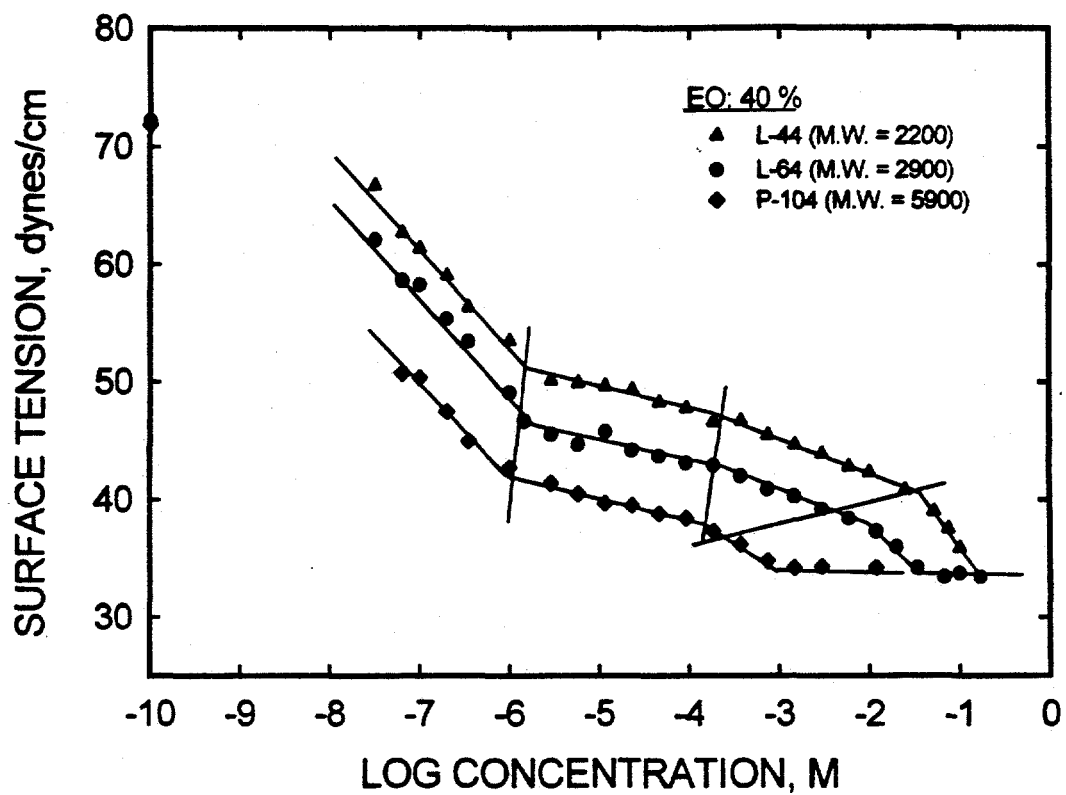


Figure 2.5. The surface tension versus concentration curves for L-44, L-64 and P-104 which demonstrate effect of the molecular weight.

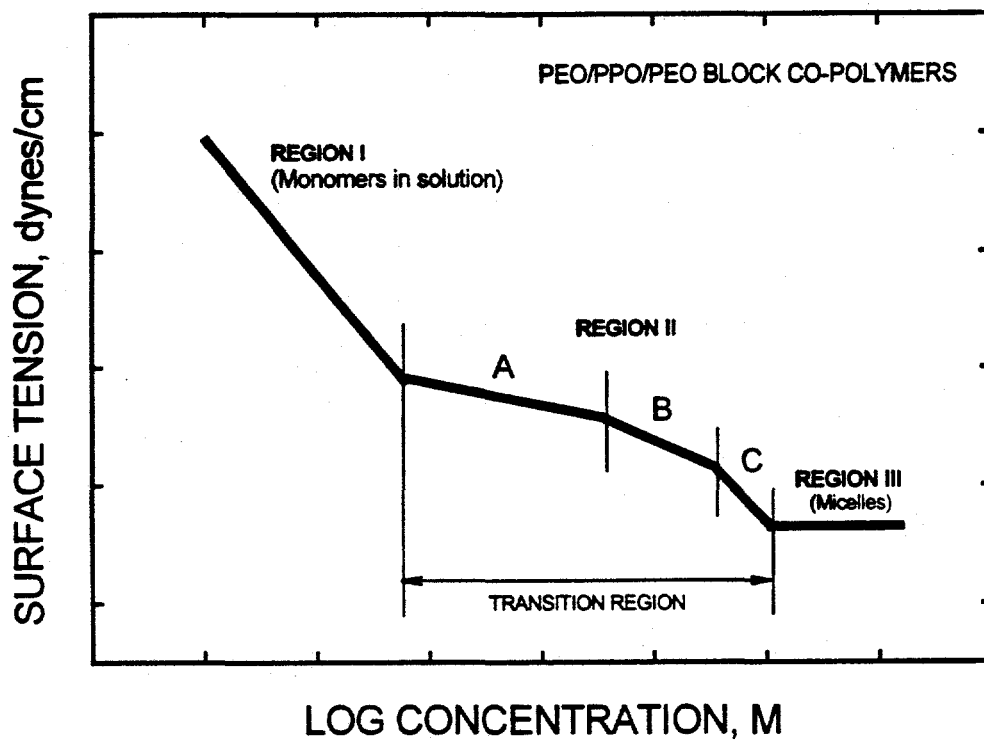


Figure 2.6. A schematic diagram of the surface tension behavior of PEO/PPO triblock co-polymers as a function of block co-polymer concentration.

contains an average of 30 PO groups (hence, a total PO parking area of about 3.3 nm^2), does not adsorb with its extended configuration and that only a fraction of its PO groups resides at the surface. The hydrophobic portions of these molecules are considered to be in a collapsed form in water by some investigators (Gao and Eisenberg, 1993).

Since an increase in the molecular weight did not affect the slope of the curve in this region, the area per molecule, 1.04 nm^2 at monolayer coverage, should be the same for all the three surfactants. Based on these results, one may conclude that only a fraction of the PO groups, which is similar for the three surfactants, anchors to the surface and the rest of the PO groups remain in water. It could be argued that those molecules which adsorb at the interface may be the same component present in each of the three surfactants. However, the time to reach the equilibrium surface tension was different for these surfactants suggesting that different molecules are involved in the adsorption process. From Figure 2.7 it can be seen that the time to reach equilibrium is longer in the case of the larger P-104 which suggests that the size of the molecules adsorbing at the surface is also larger as expected. The time was shorter in the case of smaller L-44 molecules.

The transition from Region I to II, that is concentration where the first break in the curve occurred, was about the same for all the surfactants. That is, the first break is not a strong function of surfactant type. The concentration where the first break in the curve occurred was also found to be independent of temperature and the molecular weight of the block co-polymer by other investigators (Hecht and Hoffmann, 1994; Alexandridis et al., 1994).

At a fixed concentration, say 10^{-7} M , the difference in the surface tension values of these surfactants was attributed to differences in surface activity of the molecules. The lower value was obtained with P-104 with a larger PPO group (an average of 56) which is expected to be more surface active, while the lowest value was obtained with L-44 with a smaller PPO group (an average of 23) which is expected to be less surface active.

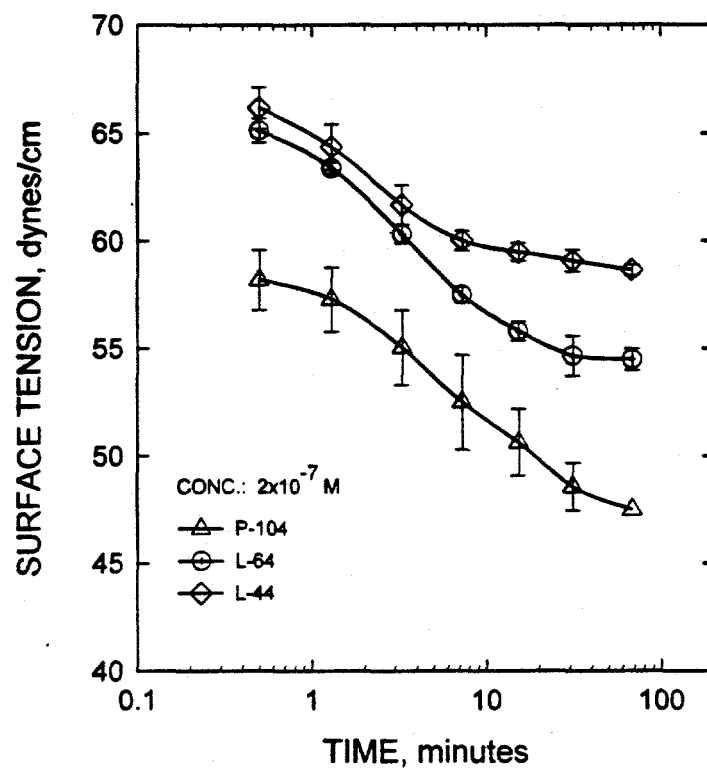


Figure 2.7. The effect of conditioning time on the surface tension of Pluronic L-44, L-64 and P-104 surfactants.

Region II. This is a transition region between Regions I (monomers) and III (micelles). The presence of such a transition region has caused confusion in the literature and a satisfactory explanation is still lacking. A plausible model is proposed here as follows: It is reasonable to assume that some of the surfactant molecules will be strongly hydrophobic since they may contain a substantially higher ratio of PO groups due to polydispersibility of PO and EO functional group. This highly hydrophobic material could aggregate at lower concentrations as dimers, trimers, etc. and still adsorb at the air/water interface because of the shape of the molecule, decreasing the surface tension with increasing concentration. The fact that such a transition region is not observed in the case of polydispersed ethoxylated phenols where the polydispersibility is due to ethylene oxide groups supports this hypothesis. Zhou and Chu (1988) state that polydispersibility of the insoluble block affects micellization considerably more than polydispersibility of the soluble block.

The presence of sub-regions in Region II can be seen in published data even though no mention of these sub-regions has been cited in the literature. These sub-regions, which are marked as A, B and C in Figure 2.6, are distinguished by an increasing slope from A to C. Since the dimers, trimers etc. will occupy a larger surface area compared to individual molecules, the slope of the surface tension versus concentration curve will be smaller. The increase in the slope of the curve as one moves from sub-region A to sub-region C could be attributed to re-configuration of the aggregates at the surface with increasing concentration³. In this case, more dimers and trimers could occupy the surface, leading to a steeper slope in sub-regions B and C. For L-64, the area per molecule was calculated to be 9.4 nm², 2.8 nm² and 1.34 nm² for sub-regions A, B and C, respectively.

³ Alexandridis et al. (1994) suggested a similar hypothesis *for monomers* to explain the first break in the surface tension versus concentration profiles. They postulated that the co-polymer layer made up of monomers became more compact at a bulk concentration of about 10⁻⁶ M due to expulsion of water.

This region became shorter as molecular weight increased due to formation of fully grown micelles at lower concentrations. The sub-region B changed most and it decreased gradually with increase in molecular weight. Disappearance of sub-region B with increasing molecular weight is most probably due to a more rapid aggregation of larger molecules in P-104 compared to smaller ones in L-44.

Region III. This concentration range corresponds to a constant value of surface tension with further increase in concentration. The reagent forms micelles in this. The concentration where Region III starts is usually defined as the CMC. The CMC changes as a function of surfactant type and temperature. The decrease in CMC with an increase in the molecular weight is in agreement with the micelle formation behavior of more traditional, monodispersed surfactants where the critical micelle concentration decreases with increasing molecular weight (Rosen, 1988; Myers, 1992).

The surface tension behavior of Pluronic type of surfactants given in Figure 2.6 partly explains the discrepancies in the literature with respect to the critical micelle concentration of these surfactants. For example, the CMC value observed by light scattering methods (see Table 1) covers a range between 3.1×10^{-4} and 6.9×10^{-3} M at a temperature range of 27°C to 40°C. A plot of the light scattering data from the literature as a function of temperature is given in Figure 2.8. An extrapolation of the data on this figure shows that the light scattering method would have predicted a CMC value of about 7×10^{-2} M at the temperature value of 21°C used in this study. This concentration coincides exactly with the transition region between Regions II and III in Figures 2.3 and 2.4 where micelle formation is observed. The CMC values observed by surface tension studies varies between 7.0×10^{-6} and 1.7×10^{-4} M for Pluronic L-64. An extrapolation gives a CMC value of about 10^{-4} M at 21°C. This concentration is within Region II in Figure 2.6. It seems that the light scattering studies were able to see only the full grown micelles, but were unable to discern the dimers, trimers, etc. from the monomers. The surface tension studies, on the other hand, seemed to be more sensitive to the changes in the system since it could distinguish the dimers and the trimers at lower concentrations. However, the reproducibility of the surface tension data obtained from the literature was

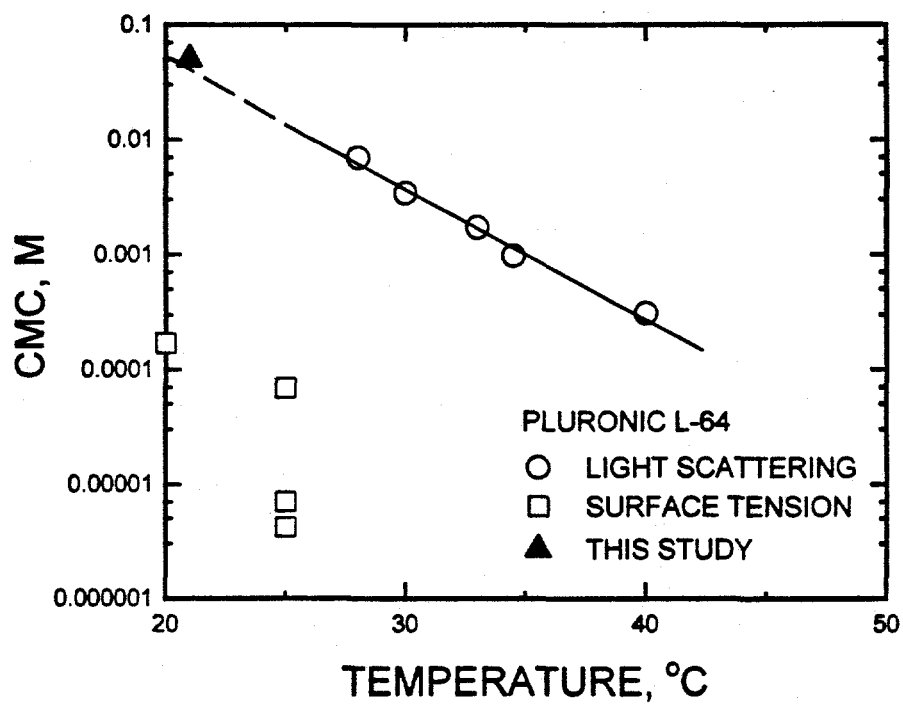


Figure 2.8. The CMC values reported in literature by light scattering and surface tension methods as a function of temperature.

not satisfactory, most probably due to the fact that these investigators were observing various points in the transition region.

2.5. Effect of Ethylene Oxide Groups

The effect of the hydrophilic portion of the surfactant structure on their surface tension behavior was investigated for L-62 and L-64. The results along with the data for P-65 which was obtained from Alexandridis et al. (1994) are presented in Figure 2.9 (see Table 2.2a for the number of EO group for these surfactants). Except Region II-A, almost no differences in the surface tension behavior was observed. In Region II-A, the slope of the curve increased and the difference between sub-region A and B disappeared in the case of L-62 and P-65.

In Region I, no change in the slope of the curve was observed. It seems that the area per molecule does not change with a change in the PPO/PEO ratio, suggesting that the area per molecule calculated may be the smallest area that these molecules could cover at the surface.

2.6. Conclusions

Adsorption of PEO/PPO/PEO type triblock copolymers at the air/water interface was investigated using surface tension measurements. Based on the studies the following conclusions could be made:

- Surface tension was a function of time at concentrations below about 10^{-6} . This was attributed to slow diffusion of the surfactant molecules to the surface.
- The surface tension versus concentration profiles for these surfactants could be divided into three distinct regions:
 1. In Region I, which extends to a surfactant concentration of about 10^{-6} M, the solution involves mainly of monomers and surface tension decreases rapidly with concentration.
 2. In Region III, the solution involves mainly of fully developed micelles and surface tension is independent of concentration.

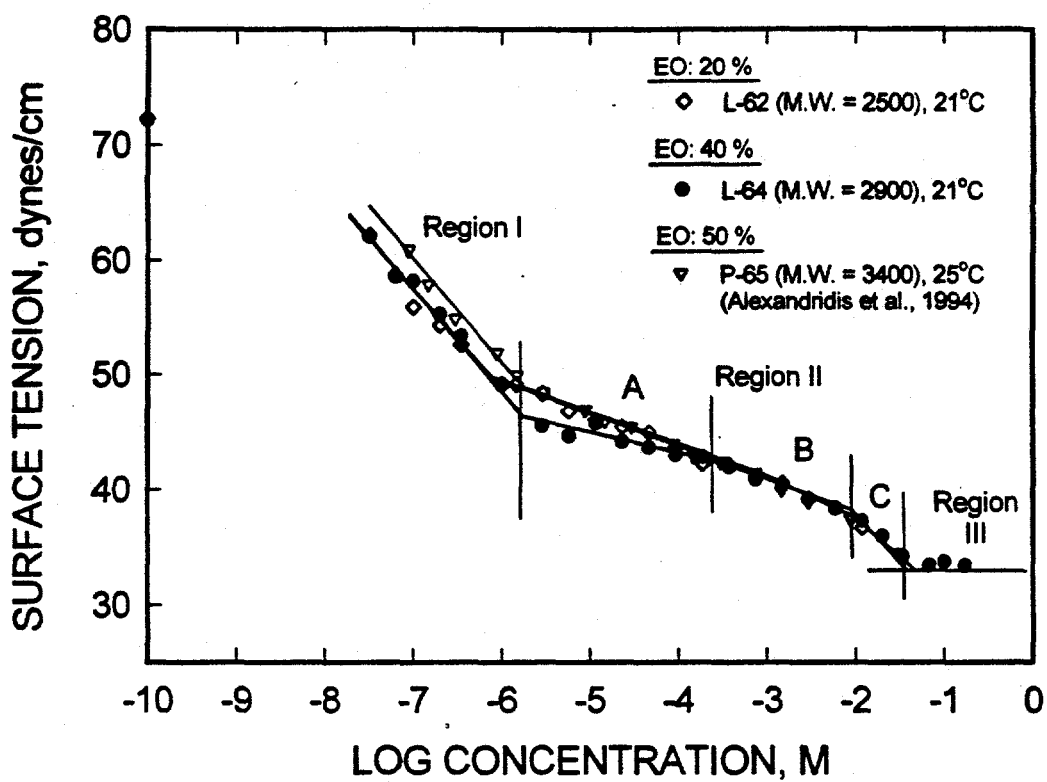


Figure 2.9. The surface tension versus concentration curves for L-62, L-64 and P-65 which demonstrate the effect of the fraction of EO groups.

3. In Region II, which is a transition between Regions I and III and was postulated that dimers, trimers, etc. are present. This region was divided into three sub-regions, namely A, B and C. These sub-regions are identified by the increase in slope with increasing concentration. Since the dimers, trimers etc. would occupy a larger surface area compared to individual molecules, the slope of the surface tension versus concentration curve would be smaller in general in the transition region compared to Region I. The increase in the slope of the curve from sub-region A to sub-region C is attributed to re-configuration of adsorbed molecules, hence closer packing of the aggregates at the surface with increasing concentration.
- The slope of the surface tension curve was not a function of molecular weight in Region I. The surface excess concentration, hence, the parking area per molecule, was found to be the same for three surfactants with different molecular weights. Nevertheless, the time which is needed by the molecules which adsorb at air/water interface should be different in size because the time to reach the equilibrium surface tension varied considerably for the three Pluronics tested (L-44, L-64 and P-104). The time increased with an increase in the molecular weight of the block copolymers.
 - The concentration at which dimers, trimers, etc., begin to form was not a strong function of molecular weight. However, the transition sub-region B disappeared with increasing molecular weight most probably due to a more rapid reconfiguration of larger molecules (P-104) compared to that of smaller ones (L-44). The concentration where fully developed micelles begin to form (transition concentration between Region II and III) decreased significantly with increasing molecular weight.
 - A change in the fraction of EO groups, keep the PO group constant, did not significantly alter the surface tension-concentration profile.

Chapter 3

KINETICS OF EMULSIFICATION IN THE ABSENCE AND PRESENCE OF PEO/PPO TRI-BLOCK CO-POLYMERS

3.1. Introduction

Emulsification of oil is important in enhancing flotation and selective agglomeration. By decreasing the droplet size the number of oil droplets in the system will increase, increasing the collision probability between the particles and oil droplets. This will affect the rate of flotation thereby influencing quality and the quantity of the product.

Emulsions are usually obtained by applying mechanical energy in a stirred tank. The mechanical energy results in deformation of the interface between the oil droplets and the continuous phase to such an extent that smaller daughter droplets form. With continuous agitation change in the size distribution of oil droplets with time depends on two sub-processes: *dispersion* and *coalescence*. Either of these sub-processes may determine the system behavior depending on the agitator speed, oil concentration and the additives present in the system. Surface active reagents, i.e., surfactants, are expected to affect these sub processes in various ways:

- *By changing oil/water interfacial tension:* Surface active agents which adsorb at the oil/water interface are known to decrease the interfacial tension significantly even at very low concentrations¹. A reduction in the restoring surface tension force against deformative stresses such as those induced by eddies in turbulent mixing promotes the dispersion of oil. In addition, oil droplets dispersed in water may develop a surface charge depending on solution chemistry (Adamson, 1990; Hiemenz, 1986) which leads to development of an electrical double layer. The presence of a such layer affects the electrostatic interaction of two oil droplets. Therefore, as adsorbed

species are expected to alter both the dispersion and coalescence sub-processes.

- *By contributing steric interactions:* Depending on the type of surfactant and the adsorption mechanism, surfactant molecules adsorbed at the oil/water interface may have hydrated sections extending outwards from each droplet surface. When two such droplets approach each other, the extended regions of the surfactant molecules physically interact, preventing coalescence (steric stabilization).
- *By altering film drainage rate:* Coalescence of two oil droplets is possible only if the water film between the two can drain away within the duration of contact. The presence of free hydrated surfactant molecules or micelles within the water film increases the energy required for drainage (Nikolov and Wasan, 1989), hence reducing rate.

Several studies have been conducted in the past to obtain mathematical models for predicting the droplet size distribution either under equilibrium conditions or as a function of agitation time. Hinze [1955] suggested that a drop would break deforming external stress was greater than a critical value of the counteracting internal stress due to the interfacial tension. Shinnar (1961) used the Hinze's approach to develop an empirical dispersion model to obtain:

$$X_{max} = D_a C We^{-0.6} \quad 3.1$$

where X_{max} is the maximum stable drop size, D_a is the impeller diameter, C is a constant and We is the Weber. It is defined as:

$$We = \rho N^2 D_a^3 \gamma^{-1} \quad 3.2$$

¹The nonionic co-polymeric surfactants employed in this study cause a decrease in the surface tension of about 20-30 dynes/cm at concentrations below $10^{-4}M$.

where N is the impeller speed in revolutions per unit time and ρ is the density of the continuous phase. Sprow (1967) used Equation 3.1 and found that the value of the constant, C was between 0.126 and 0.15. Based on Equation 3.1, Coulaloglou and Tavlarides (1976, 1977) discussed various data available in the literature and found the equation to be generally valid. The viscosity of the dispersed phase was found also to be important with regard to the droplet size (Arai et al., 1977; Konno et al., 1982). In the model proposed by Shinnar (1961) the viscous properties of the dispersed phase are neglected. An alternate model that takes into account viscous properties of the dispersed phase was proposed by Lagisetty et al. (1986). Koshy et al. (1988) considered that all these models overpredict the maximum stable drop size in the presence of surfactants. They developed a modified model incorporating the dynamic and static interfacial tensions to account for the effect of surfactant.

Other approaches have also been used to estimate the droplet size distribution in an agitated vessel. Narsimhan et al., (1980) utilized the experimental measurements of drop distributions along with a population balance model to determine the probability of breakage rate based on similarity concept. They restricted the considerations to lean dispersions since identification of rate probability functions characterizing both droplet breakage and coalescence was difficult. In their study, the similarity transformation proposed was based on the drop size distributions obtained from kinetics experiments conducted under different stirring and dispersed phase conditions. In another study, Nishikawa et al. (1990) observed that a combination of three normal distribution curves gave a good fit for the volumetric size distributions and a combination of two normal distributions generated a good correlation for the number size distribution. In addition to these studies, computer simulations of the emulsification process under turbulent flow conditions were carried out by several investigators (Becher and McCann, 1991; Tjaberinga et al., 1993; Lachaise et al., 1995). But, these models are not suitable for predicting the droplet size distributions used in this investigation.

3.2. Experimental Set-up

An apparatus was designed and set-up to carry out *in-situ* size distribution measurements of emulsion droplets as a function of time. A schematic of the experimental set-up which is based on light scattering is given in Figure 3.1. It contained a two-liter vessel of standard geometry (Holland and Chapman, 1966) with four baffles and a turbine type stirrer (Figure 3.2). The agitation speed was maintained constant at 1000 rpm. The vessel was connected to a flow-through cell with a 1/8" tubing. The flow through cell was placed in the light beam path of a light scattering size measurement device, Malvern Model 2600c. An adjustable speed peristaltic pump was used for circulating the solution. A known amount of dodecane was added to the agitated vessel in the form of a pulse input and the time of addition was recorded as the zero time of emulsification. Size distribution measurements were obtained at preset time-intervals. The data acquisition time for each size distribution measurement was about 5 seconds.

Calibration: To confirm that the *in-situ* size distributions obtained using the set-up in Figure 3.1 corresponded to the actual size distribution of the oil droplets in the agitated vessel at that time, the following experiment was conducted. An oil soluble monomer (terephthaloyl chloride, 0.05% by volume based on the amount of oil in the system) was dissolved in the oil phase prior to the experiment. The necessary amount of oil (0.1% by volume) containing the dissolved monomer was added into the agitated vessel. After 16 minutes of agitation, size distribution of the droplets was measured while the solution containing the droplets was passing through the flow-through cell using the light scattering device. As soon as the size measurement was complete, the water soluble monomer (piperazine, 0.05% by volume based on the amount of water in the system) was added to the agitated vessel. Following the addition of piperazine the agitation speed was reduced to 200 rpm, which was enough to keep the droplets suspended but not so intense as to cause further dispersion. Addition of piperazine formed an encapsulating polymeric film around each droplet by reaction of piperazine with terephthaloyl chloride at the oil/water interface, hence effectively freezing the dispersion process. The details of the encapsulation process are given by Mlynek and Resnick (1972). An aliquot of sample

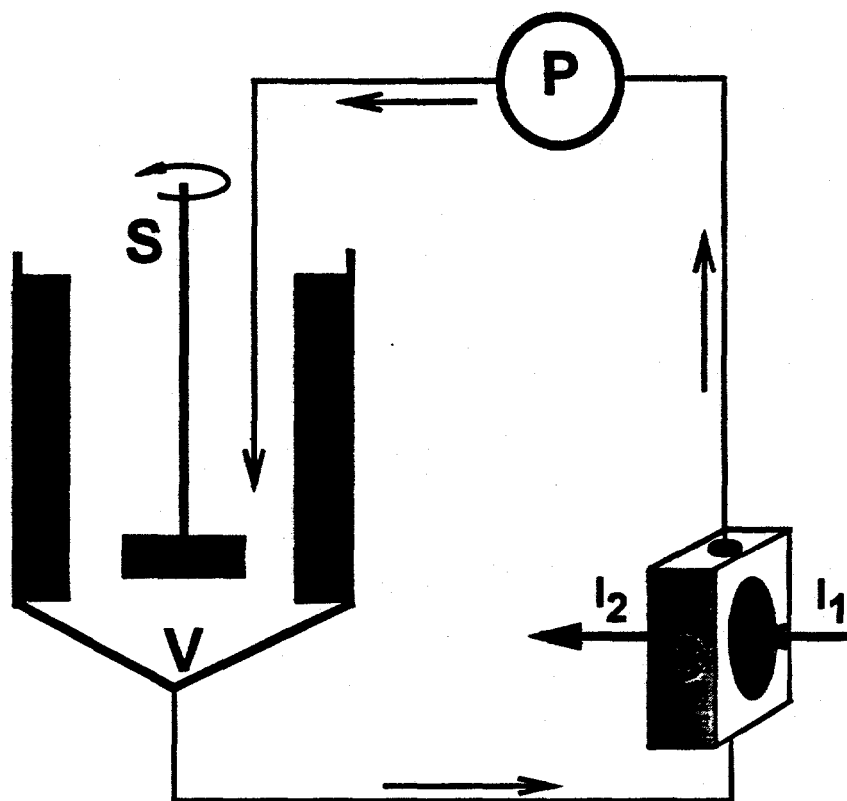


Figure 3.1. Experimental set-up used in the study.

- V:** agitated vessel;
S: stirrer;
C: flow through cell of the size measurement device;
P: peristaltic pump;
I₁, I₂: the lights coming from the laser source and going to the detector respectively.

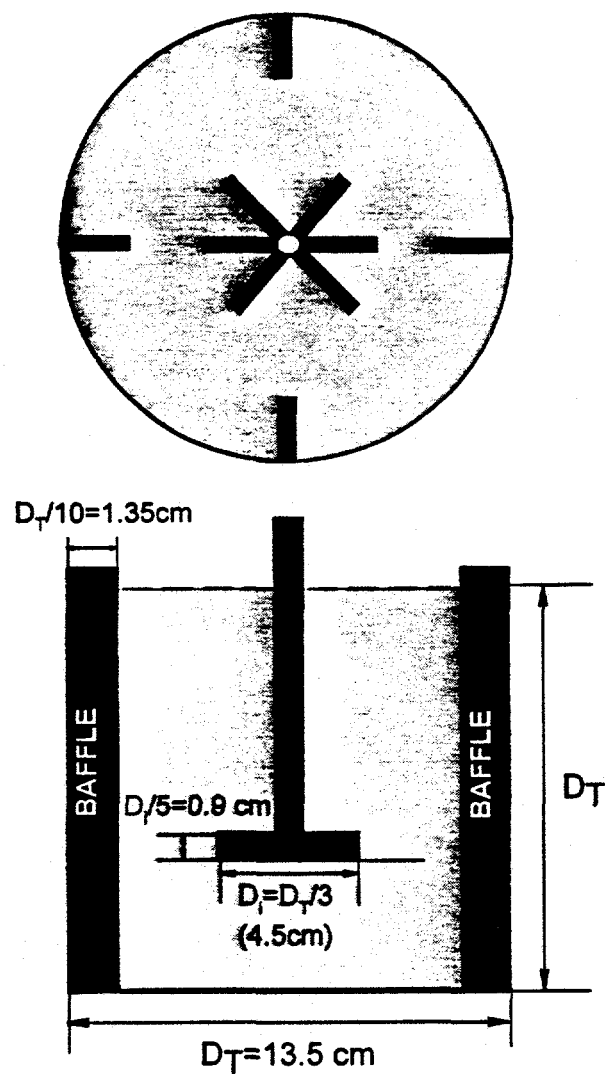


Figure 3.2. A schematic representation of the agitation vessel and the turbine type stirrer used in this study.

taken from the agitated vessel was diluted and transferred into a batch measurement cell with gentle, built-in agitation mechanism. Size distribution of the encapsulated droplets in this batch cell was measured subsequently using the light scattering device. Figure 3.3 gives the two size distributions, one in-situ while the solution containing the actual oil droplets was passing through the flow-through vessel and the other from the batch measurement with the encapsulated oil droplets. The figure shows that the two size distributions are quite similar. This demonstrates that the size distributions which were measured in-situ by the flow through vessel indeed represent the actual size distribution in the agitated vessel.

In the present study, a set-up was designed to carry out *in-situ* size distribution measurements as a function of time using light scattering.

3.3. A Phenomenological Dispersion Model

A phenomenological model for lean dispersion systems was developed to predict the mean droplet size as a function of time. The model allows the kinetics of emulsification to be summarized by two parameters; the mean droplet size after 1 minute of dispersion and a dimensionless breakage rate constant. To determine the parameters of the model, the kinetics of emulsification of oil was investigated in the absence and presence of the block co-polymeric surfactants and the results are discussed in the paragraphs that follow.

The droplet size distributions for the emulsification of 0.1% of dodecane in water are given in Figure 3.4a as a function of agitation time. The normalized size distributions for the same data are presented in Figure 3.4b which demonstrates that the size distributions are self-preserving. Thus, an appropriate droplet size, such as the median droplet size (X_{50}), can be used to represent the changes in the drop size as a function of time. The time dependence of the median droplet size, X_{50} , for the data in Figure 3.4 is given in Figure 3.5.

The emulsification model developed in this study correlates with the median droplet size of oil with the time of dispersion. The model includes two empirical parameters, the median droplet size at 1 minute of dispersion and a dimensionless

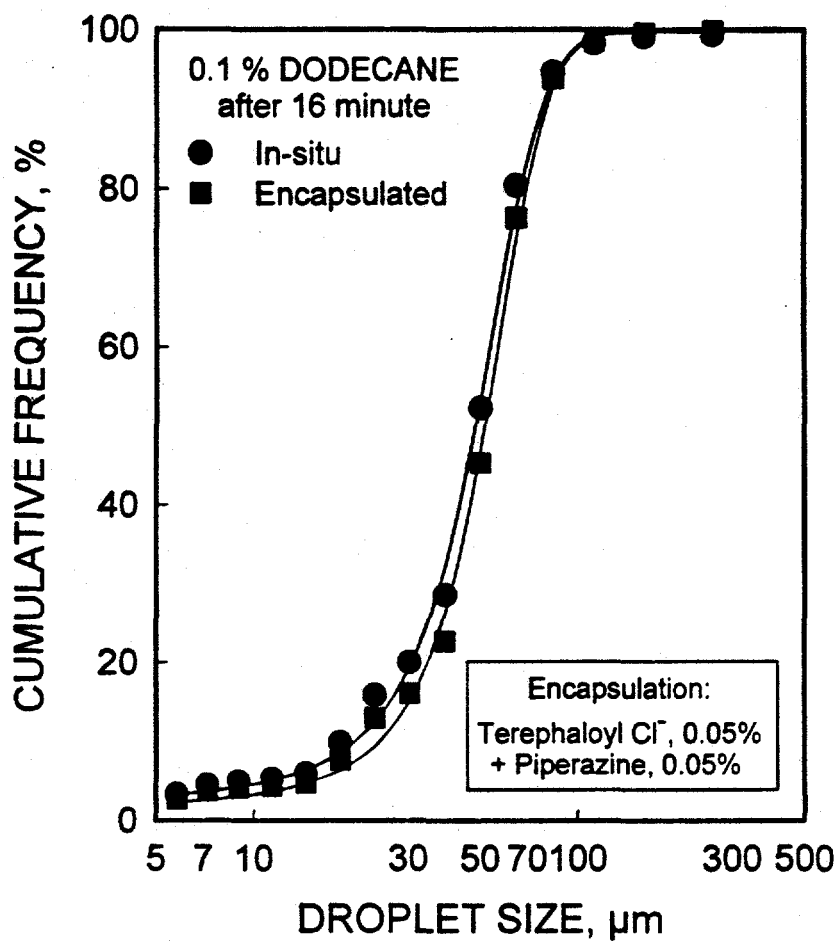


Figure 3:3. The size distribution of oil droplets measured in-situ in the flow through vessel and after encapsulation using piperazine and terephaloyl chloride.

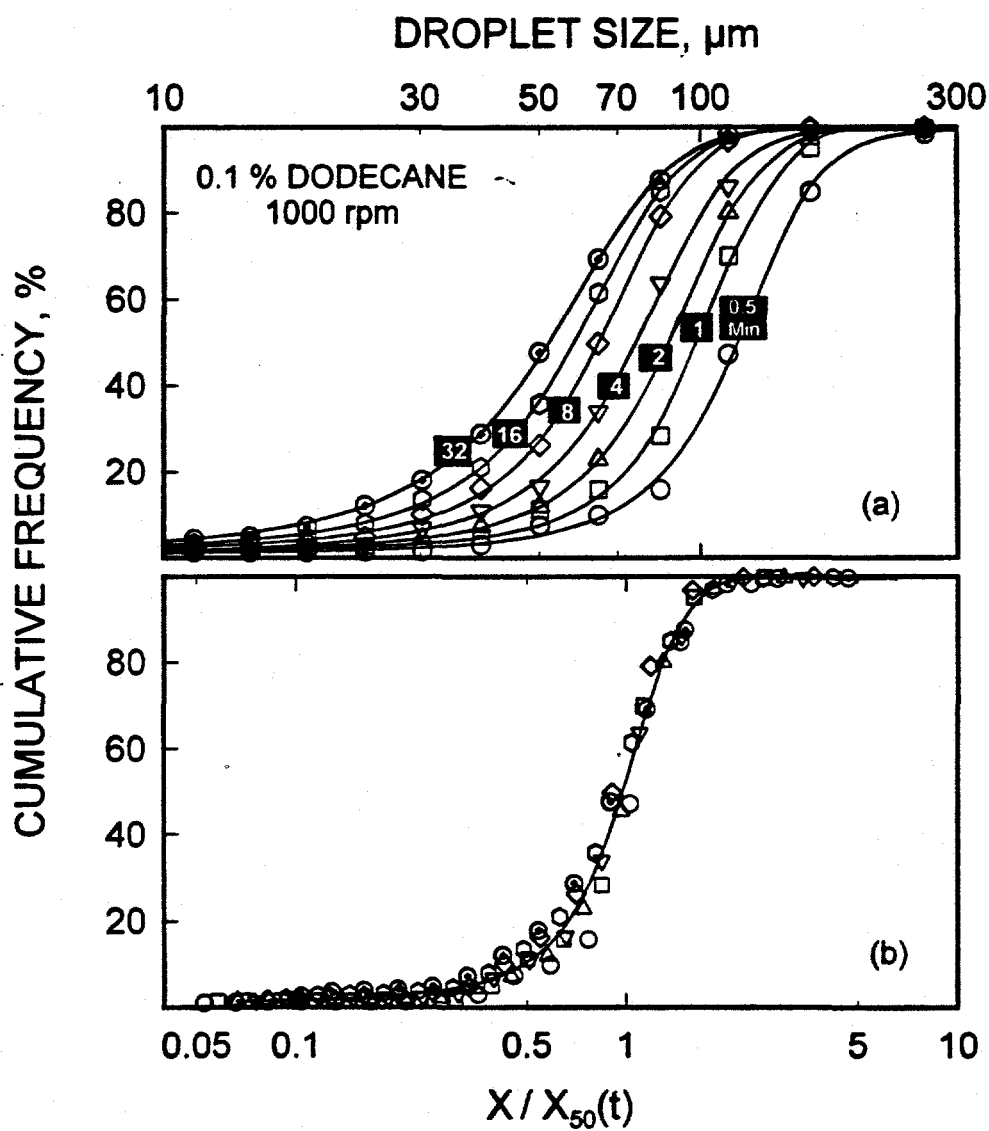


Figure 3.4. a) Size distribution of dodecane droplets in water at various times.
 b) Normalized size distribution of dodecane droplets in water.

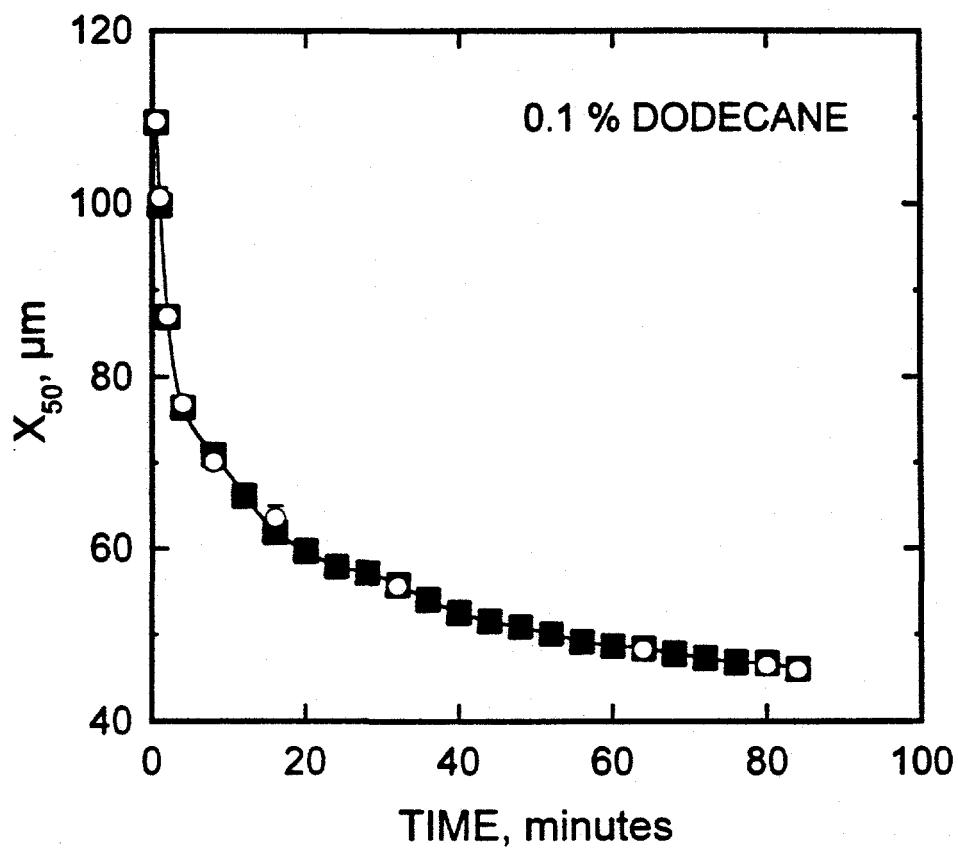


Figure 3.5. Change in the median droplet size, X_{50} , as a function of time of agitation for 0.1 % dodecane.

(Open symbols represent two other measurements and the reproducibility of these measurements).

breakage rate. Expressing the emulsification data using two distinct parameters is of significant value in the evaluation of process kinetics. The model was developed following Hinze [1955] who suggested that breakage of an isolated droplet is determined mainly by the ratio of external and internal stresses acting on such a droplet. The external stress τ is the force per unit surface area and acts in such a way as to cause deformation of the droplet. However, the interfacial tension γ will give rise to a surface force that will counteract the deformation. If X is the diameter of the droplet, the internal stress due to the surface tension force will be of the order of magnitude $[\gamma/X]$. Hinze proposed that the probability of breakage would be related to a generalized Weber number which is defined as the ratio of external and internal stresses such that:

$$We = \frac{\tau X}{\gamma} \quad 3.3$$

Hinze stated that:

" The greater the value of We , that is, the greater the external force τ compared with the counter acting interfacial tension-force γX^{-1} , the greater the deformation. At a critical value $(We)_{crit}$, breakup occurs."

As discussed above, this approach was used by other investigators (Shinnar, 1961; Sprow, 1967; Coualoglou and Tavlarides, 1976,1977; Lagisetty et al., 1986; Koshy et al., 1988) to develop an empirical dispersion model to predict the maximum stable droplet diameter, X_{max} under steady state conditions.

In a standard vessel with 4 baffles and the agitation speed at 1000 rpm the flow regime is turbulent (1000 rpm). In such a system there will be a distribution of eddies (Walstra, 1983) of various sizes which induce the external stresses that lead to deformation of droplets. The efficiency of breakage is a function of both the size of the eddies and the droplets. Glasgow et al. (1985) stated that:

“ clearly, large eddies cannot break small drops and small eddies can not break large drops. Further, so little energy is contained at very small scales that little or no breakage can occur for comparable entity sizes. Thus, a practical limit for particle size reduction in a given system is a length scale on the order of the Kolmogorov(s) microscale (of turbulence)...”.

If the energy input into the dispersion vessel is constant, it is reasonable to assume that the distribution of eddy sizes will be relatively stable, resulting in a time-invariant microscale of turbulence. Nevertheless, the average droplet size will gradually decrease with time. If the microscale of turbulence is comparable to the droplet size, a significant and increasing fraction of droplets with sizes less than the microscale of turbulence will be generated during the dispersion process. In other words, the number of effective eddies, hence the breakage rate, should be expected to decrease as a function of time. Hence, it could be suggested that the rate of change in the droplet size would be inversely proportional to the dispersion time. The functional form, which is not known, could be estimated from actual emulsification experiments. After calculating the Kolmogorov's microscale of turbulence, λ_0 , for the system, one could experimentally determine the fraction of droplets which are finer than λ_0 , $F(\lambda_0, t)$, as a function of time. The functional relationship between breakage rate and the dispersion time could be estimated from a plot of $F(\lambda_0, t)$ versus t . This exercise has been carried out for our system as follows:

By dimensional analysis, Kolmogorov (1949) suggested that the dissipation rate, ε , and kinematic viscosity, ν , can be arranged to give a length-scale for the turbulence, λ_0 , in the system.

$$\lambda_0 = \left(\frac{\nu^3}{\varepsilon} \right)^{\frac{1}{4}} \quad \text{and} \quad \varepsilon = \frac{P}{m} \quad 3.4$$

where ν is the kinematic viscosity, P is the power input into the system and m is the mass of the medium in the tank. Power input is given by:

$$P = N_p D_a^5 N^3 \rho \quad 3.5$$

where N_p is the power number which is a function of the Reynolds number². For the standard four-baffled vessel with a turbine type stirrer operated at 1000 rpm, the flow regime is turbulent, resulting in a Reynolds number of about 10,000. In this region N_p is constant and equal to 4 [Tatterson, 1991]. This results in a power input of about 1.025 watts, which in turn gives a λ_0 value of about 30 μm .

The change in the fraction of droplets which are finer than $\lambda_0 = 30 \mu\text{m}$ as a function of time is given in Figure 3.6. The figure shows that the fraction of droplets that fall below the microscale of turbulence increases linearly with time, with the exception of very short times at which this quantity increases rapidly. This means that the breakage rate will be inversely proportional to the first power of time.

Using the two hypothesis presented above, Hinze's criterion and the inverse relationship between the breakage rate and the time of dispersion, a phenomenological model is proposed. If breakage is dominant, the change in the mean droplet size with time will be proportional to the generalized We defined by Hinze while it will be inversely proportional to dispersion time. That is :

$$\frac{d}{dt} [X_{50}(t)] = -k' \left[\frac{\tau(t) X_{50}(t)}{\gamma} \right] \frac{1}{t} \quad 3.6$$

where $X_{50}(t)$ and $\tau(t)$ are the mean droplet size and the external stress per unit area at time t , respectively. γ is the interfacial tension and k' is a proportionality constant.

Assuming that $\tau(t)$ can be replaced with a time-averaged stress per unit area, τ (Tatterson,

²The Reynolds number for an agitated vessel is given as $Re = \rho D_a v_a \mu^{-1}$ where v_a is the tip speed of the impeller ($v_a = 2\pi r N$ where r is the radius of the impeller) and μ is the viscosity of the continuous medium.

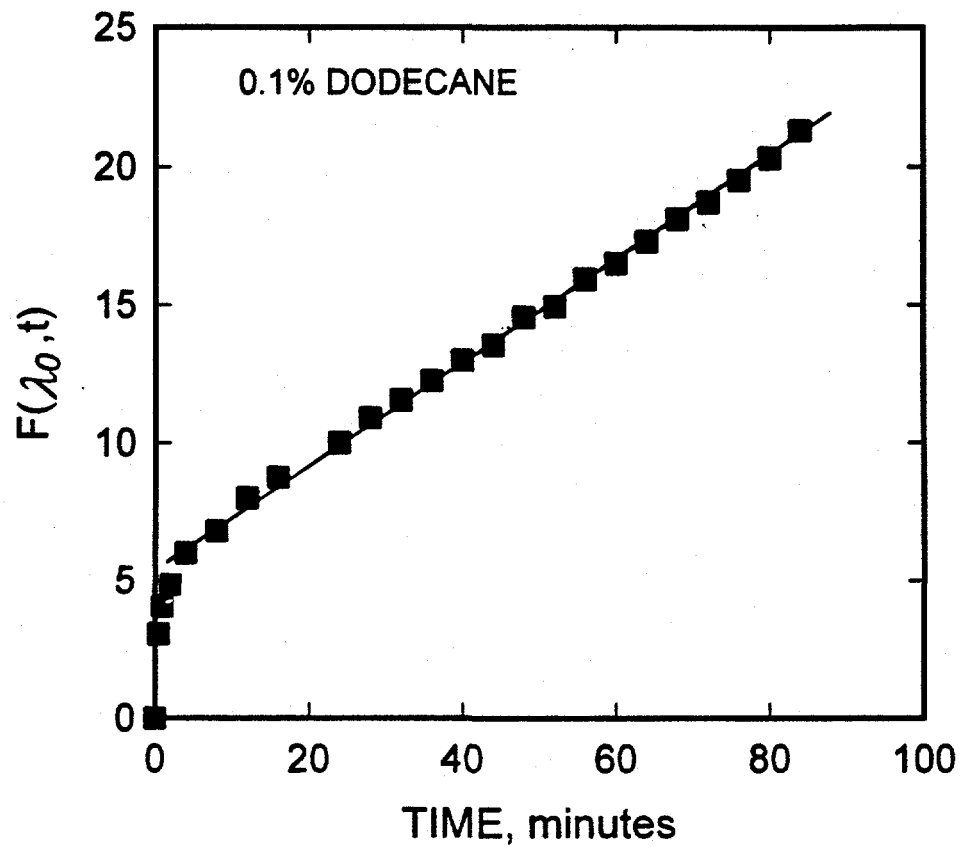


Figure 3.6. A plot of the fraction of droplets that are smaller than λ_0 (Kolmogorov's microscale of turbulence) as a function of agitation time. Dodecane concentration 0.1% by volume.

1991), k' , $\tau(t)$ and γ could be collected as a new, dimensionless constant k . It follows that:

$$\frac{d}{dt}[X_{50}(t)] = -k \frac{X_{50}(t)}{t} \quad 3.7$$

where $k = k' \frac{\tau(t)}{\gamma}$, integration of Equation 3.7 yields:

$$\ln[X_{50}(t)] + \ln(C) = -k \ln(t) \quad 3.8$$

Where C is the constant of integration. Defining $X_{50}(t=1)$ as the mean droplet size at 1 minute of dispersion, one can determine the constant C . Hence,

$$\ln[X_{50}(t)] = \ln[X_{50}(1)] - k \ln(t) \quad 3.9$$

A plot of $\ln[X_{50}(t)]$ versus $\ln(t)$ should result in a straight line with an intercept of $\ln[X_{50}(t=1)]$ and a slope of k . A plot of the emulsification data previously given in Figure 3.5 is presented in Figure 3.7 on a log-log scale as demanded by Equation 3.9. It can be seen that the variation in the mean droplet diameter with agitation time can be represented by a straight line. The model was also applied to the data from Narsinhan et al. (1980). The results are given in Figure 3.8 and demonstrate that their data could also be represented by a straight line in a log-log scale³.

³ The quantity of the parameters, the breakage rate constant $[k]$ and the mean droplet size at one minute dispersion $[x_{50}(t=1)]$, however, can not be compared due to the differences in the variables of two systems (such as impeller type and speed, interfacial tension between dispersed phase and continuous phase, etc.) which determines the quantity of these parameters (see Equation 3.7).

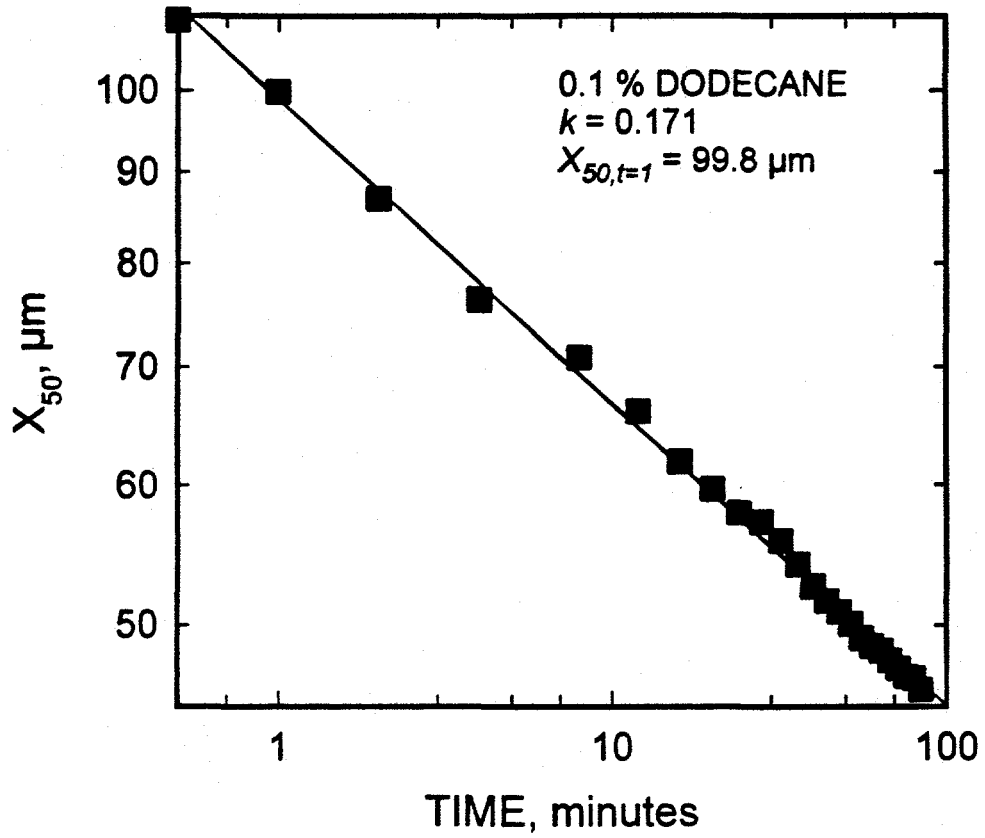


Figure 3.7. The median droplet sizes as a function of agitation time; symbols: experimentally determined; solid line: predicted by Equation 8.

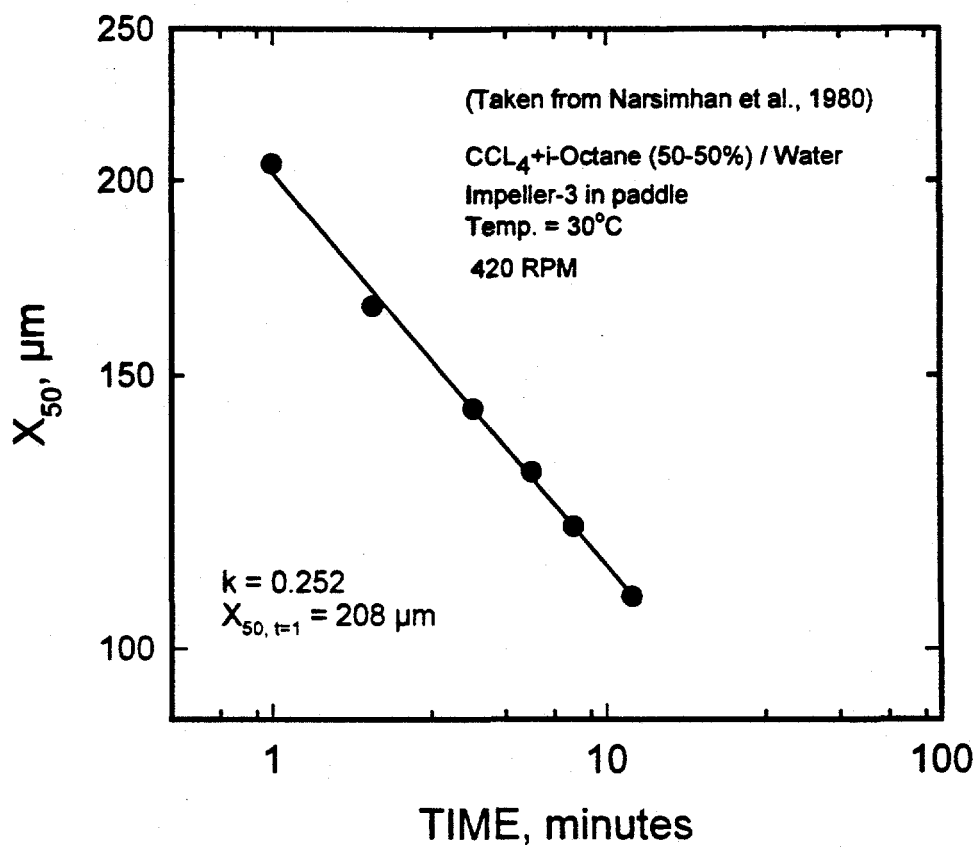


Figure 3.8. The mean droplet sizes as a function of agitation time (data obtained by Narsimhan et al., 1980).

3.4. Effect of Dodecane Concentration

The mean droplet sizes given in Figure 3.7 are for a dodecane concentration of 0.1% by volume. It is known that the dominant process should be dispersion at this low concentration. The model whose main assumption was that the dispersion is the dominant mechanism represents the kinetics data quite well under these conditions. When emulsification was carried out at a dodecane concentration of 1.0 % by volume, the behavior of the system was quite different, however. The median droplet sizes as a function of agitation time are given for 1.0% along with the 0.1% data in Figure 3.9. It can be seen that the model can not represent the high oil concentration data for the entire time scale. However, it is able to show that there is an initial period of about 2 minutes where dispersion is the dominant mechanism as expected, but coalescence becomes significant at longer times. The slope of the curve is different for these two regions; it is high in the dispersion dominated region, resulting in a rapid decrease in the mean droplet size and becomes lower as coalescence increases, resulting in a slower decrease in the mean droplet size.

3.5. Effect of Block co-polymer Concentration and Type

Size distribution studies in the presence of block co-polymers were conducted to investigate the effect of these surfactants on the kinetics of emulsification of dodecane. The results of these studies are discussed in the following paragraphs.

3.5.1. Water soluble PEO/PPO/PEO

Addition of Pluronic L-64 surfactant increased the dispersibility of the oil droplets, resulting in various regions with different emulsification characteristics. The location of these regions along the time axis was a function of surfactant concentration. The results are presented in Figure 3.10. Another block co-polymer with a higher molecular weight, Pluronic P-104, was also tested in this series of tests and the results are given in Figure 3.11. It can be seen that the general behavior is very similar to that of L-64. However, the droplet size obtained for the same concentration was smaller in the case of P-104. This might be due to the difference in the surface activity of these two

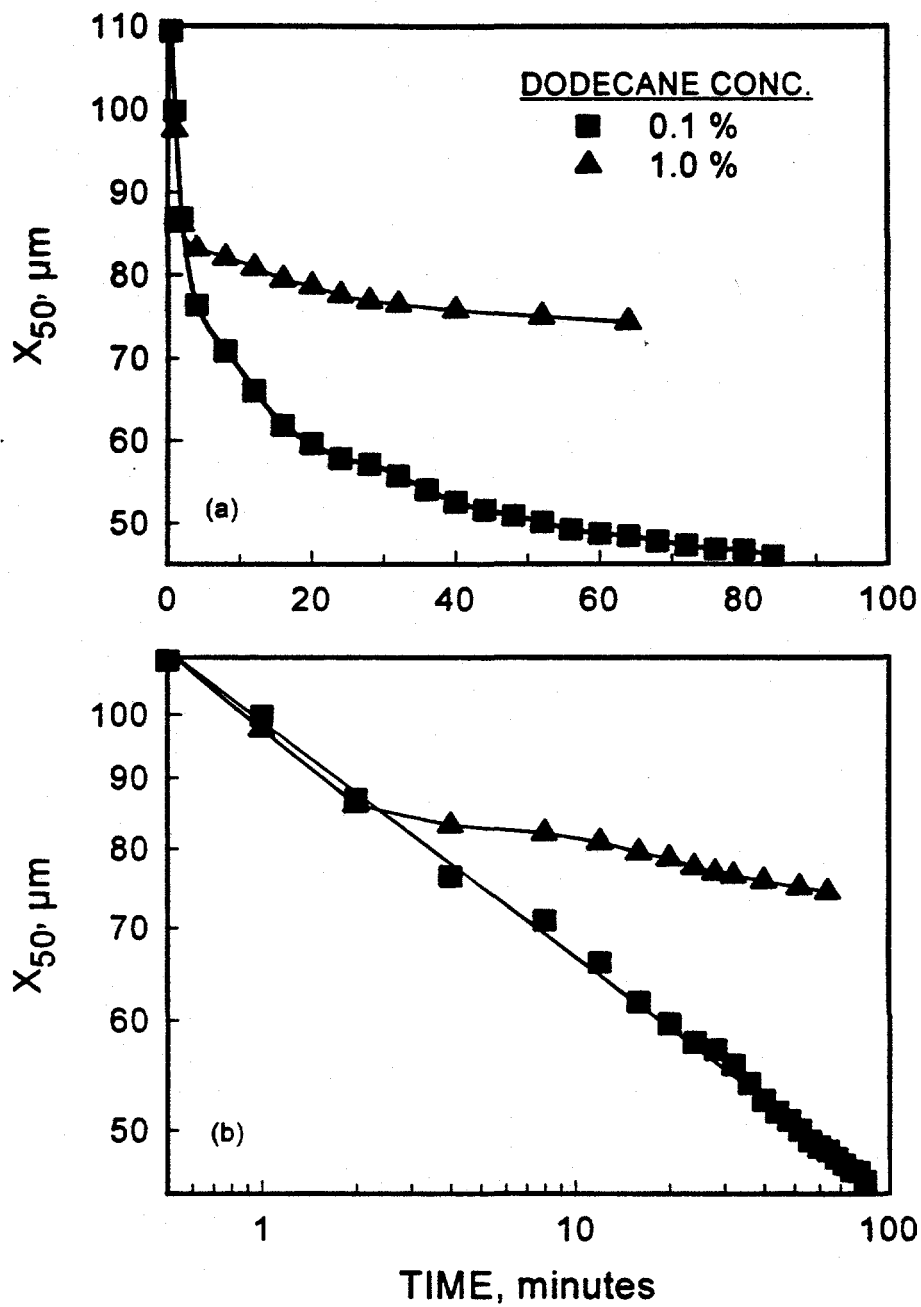


Figure 3.9. Change in the median droplet size as a function of time at dodecane concentrations of 0.1 % and 1.0% by volume. a) in a linear-linear scale, b) in a log-log scale.

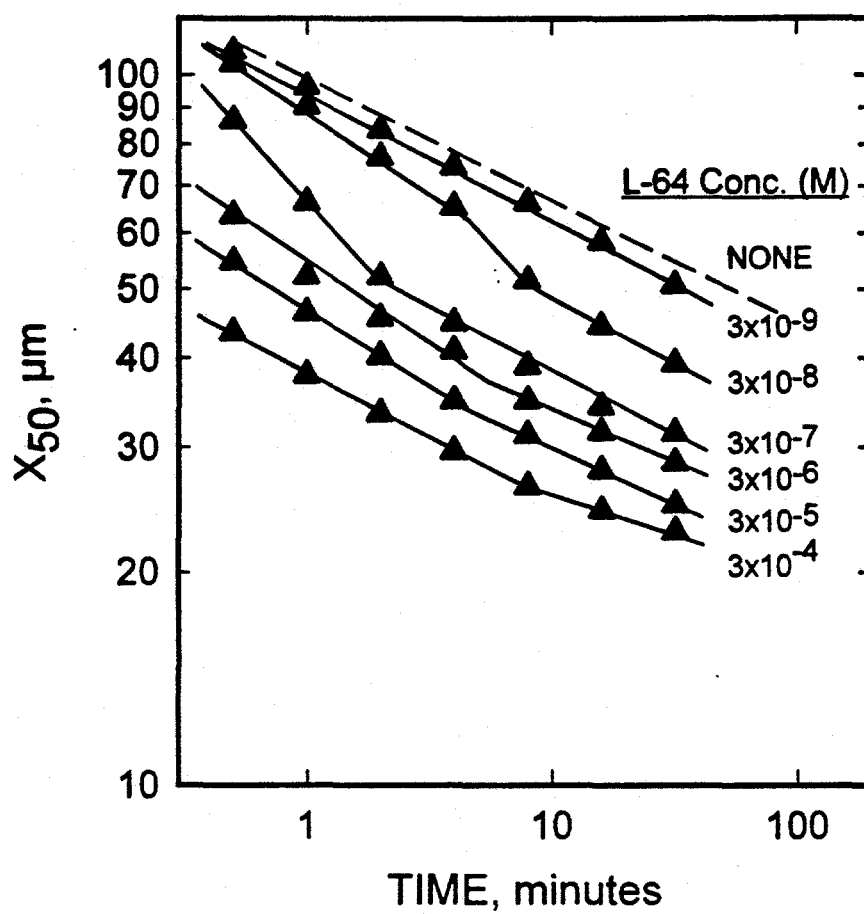


Figure 3.10. Effect of the concentration of Pluronic L-64 on the kinetics of emulsification of dodecane. Amount of dodecane: 0.1% by volume.

block co-polymers. Results in a previous chapter show that the decrease in the surface tension was more for P-104 compared to L-64 for all concentrations below 10^{-6} M.

A conceptual model based on the experimental results discussed above is presented in Figure 3.12 in order to explain the regions observed along the time axis. Some calculations were carried out to provide an estimate of the number of surfactant molecules and the available droplet surface area for adsorption in the system. The results are given in Table 3.1. It can be seen that the droplet surface area available for surfactant adsorption is greater than the area under maximum monolayer coverage for the surfactant concentration, 10^{-8} M, about equal for the concentration of 10^{-6} M and low for the concentration of 10^{-4} M. However, even in this case, the diffusion of molecules from solution to surface becomes a problem with time due to a decrease in the number of surfactant molecules in the bulk. The emulsification behavior could be divided into two distinct regions with different emulsification characteristics. The placement of these regions along the time axis is a function of surfactant concentration and type. These characteristics are discussed in the following paragraphs.

- *Region I*: In this region, there are free surfactant molecules in solution. Therefore the interfacial tension is lowered by the adsorption at the oil/water interface. This will increase the breakage rate as can be seen from large value of the slope of the kinetic curve. (Figure 3.10, 3.11 and 3.12).
- *Region II*: In this region, the breakage rate approaches that of "no surfactant" case. In the case of high surfactant concentrations, Region I might be so short that it can not be detected in the period of time used. For example in the case of 10^{-4} M, only Region II is observed. A lower breakage rate was observed in this region which resulted from a decrease in the number density of the molecules per unit droplet surface area due to constant concentration of the block co-polymer. This was attributed to both the depletion of the reagent from the solution and the decrease in the diffusion rate of molecules from bulk to surface with time (due to decrease in the number of molecules) at low surfactant concentrations. At high concentrations, however, the slow diffusion of molecules may be the main reason for a decrease in

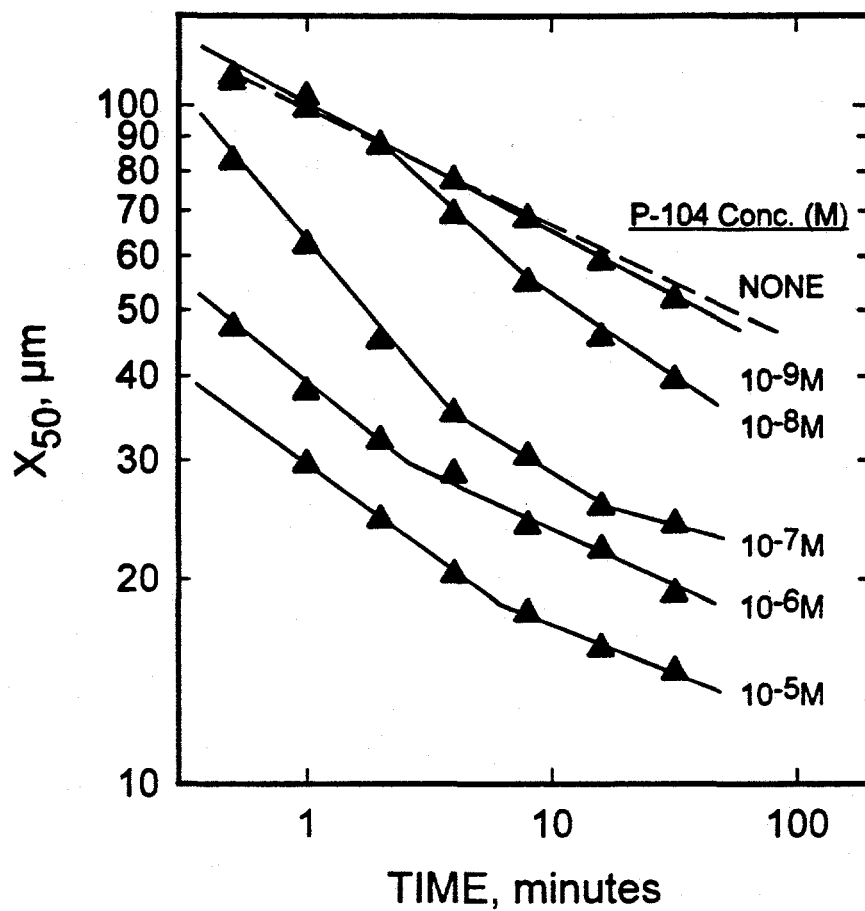


Figure 3.11. Effect of the concentration of Pluronic P-104 on the kinetics of emulsification of dodecane. Amount of dodecane: 0.1 % by volume.

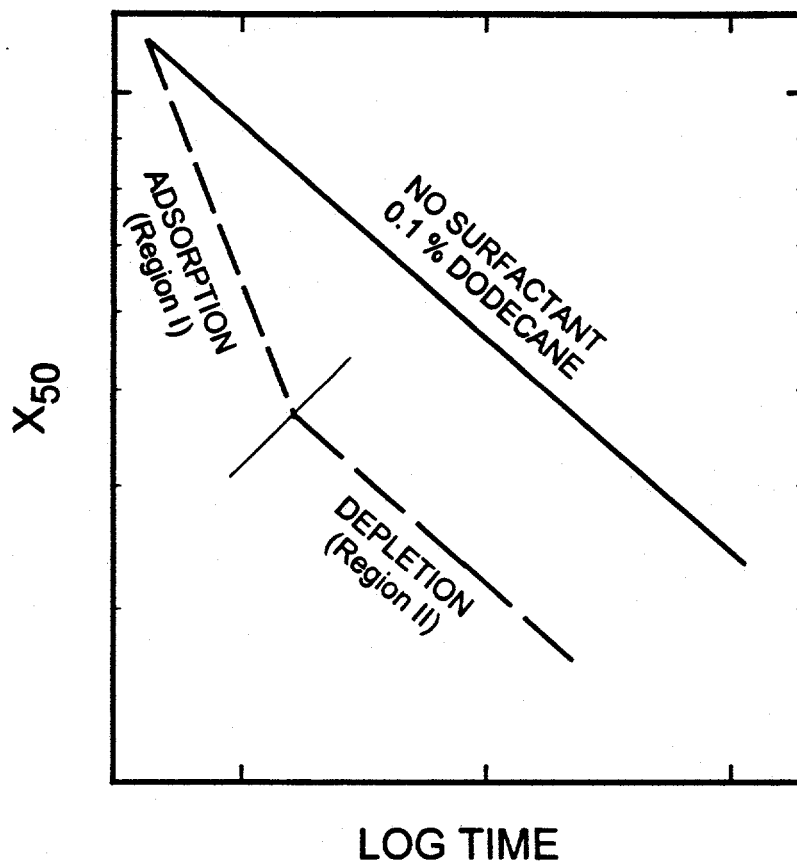


Figure 3.12. A schematic figure to explain the effect of surfactant on the kinetics of emulsification of dodecane.

the number of molecules at surface. A high breakage rate was observed in the first region and is associated with adsorption at oil/water interface.

Table 3.1. The calculated surface area of droplets in the system and the number of molecules at monolayer coverage (Γ_m) as a function of time (assuming a parking area of 1.04 nm^2).

Time min.	Droplet Surface area, 10^3 cm^2			# of Surfactant Molecules at $\Gamma_m, 10^{17}$		
	10^{-8} M	10^{-6} M	10^{-4} M	10^{-8} M	10^{-6} M	10^{-4} M
0.5	2.03	3.93	5.50	1.95	3.78	5.00
1	2.52	4.50	6.21	2.43	4.32	5.97
2	2.76	5.23	6.95	2.66	5.03	6.69
4	3.49	6.10	7.80	3.36	5.87	7.50
8	4.35	6.83	8.59	4.18	6.56	8.26
16	5.34	7.54	9.14	5.13	7.25	8.79
32	6.13	8.18	9.63	5.89	7.87	9.26
Number of molecules in bulk \rightarrow				6.02×10^{15}	6.02×10^{17}	6.02×10^{19}

3.5.2. Oil soluble PPO/PEO/PPO

Addition of an oil soluble PPO/PEO/PPO type block co-polymer, 25R-1, also enhanced the rate of dispersion with increasing concentration. The results are given in Figure 3.13. The presence of different regions along the time axis was also identified in the case of this surfactant. The reagent P-25R1 was more effective in decreasing the droplet size especially at low concentrations. At higher concentration of $3 \times 10^{-5} \text{ M}$, the rate of breakage in the first region is not very different than that of L-64 while it was higher in the second region. But, the droplet size obtained after about 30 minutes of dispersion was still smaller ($19 \mu\text{m}$) in the case of oil soluble surfactant than that of water soluble surfactant ($25 \mu\text{m}$). This was attributed to the difference in their influence on the interfacial tension at oil/water interface. The Pluronic L-64 is less hydrophobic block co-polymer than P-25R-1 and it is expected to be less effective in decreasing interfacial tension.

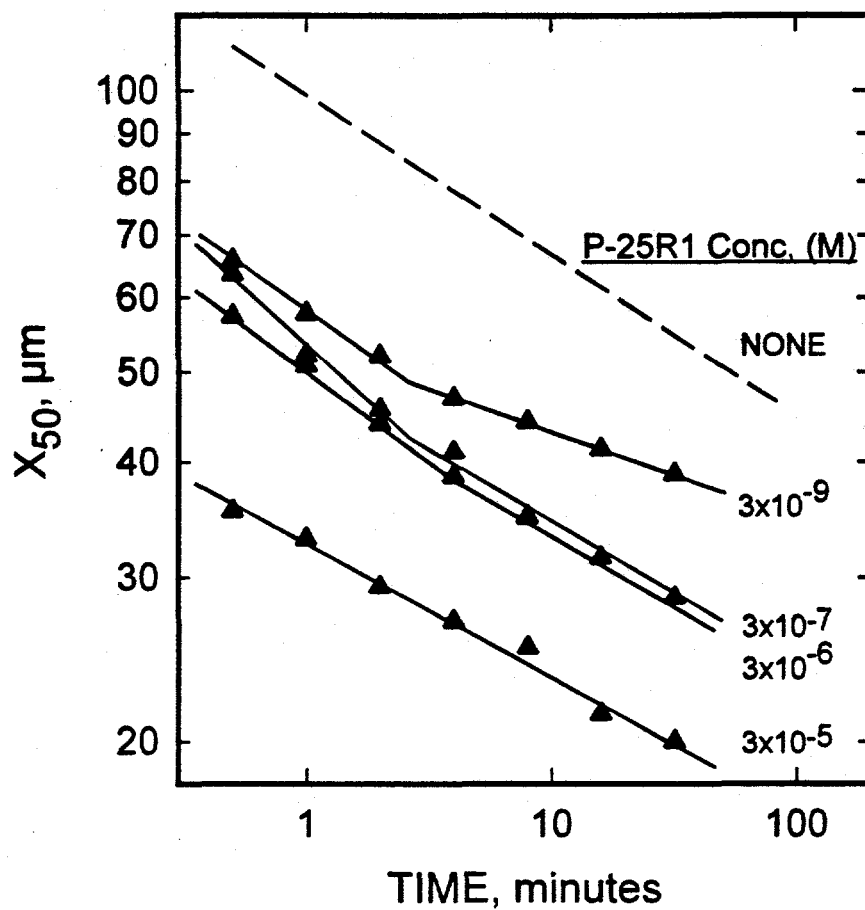


Figure 3.13. Effect of the concentration of Pluronic P-25R1 on the kinetics of emulsification of 0.1 % dodecane.

3.5.3. Effect of Time of Reagent Addition

The effect of the time of surfactant addition was investigated by introducing the block co-polymer (L-64) into the emulsion at different times during dispersion. The results are presented in Figure 3.14. The experiments were designed to investigate the significance of the available droplet surface area for the adsorption of surfactant molecules at the point of surfactant addition. In three separate tests the surfactant was added into the system at different times: a) simultaneously with dodecane, b) after 4 minutes of emulsification and c) after 84 minutes of emulsification. Even though the time of addition resulted in a significant difference in the kinetics of emulsification, it had no effect on the droplet size distribution at long times (after about 150 minutes). That is, whether the surfactant was added simultaneously with oil or after the oil was emulsified, the final state of the system was the same. This observation suggests that the surfactant is completely depleted from solution after sufficient time of emulsification independent of the time of reagent addition. The fact that the droplet size distributions became identical at long times implies that the droplets have similar surface coverage.

3.6. Conclusions

Kinetics of emulsification of oil in the absence and presence of the block co-polymer surfactants was investigated using a specially designed. Based on the studies presented in this chapter, a phenomenological model was proposed to describe drop breakup in an agitated dodecane/water system. The following conclusions were made:

- The emulsification behavior of oil can be described by two empirical parameters, namely, the median droplet size at one minute dispersion, $[X_{50}(t=1)]$, and a breakage rate constant, $[k]$.
- The model fitted the data quite well for dispersed phase concentrations less than 0.1% by volume. At higher oil concentrations (greater than 1.0 % by volume) the contribution of coalescence sub-processes became important. At 1% volume of the dispersed phase, dispersion was dominant at short times, and coalescence became

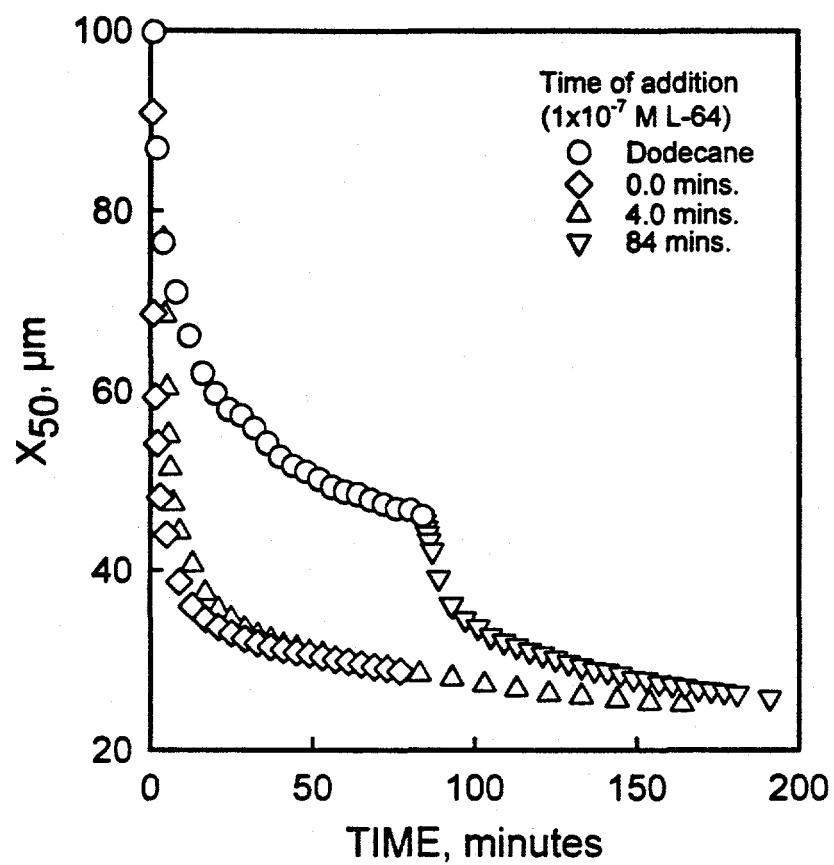


Figure 3.14. Effect of the time of surfactant addition on emulsification of 0.1 % by volume dodecane.

significant at times longer than about 2 minutes, when the number of droplets increased substantially.

- Addition of block co-polymers was found to enhance the dispersion of dodecane at all the concentrations tested. This effect was a function of surfactant type and concentration. At a fixed concentration, the drop size obtained was smaller for the more surface active molecule.
- The presence of the block co-polymers resulted in two distinct regions in the X_{50} vs time plots with different emulsification characteristics. The placement of these regions along the time axis was a function of surfactant type and concentration. A lower breakage rate was observed in the second region which resulted from a decrease in the number density of the molecules per unit droplet surface area due to constant concentration of the block co-polymer. This was attributed to the depletion of the reagent from the solution at low surfactant concentrations and slow diffusion of molecules from bulk to oil/water interface at high surfactant concentrations. A high breakage rate was observed in the first region and is associated with adsorption at oil/water interface.
- The kinetics of emulsification changed considerably when the block co-polymer was added at different times during emulsification (simultaneously with dodecane, 4 minutes and 84 minutes after emulsification of dodecane). However, the droplet size distributions became identical at long times of emulsification (about 150 minutes) in three different tests. At long times the block co-polymer was completely depleted from solution and the rate became similar to that of surfactant free solution.

Chapter 4

WETTING CHARACTERISTICS OF PEO/PPO/PEO BLOCK CO-POLYMERS IN COAL/AIR/WATER AND COAL/DODECANE/WATER SYSTEMS

4.1. Introduction

The PEO/PPO/PEO tri block co-polymers are widely utilized as wetting agents. These polymers adsorb on hydrophobic surfaces through the PPO segment, while the PEO segments interact with water molecules (Kayes and Rawlings, 1979). The wetting tendency usually increases with the number of ethylene oxide groups in the structure of the surfactant (Nevolin et al., 1963; Schmolka, 1967; Chander et al, 1987). However, in studies with ethoxylated octyl phenols, Chander et al. (1987) observed that the hydrophobicity of coal increased at lower surfactant concentrations (usually below 10^{-6} M) while it decreased at higher surfactant concentrations as expected. An effort was made in this investigation to exploit this behavior to enhance coal cleaning.

The wetting characteristics of coal in the presence of various block co-polymers were investigated in coal/air/water and coal/dodecane/water systems using a modified contact angle measurement technique. With this technique, about 10 readings per square cm of substrate were made to obtain the distribution of contact angle. The effect of such variables as reagent concentration, the HLB value and the molecular weight of these surfactants on the wettability of coals of different rank was studied. The results are presented in the following paragraphs.

4.2. Contact Angle Studies in the Presence of Block Co-polymers

4.2.1. Coal /Air/Water/ System

To determine the wettability characteristics of coal by block co-polymers as a function of concentration, four sets of contact angle studies were carried out with co-polymers of different molecular characteristics. First, contact angle distributions on a Pittsburgh coal sample were obtained in distilled water to establish the base line for determining the effect of surfactant. Second, the effect of surfactant (L-64) concentration

was studied. Third, the fraction of the hydrophilic ethylene oxide group was varied from 20% to 50% to determine the effect of HLB. Fourth, the fraction of the EO groups was fixed at 40% and the molecular weight of surfactant was varied between 2250 and 5900 to determine the effect of molecular weight.

Effect of Block Co-polymer Concentration. The reproducibility of contact angle measurements was determined by conducting replicate tests in the absence of surfactant with the Pittsburgh coal as substrate. The results are given in Figure 4.1 for four different tests. It can be seen that a normal probability function with a mean contact angle, θ_m , of 47.3° and standard deviation, θ_σ , of 3.3 could be used to approximate all the four distributions. Addition of a block co-polymer, L-64, changed the distribution of contact angles significantly (Figure 4.2). The mean contact angle value increased gradually from 47.3° to 57.5° with the addition of surfactant up to a concentration of about 3×10^{-7} M, which was the concentration where a maximum in the contact angle was observed for all the block co-polymers tested. The standard deviation first decreased from 3.3 in distilled water to 2.5 at a surfactant concentration of 3×10^{-9} M. It increased to 3.8 with further increase in concentration to 3×10^{-8} M. The distribution became narrow again as the concentration was further increased to 3×10^{-7} and 3×10^{-6} M. The contact angle was reduced to zero when the concentration exceeded 3×10^{-5} M. This concentration corresponds to transition Region II in the surface tension results (see Chapter 2). The magnitude of θ_m and θ_σ varied depending on the type of surfactant. The decrease in contact angle coincides with the critical wetting concentration of these polymers (Mohal, 1988).

The increase in the standard deviation at low concentrations was attributed to local adsorption of surfactant was expected due to heterogeneity of coal surface. The results show the surface became more homogeneous in the presence of small amounts of the surfactant. The increase in the contact angle is proposed to result from preferential coverage of the hydrophilic sites on the coal surface. To substantiate this hypothesis and to establish an adsorption mechanism additional studies were conducted using polymers

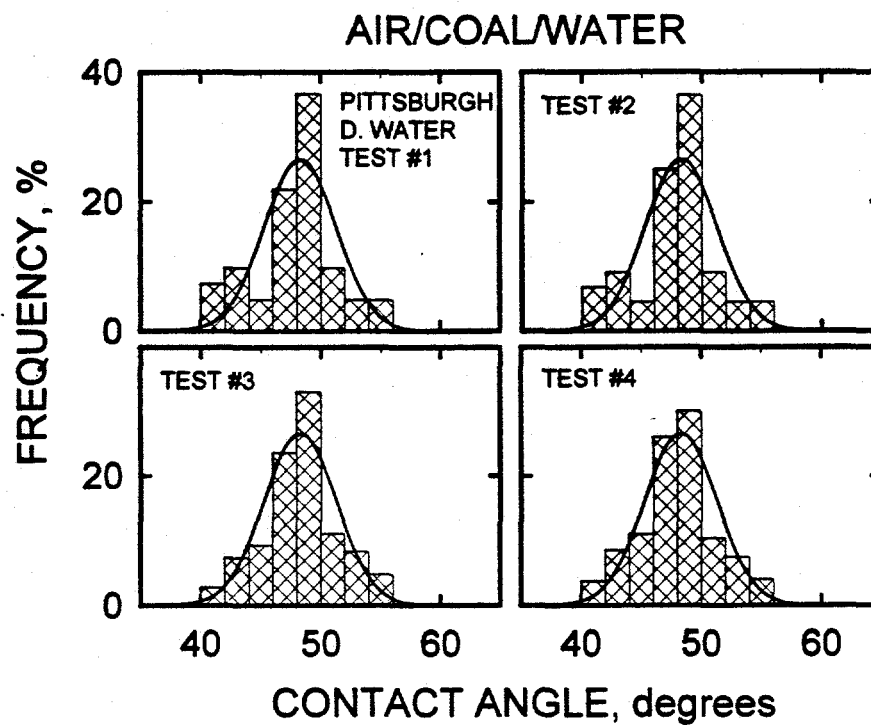


Figure 4.1. Contact angle of Pittsburgh Seam sample in distilled water. Test #1, Test #2, Test #3 and Test #4 are replicate measurements.

(The normal distribution curves super-imposed on the histograms are identical with a mean and standard deviation of 47.3 and 3.3 degrees, respectively)

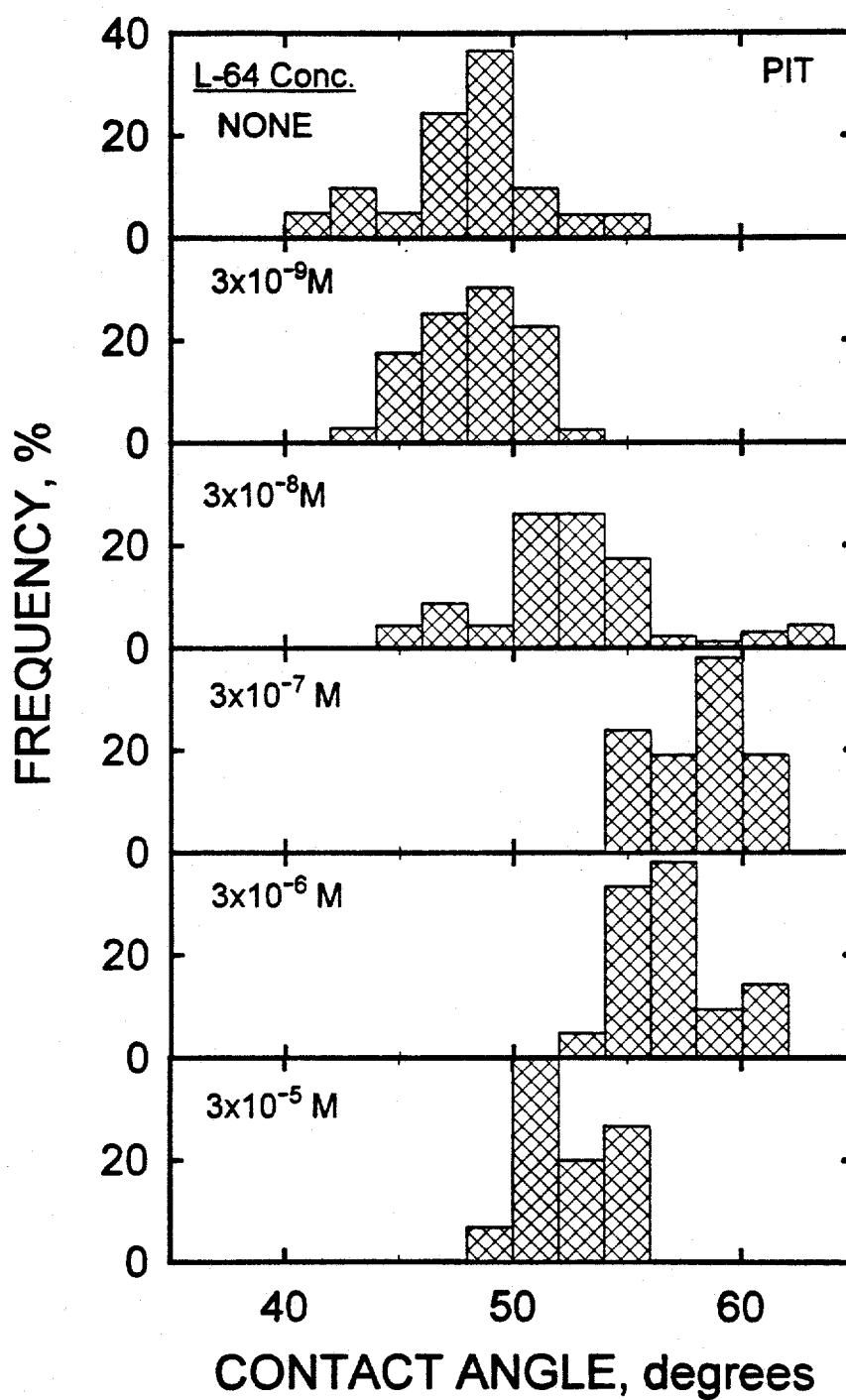


Figure 4.2. Change in the contact angle distribution of Pittsburgh Seam sample (PIT) as a function of L-64 concentration.

with different molecular weights and HLB. The results are discussed in the following sections.

Effect of Ethylene Oxide Groups. To determine the effect of the ethylene oxide group on the contact angle of the coal, 105 Pluronic surfactants L-62, L-63, L-64, P-65 and P-103, P-104, P- were tested. The results of these studies are presented in Figures 4.3 and 4.4 in terms of mean contact angle values as a function of surfactant concentration for the two series of polymers, Pluronic 60- and 100-series respectively. Standard deviations of the contact angle distributions are given in the right margins. The results show a nonlinear relationship between the contact angle and the size of the hydrophilic group. Pluronic L-64 and Pluronic P-104 with an ethylene oxide fraction of 40% were found to be the most effective surfactants in increasing the contact angle of coal within the 60 and 100 series of these surfactants, respectively. This suggests that there is an optimum propylene oxide/ethylene oxide ratio which renders the surface more hydrophobic.

Effect of Molecular Weight. The contact angles observed with the three Pluronic surfactants containing 40% EO fraction and molecular weights of 2200, 2900 and 5900 g/mole (L-44, L-64 and P-104 respectively), are given in Figure 4.5. A comparison of the data for the three surfactants shows that the surfactants Pluronic L-64 and P-104 increased the contact and concentration in the range of 10^{-8} to 10^{-6} . The contact angle reached its maximum value of 55.5° in this range. This might be due to a better coverage of the hydrophilic sites of the surface by the large molecules of this surfactant, even at lower concentrations. The surfactant with the smaller molecular weight, Pluronic L-44, increased the contact angle only slightly, from 47 to 51° .

Contact Angle and HLB Value. The maximum value of the contact angle is plotted in Figure 4.6 as a function of the HLB value of the surfactant. For the homologous series of block co-polymers that were tested, the mean contact angle first increased and then decreased with increase in HLB. The standard deviations of the contact angle distributions are also given, as error bars. The effect of HLB is considered to be statistically significant because the change in contact angle is much larger than the

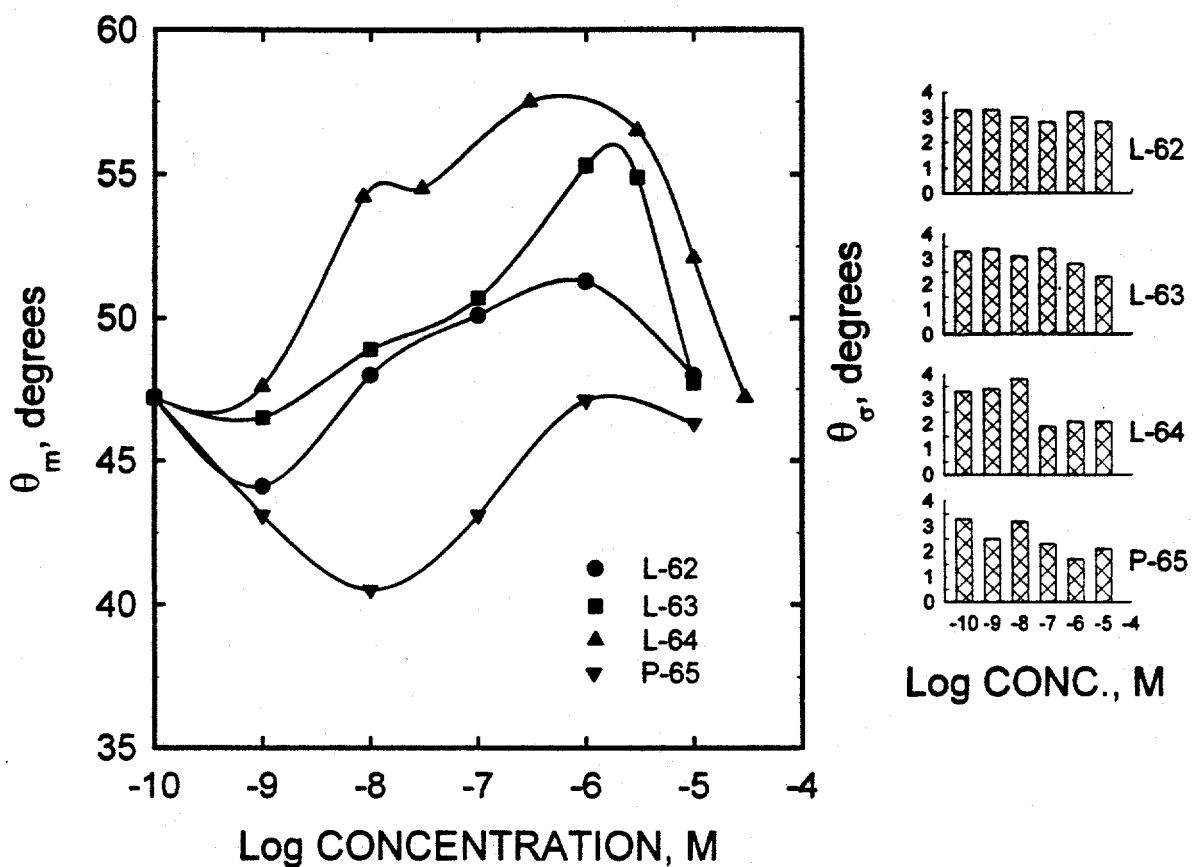


Figure 4.3. Effect of ethylene oxide fraction of PEO/PPO/PEO triblock co-polymer on the mean contact angle of Pittsburgh Seam sample as a function of Pluronic-60 series.

θ_m : Mean Contact Angle, θ_σ : Standard deviation of contact angles about the mean.

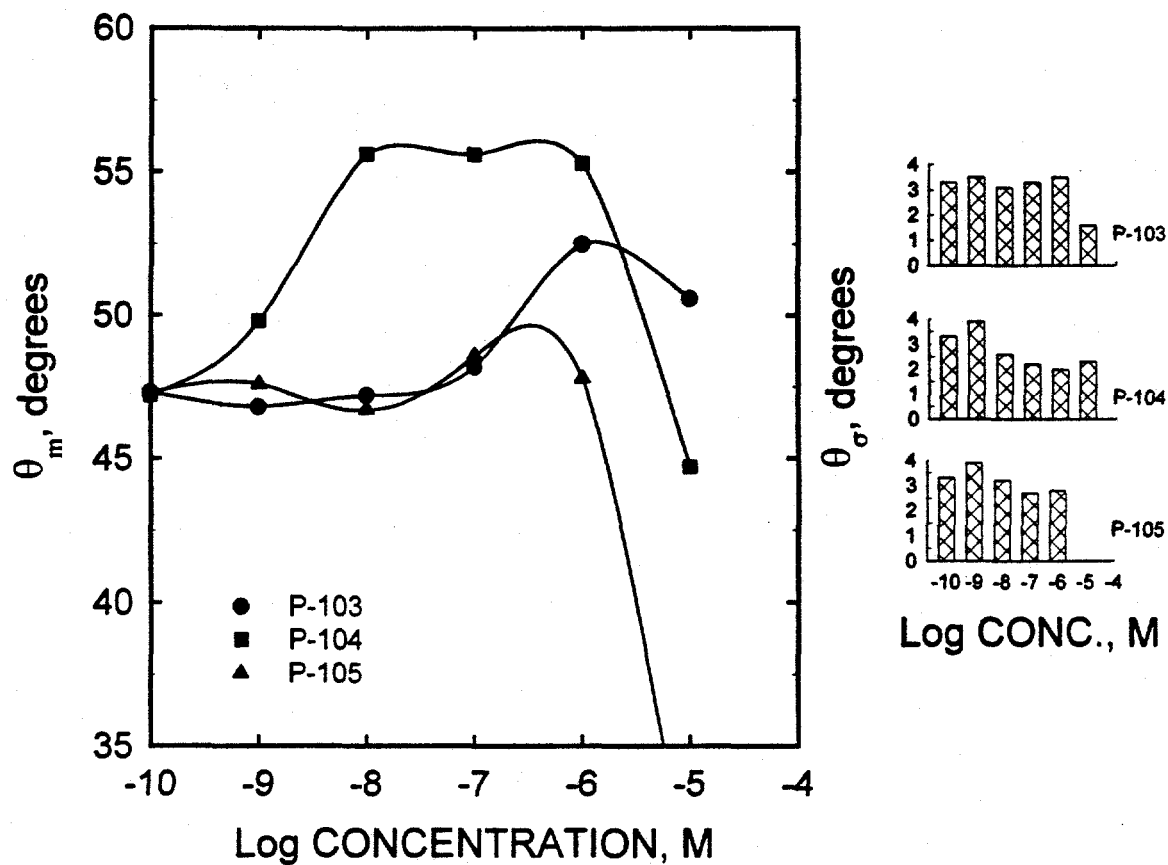


Figure 4.4. Effect of ethylene oxide fraction of PEO/PPO/PEO triblock co-polymer on the mean contact angle of Pittsburgh Seam sample as a function of Pluronic-100 series.

θ_m : Mean contact angle, θ_σ : Standard deviation of contact angles about the mean.

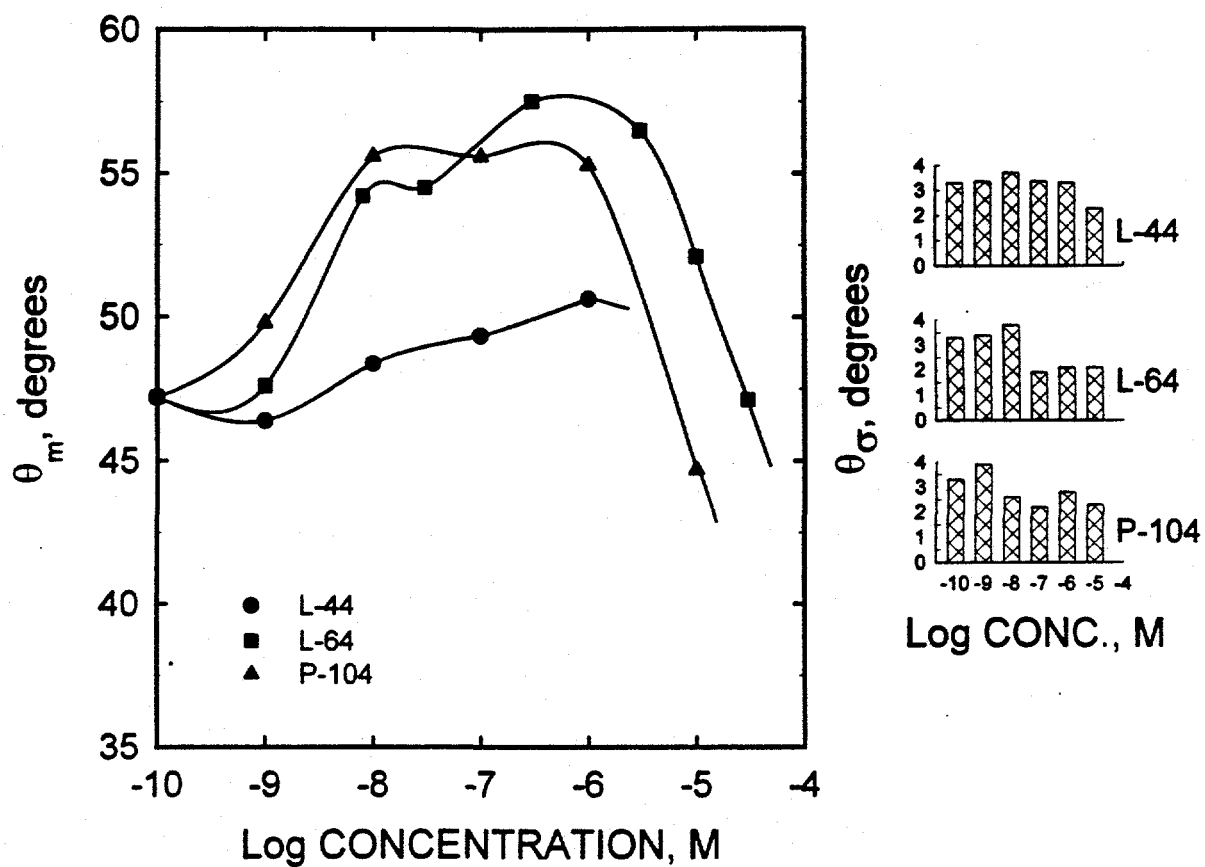


Figure 4.5. Effect of molecular weight of the PEO/PPO/PPO triblock co-polymers on the mean contact angle of Pittsburgh Seam sample.

θ_m : Mean contact angle, θ_σ : Standard deviation of contact angles about the mean.

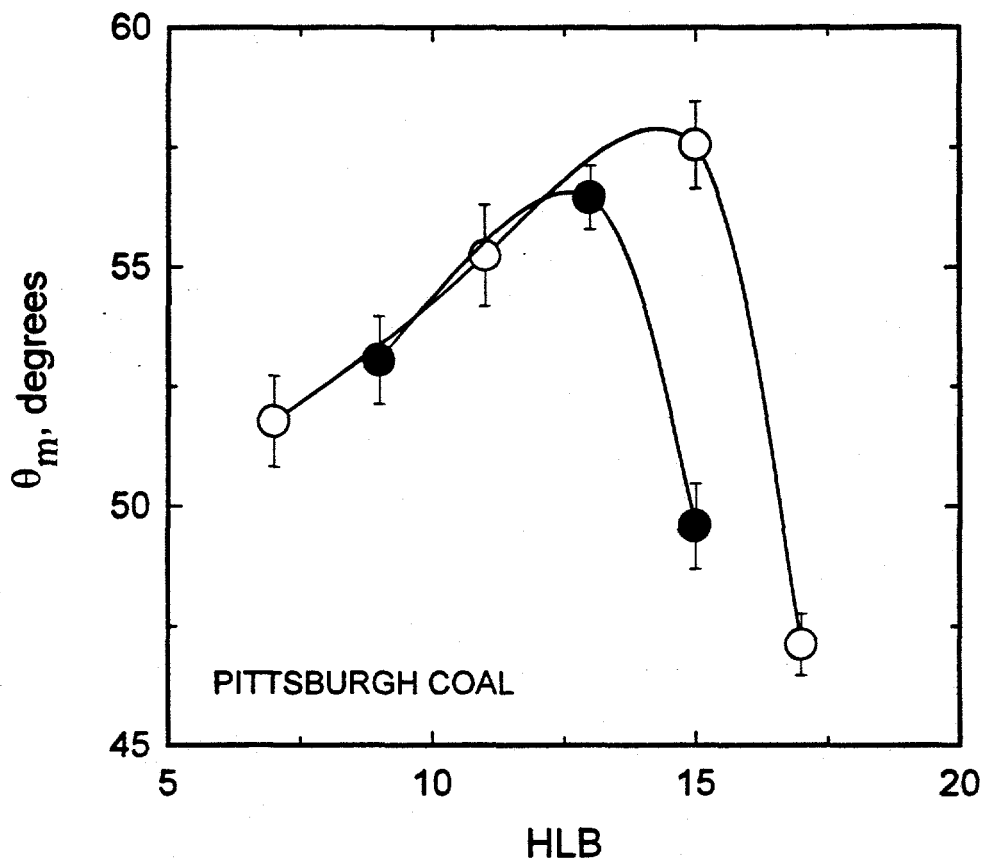


Figure 4.6. Effect of HLB value of the PEO/PPO/PPO triblock co-polymers on contact angle of Pittsburgh Seam sample for two series of Pluronic surfactants; ● : 60-series; ○ : 100-series. θ_m : Mean contact angle.

standard deviation. The optimum HLB value was found to be 13 and 15 for the 60- and the 100-series of Pluronic surfactants. The results demonstrate the importance of the hydrophilic part of the surfactant in increasing the hydrophobicity of coal. A critical number of ethylene oxide groups seem to be necessary for the adsorption of these co-polymers on the coal surface to render it more hydrophobic. From the results one may consider that adsorption occurs at the hydrophilic sites on the coal surface, probably involving hydrogen bonding.

Effect of Coal Type. Four coal samples, differing in rank, namely, coals from the Pittsburgh, Upper Freeport, Lower Kittanning and Illinois No.6 Seams, were studied to determine the effect of coal type on the contact angle distributions. The results are presented in Figures 4.7 and 4.8. In the absence of surfactant, the Pittsburgh and Lower Kittanning coal samples gave narrower contact angle distributions compared to the Upper Freeport and Illinois No.6 coal samples, suggesting a more homogeneous surface. The effects of surfactant on the contact angle distributions were found to be different for different type of coals. The behavior of the Illinois No.6 coal was different from the other coals. This coal contained a relatively large fraction of surface with zero contact angle. This was attributed to the presence of oxidized areas on the surface of this medium rank coal. With increase in surfactant concentration the fraction of the hydrophilic areas first increased then decreased. The results confirm the hypothesis that adsorption of these reagents is site specific.

Contact Angles in the Presence of Triton X-100 and Aerosol-OT. A limited number of measurements was carried out with two different types of surfactants, Triton X-100 and Aerosol-OT to compare the effectiveness of block co-polymers in making coal more hydrophobic. These two surfactants were selected because of their wide use in the wetting of coal and emulsification of oil. The results are presented in Figure 4.9 along with those obtained with L-64 block co-polymer. Since no contact was obtained with Aerosol-OT, the results for this surfactant are excluded from the figure. A non-zero contact angle whose magnitude was a function of surfactant concentration was obtained

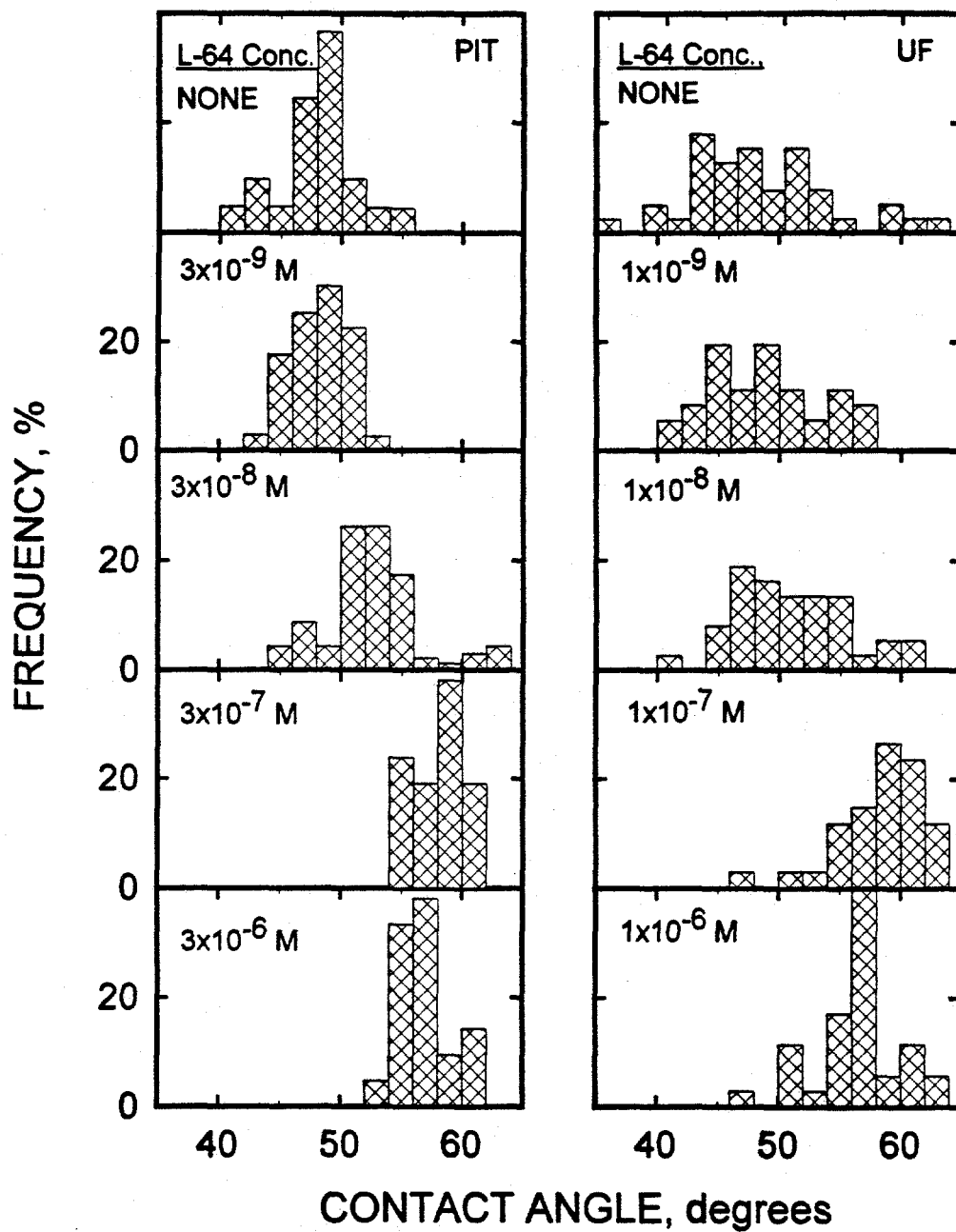


Figure 4.7. Change in the contact angle distribution of Pittsburgh (PIT) and Upper Freeport (UF) coal samples as a function of L-64 concentration.

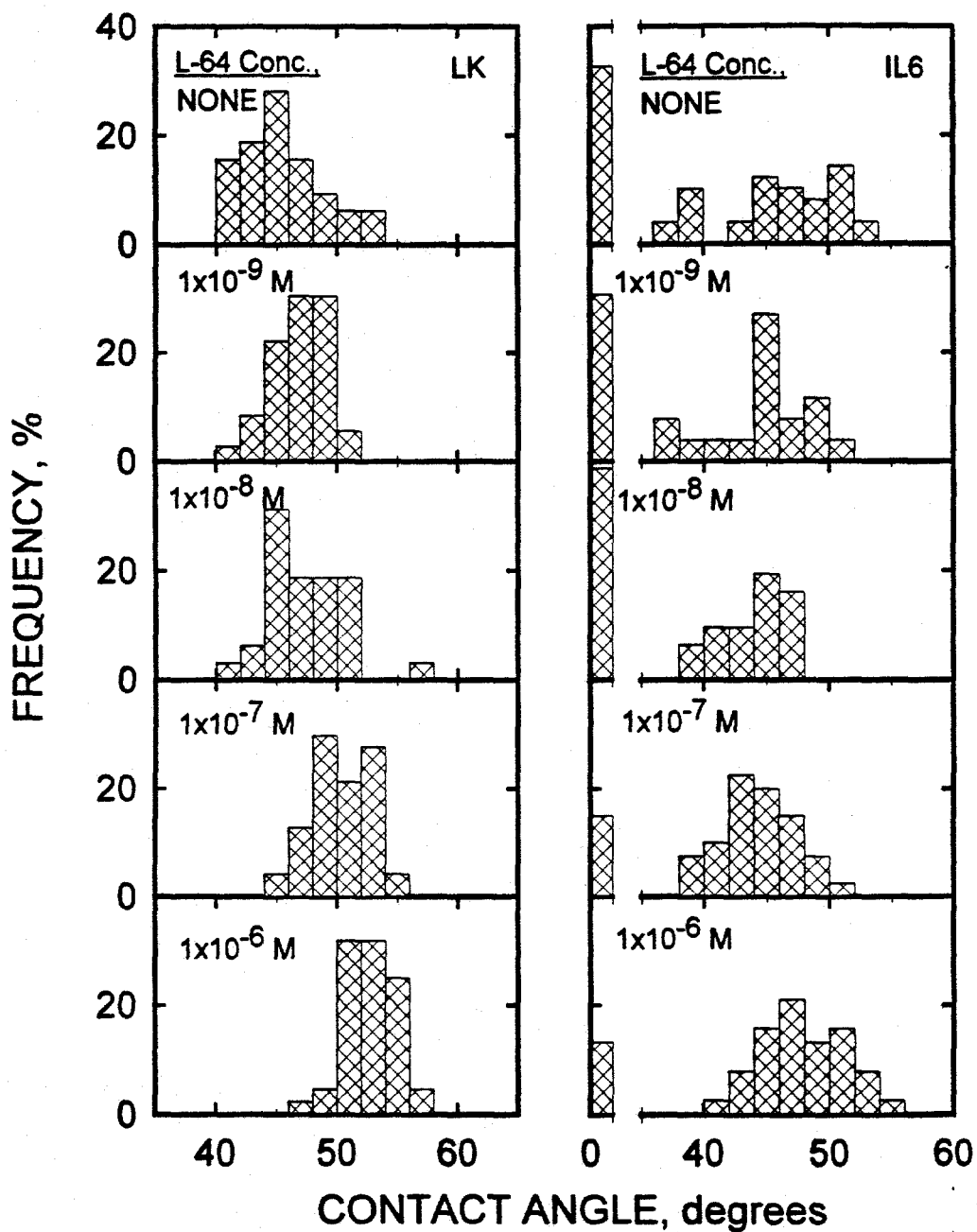


Figure 4.8. Change in the contact angle distribution of Lower Kittanning (LK) and Illinois No.6 (IL6) coal samples as a function of L-64 concentration.

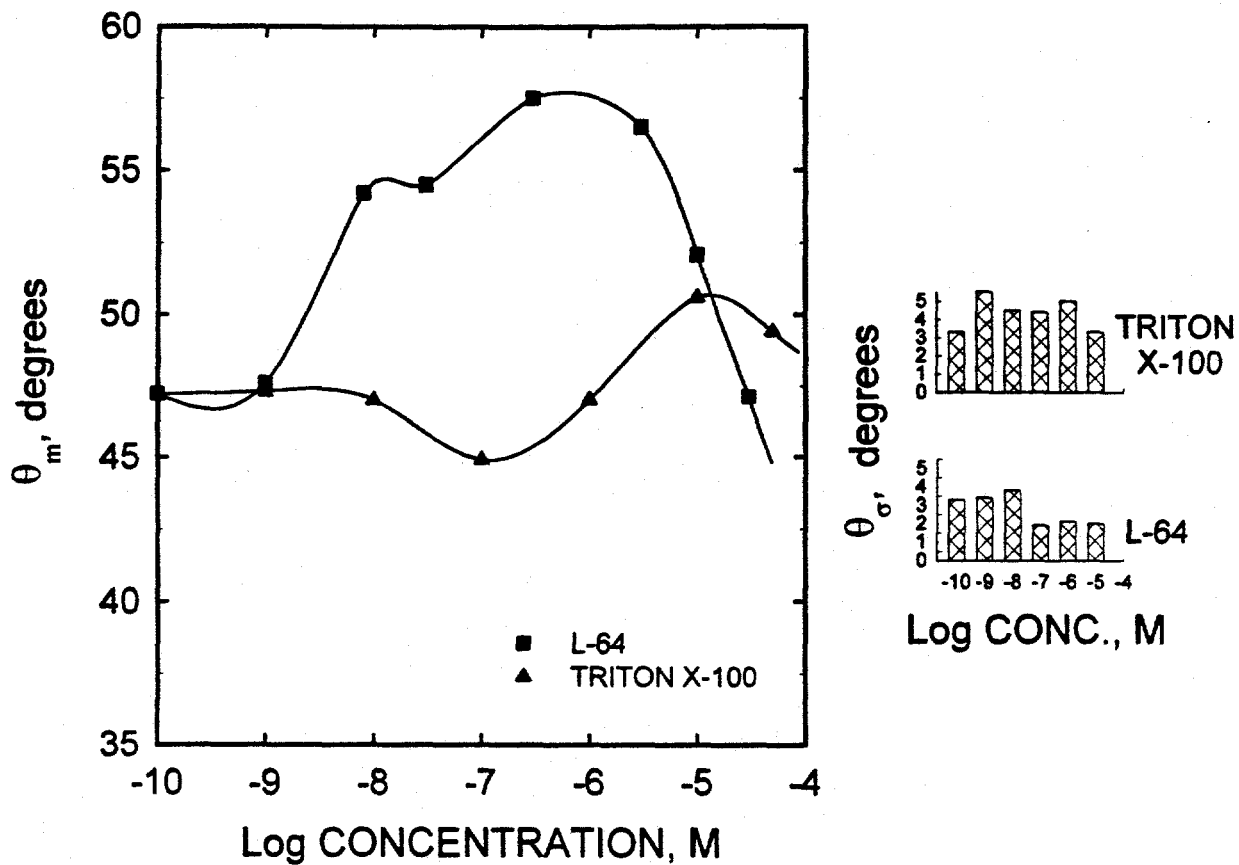


Figure 4.9. A comparison between the mean contact angles of Pittsburgh Seam sample as a function of L-64 and Triton X-100 concentration.

θ_m : Mean contact angle, θ_σ : Standard deviation of contact angles about the mean.

in the case of Triton X-100. It was observed that the contact angle values obtained in the presence of L-64 were much larger compared to Triton X-100 at concentrations below about 10^{-5} M demonstrating superior performance of this class of reagents.

4.2.2. Coal/Dodecane/Water System

The contact angle of a drop of dodecane on coal immersed in water was measured in the absence and presence of L-64 surfactant. The concentration selected for this test was 10^{-7} M where a maximum in the mean contact angle was obtained in the coal/air/water system for this surfactant. The results are presented in Figure 4.10. For comparison, the results for the coal/air/water system are included. Since the wetting characteristics of an air bubble and oil droplet will be different, the actual magnitudes of the contact angles can not be directly compared. However, there are some similarities between the two sets of data. The addition of surfactant increased the average contact angle by about 10 degrees in both cases. However, the contact angle distribution was broader with dodecane possibly due to differences in sites at which adsorption occurs in the two cases.

4.3. Adsorption of Block Co-polymers on Solid/Liquid Interface

Very little information is available on adsorption of block co-polymers on coal surfaces. Since coal is a heterogeneous substance consisting of surfaces with different properties, a brief review of adsorption on selected solids is presented in the following paragraphs.

4.3.1. Pure Hydrophobic and Hydrophilic Surfaces

Based on their ellipsometry measurements Kayes and Rawlings, (1979) proposed that the adsorption of PEO/PPO triblock co-polymers onto polystyrene latex particles followed a Langmuirian model. These polymers were suggested to be adhering to the latex with their hydrophobic PPO segments while the PEO groups extended into the solution as tails. The thickness of the adsorbed layer depended on the molar mass of the PEO groups and bulk polymer concentration. Several investigators have proposed that

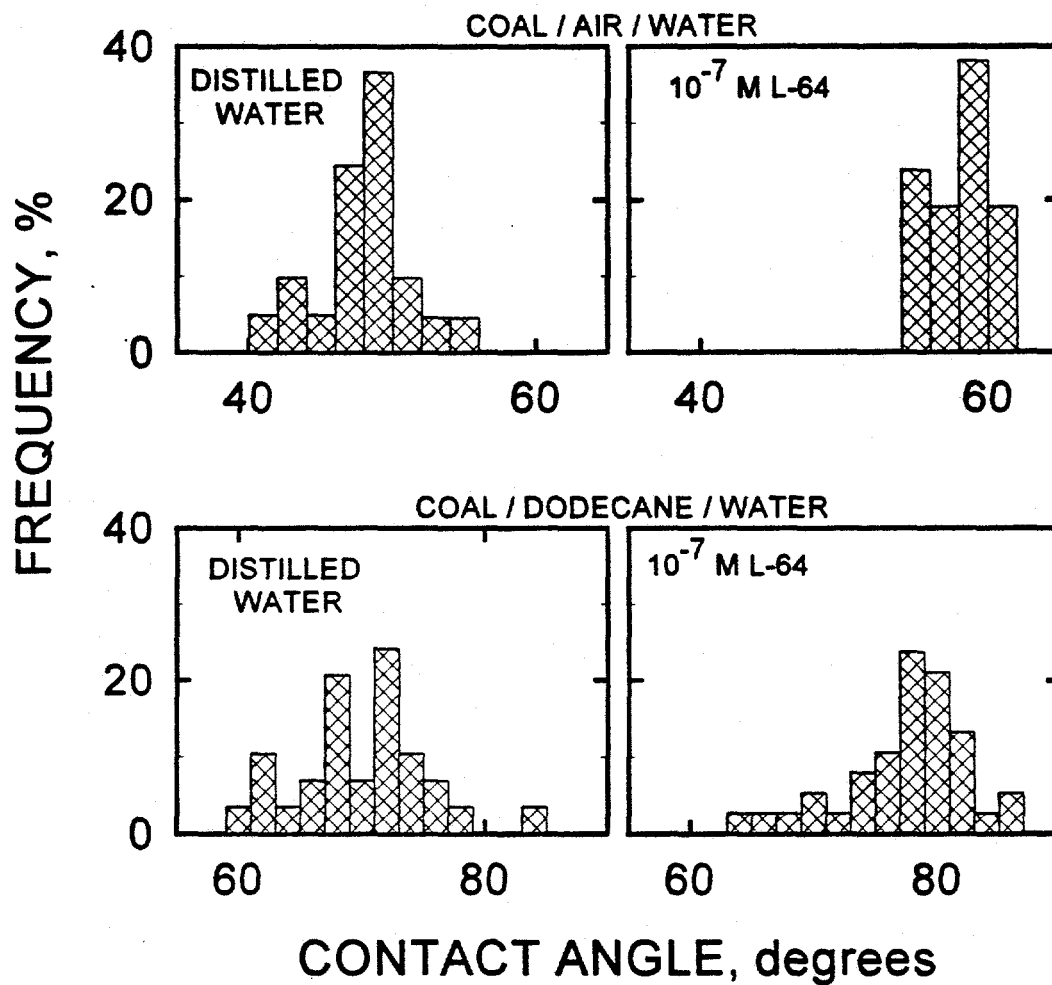


Figure 4.10. Contact angle distribution of Pittsburgh Seam sample in the absence and presence of L-64 (10^{-6} M) in both the coal/air/water and the coal/dodecane/water systems.

the adsorbed PPO blocks formed small loops or were tightly coiled on the surface (Kayes and Rawlings, 1979; Baker and Berg, 1988; Killmann et al., 1988). The area covered by each molecule was determined to be 2.85, 3.20, 5.90, 6.51, 15.10, 17.52 and 24.26 nm² for Pluronics L-61, L-62, L-64, F-38, F-68, F-88 and F-108, respectively (Kayes and Rawlings, 1979). The adsorbed amount was around 1.00 mg/m² for these surfactants.

In the case of silica, both the PEO and PPO chains adsorbed, giving thin layers of constant thickness. This thickness of adsorbed layer was comparable to the thickness of PEO layers on silica (Killmann et al., 1988). The adsorbed amount was very low (0.35-0.40 mg/m²) and independent of the PPO content in the range between 0-30% PPO. In comparison, the adsorbed amount was 0.20 mg/m² in the case of a reagent with 4000 molecular weight and 50% PPO content. The adsorbed layers were also found to be thin in the case of all the polymers (about 2-5 nm) by Tiberg et al. (1991) and Malmsten et al. (1992). The thickness of the layer was also found to increase with particle size (Baker et al., 1989).

The area occupied by a block co-polymer molecule at a hydrophobic surface was found to be greater than those observed at the air/water interface (Alexandridis et al., 1994; Prasad et al., 1979) and considerably less than those at a hydrophilic surface e.g. silica-water interface (Heydegger and Dunning, 1959). These results show the importance of the nature of the solid.

4.3.2. A Hypothesis for Block Co-Polymer Adsorption on Coal

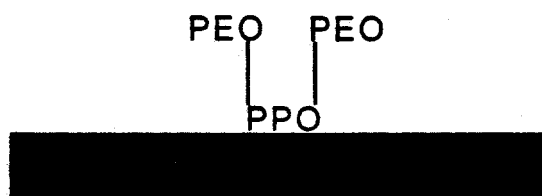
As indicated earlier, coal has a heterogeneous surface structure where strongly hydrophobic (paraffin, graphite, naphthalene) and hydrophilic (methoxyl, carboxyl, carbonyl, hydroxyl) groups co-exist. The degree of hydrophobicity and respective ratios of these groups depend on the rank of coal. Lignite and low rank coals are known to contain large amounts of methoxyl, carboxyl, carbonyl and hydroxyl groups (up to 35%). The carboxyl and methoxyl groups are absent and the carbonyl groups amount to 2% in bituminous coals. The hydroxyl content was observed to decrease as carbon content increases (Yarzab et al., 1979). It has been found that the lower the rank of the coal, the higher its oxygen content, and the greater its susceptibility to attack by oxygen.

Oxidation of coal increases the amount of the oxygen-containing groups, hence, causes a further reduction in the hydrophobicity of coals.

The adsorption studies in the literature (Kayes and Rawlings, 1979; Tadros and Vincent, 1980; Malmsten et al., 1992; Miano et al., 1992; Faers and Luckham, 1994) elucidate the mechanism of adsorption of block co-polymers onto pure hydrophobic (polystyrene latex) and hydrophilic (silica) substrates. Hence, two main types of mechanisms could be proposed for the adsorption of block co-polymers onto coal surface if it is assumed to consist of either completely hydrophilic or completely hydrophobic sites (Figure 4.11).



a. Hydrophilic coal surface
(Oxygen functional groups, methoxyl, carboxyl, carbonyl, hydroxyl)



b. Hydrophobic coal surface
(Paraffin, Graphite, Naphthalene, Anthracene)

Figure 4.11. A schematic illustration of PEO/PPO/PEO type block co-polymer adsorption on hydrophobic and hydrophilic sites of coal surface.

For a completely hydrophilic surface (Figure 4.11-a), adsorption occurs through ethylene oxide groups (hydrogen bonding between the oxygens of the EO groups and functional groups). Adsorption of these molecules should make the surface more hydrophobic because both the EO and PO groups are more hydrophobic than all the hydrophilic groups in the coal structure. This can be seen from Table 4.1 where the HLB

values of EO and PO are presented along with the main surface functional groups of coal structure. The table shows that the HLB values of all the hydrophilic functional groups are higher than the HLB values of ethylene oxide whereas the HLB values of all the hydrophobic functional groups are higher than that of the propylene oxide (Myers, 1988). Therefore, the coverage of these hydrophilic functional groups with surfactant molecules, whether it is an EO or PO group, will make these surfaces less hydrophilic.

Table 4.1. HLB values for selected functional groups (after Davies and Lin, 1972).

Hydrophilic group	HLB	Hydrophobic group	HLB
-COONa	19.1	-CH-	-0.475
-Ester (Free)	2.4	-CH ₂	-0.475
-COOH	2.1	-CH ₃	-0.475
-OH (Free)	1.9	=CH-	-0.475
-O-	1.3		
PEO: -(CH ₂ CH ₂ O)-	0.33	(PPO): -(CH ₂ CH ₂ .H ₂ O)-	-0.15

In the case of a completely hydrophobic surface (Figure 4.11-b), the adsorption of block co-polymer occurs via the hydrophobic portion (PPO) of the molecule through hydrophobic attraction while the PEO groups will be exposed to the bulk solution. This type of adsorption would decrease the hydrophobicity of such a surface.

A coal surface is likely to consist of a random mixture of both hydrophilic and hydrophobic sites. The relative ratio and distribution of these surface sites will depend on such factors as the coal rank and degree of oxidation. Therefore, the total adsorption of block co-polymer molecules on the heterogeneous coal surface is expected to depend on adsorption on both the hydrophobic and hydrophilic sites. For example, the contact angles measured on the Pittsburgh coal sample were distributed with a standard deviation of 3.3° about a mean of 47.3°, demonstrating the presence of the surface sites with varying hydrophobicities. One can consider that the surface of this coal consists of three

type of surfaces: weakly hydrophobic Type 1, moderately hydrophobic Type 2, and strongly hydrophobic Type 3 (Figure 4.12). The relative ratios of these surfaces in a given coal sample would influence the type and the magnitude of adsorption, hence the contact angle.

The fraction of hydrophobic sites for a given coal could be estimated by use of contact angle measurements (Gutierrez et al.,1984). The details of this procedure are discussed in Appendix D. For the Pittsburgh coal sample, the fraction of Type 3 surface was found to be around 32% by use of this method. Similarly, the fractions of hydrophobic sites for some other coals used in this study are tabulated in Table 4.2. It should be noted that coals the fraction of Type 3 sites is zero for low rank when estimated by this method.

Table 4.2. The estimated fractions of hydrophobicity of coal.

Coal Samples	Hydrophobic fraction, %
Pittsburgh	32
Illinois No.6	14
Lower Kittaning	29
Upper Freeport	33

Since all three sites are present together on the coal surface, the adsorption will be affected by the relative affinity of the PEO and PPO groups surfactant molecules onto a given site. However, the preference of a specific surface site by a given surfactant molecule will be a function of surfactant structure (fraction of EO groups). It seems that a block co-polymer molecule with 40% EO group prefers to adsorb on Type 1 and 2 surfaces rather than Type 3. This conclusion was reached based on the experimental observation that an optimum HLB value of 15 was needed to increase contact angle. A decrease in the contact angle which was observed for relatively more hydrophobic block co-polymers such as L-63 and L-62, supported the hypothesis that a certain fraction of

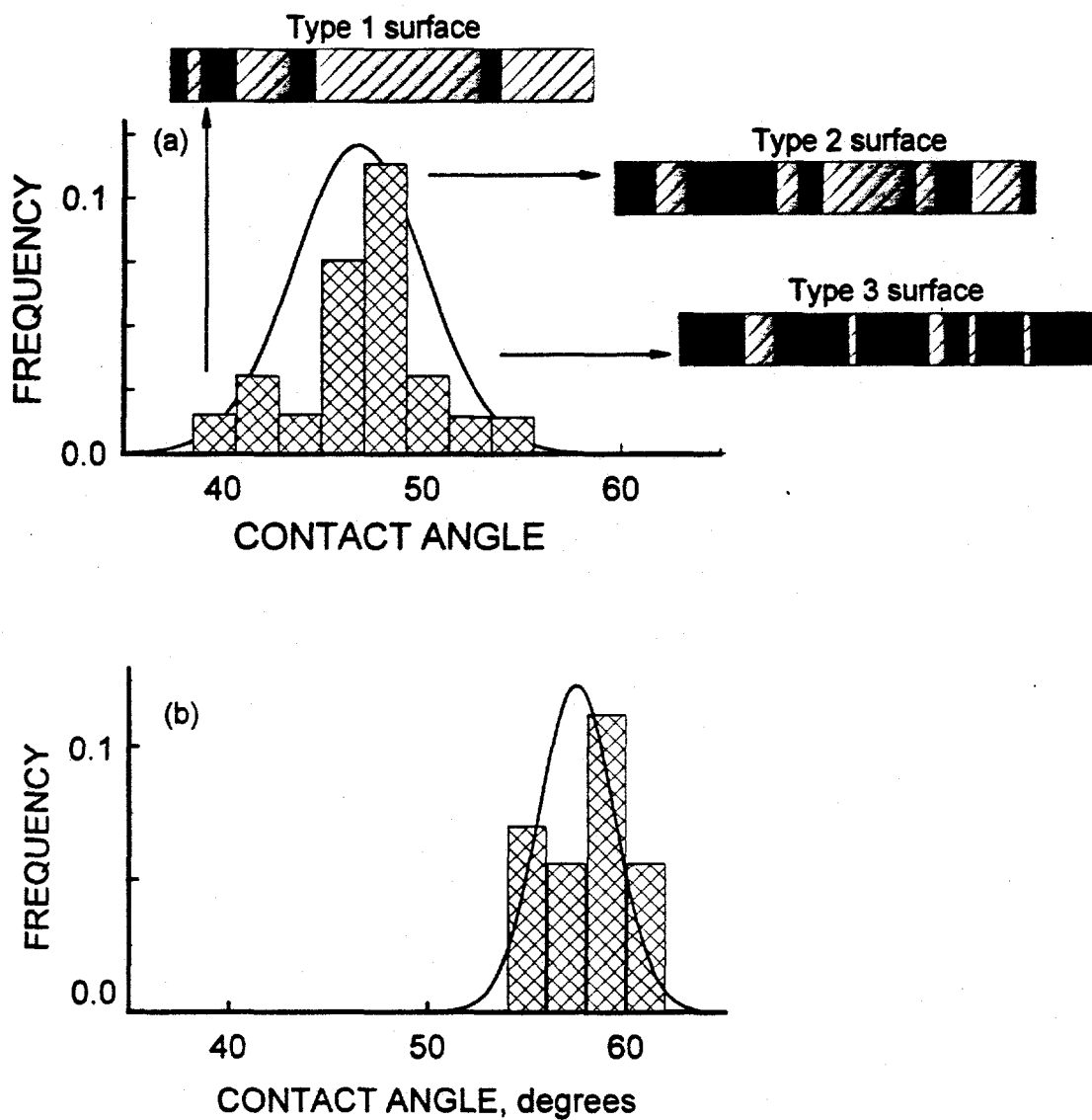


Figure 4.12. The proposed surface types present on the surface of Pittsburgh Seam sample. : Hydrophobic site : Hydrophilic site.

- a) in the absence of block co-polymer
 b) in the presence of L-64 (10^{-7} M)

hydrophilicity is necessary to increase the contact angle. For the same HLB, an optimum number of EO groups hence an optimum molecular weight (>2900), is required to increase contact angle.

Even though there was not a significant change in the mean contact angle at low concentrations, the narrower contact angle distributions given in Figures 4.6 and 4.7 suggest a decrease in the fraction of hydrophobic and hydrophilic sites. The decrease in the fraction of hydrophobic sites was explained by the adsorption of the low molecular weight, most hydrophobic component (high PO%) of the surfactant on the most hydrophobic sites of the coal surface. As discussed in Chapter 2, these surfactants are polydispersed with respect to the PO groups as well as to overall molecular. It is reasonable to assume that some of the surfactant molecules may have a substantially higher ratio of PO groups to EO groups since there is a distribution of both. Hence, some strongly hydrophobic molecules (large PO/EO ratio) with low molecular weight are present in the system. Due to the high hydrophobicity and diffusion rates of these molecules, a decrease in the contact angle is not surprising at low concentrations. The decrease in the fraction of hydrophilic sites, on the other hand, could be explained by the adsorption of a low molecular weight, moderately hydrophobic (~40%) component of the surfactant on weakly hydrophobic sites of the coal surface. At high concentrations, however, the effect of this type of diffusion disappears¹ (Chapter 2). Therefore, the main component of the surfactant which adsorbs mainly on the hydrophilic sites of the surface becomes more effective and thereby increases the contact angle. At a high concentration, $> 10^{-5}$ M, surfactants adsorb indiscriminately on both hydrophobic and hydrophilic surfaces, decreasing the contact angle. In this study, the suitable structure to obtain the highest contact angle in the presence of block co-polymers was 40% EO and > 2900 molecular weight (as in the case of L-64).

¹ As discussed in Chapter 2 where the adsorption of these surfactants at air/water interface was discussed, the effect of diffusion on the adsorption becomes insignificant at concentrations greater than 10^{-6} M.

4.4. Conclusions

The wetting characteristics of triblock co-polymers of ethylene and propylene oxide were investigated using contact angle measurements. A modified captive bubble technique was employed to measure the magnitude of the three-phase contact at the coal/air/water and coal/dodecane/water systems as a function of surfactant concentration. A normal distribution of contact angles was observed, therefore the surface could be characterized by two parameters: the mean and the standard deviation. By use of this technique, the effect of such variables as the concentration, the HLB value and the molecular weight of these surfactants on the wettability of coals of varying rank was studied. The following specific conclusions could be made:

Coal/Air/Water/ system:

- The contact angle increased initially with an increase in the surfactant concentration and reached a maximum value in the concentration range of about 10^{-8} to 10^{-6} M. It decreased precipitously with further increase in concentration. No contact was obtained at concentrations above 10^{-5} to 10^{-4} , depending on surfactant type. The point of no-contact was within Region II of the surface tension versus concentration curves where molecules are believed to be in the form of dimers, trimers, etc. (this range of concentration was reported as the critical micelle concentration in some surface tension studies)².
- The contact angle was found to be a function of molecular weight of the surfactant and the fraction of ethylene oxide groups.
- Contact angle increased with an increase in the HLB value and reached a maximum at an HLB which was a function of the molecular weight.
- As expected, contact angle was also a function of coal type. Some coals (Pittsburgh, Lower Kittaning) gave narrow contact angle distribution while others (Upper

² The results of the surface tension experiments which support this hypothesis are given in Chapter 2.

Freeport, Illinois No.6) had a broad distribution of contact angles, suggesting a more heterogeneous surface structure.

- The coverage of the hydrophilic surface sites by the surfactant molecules through the PEO groups was proposed to be the mechanism for the increase in the hydrophobicity of coal. The investigation suggested that the most suitable structure to obtain the highest contact angle was about 40% EO and a molecular weight greater than 2900 g/mole (as in the case of Pluronic L-64).
- At low concentrations of block co-polymers, the polymer adsorbed through hydrogen bond interaction at hydrophilic sites at the coal surface.

A decrease in the contact angle was observed with more hydrophobic block copolymer (EO% < 40) also suggested that such molecules prefer to adsorb at more hydrophobic sites on the coal surface.

Coal/Dodecane/Water/ system:

- Surfactant addition increased the wetting of coal by oil. The contact angle distribution was found to be broader in the case of a dodecane droplet than that measured in the coal/air/water system using an air bubble. The effect of surfactant concentration was not investigated in this study.

Chapter 5

AGGLOMERATE GROWTH AND STRUCTURE

5.1. Introduction

The formation and growth of agglomerates in an agitated fine coal - water - oil mixture is a highly complex process involving numerous simultaneous, interacting and often competing sub-processes. In the context of micro-agglomerate flotation, the objective is to produce dense agglomerates which are large enough to minimize water carryover during flotation and which contain as little entrapped water and mineral matter as possible. It appears (Chander and Polat, 1995) that fine coal flotation invariably involves some degree of agglomeration of the particles; our goal in this project has been to control the process in such a way as to maximize potential benefits in coal recovery and process selectivity.

For analytical purposes, it is convenient to break the process down, conceptually, into various component sub-processes. It should be emphasized, however, that these are not independent processes and that the outcome of each is highly dependent on what happens in each of the others. The principal components of the overall process can be regarded as collision/adhesion processes and disruption or breakage processes, and refer to fine-particle aggregation, oil emulsification, solid-oil interaction and agglomerate breakage. An additional process: agglomerate compaction can also be included.

5.2. Collision Processes

Collisions between dispersed species are responsible for establishing contact between oil and coal and for the formation and growth of agglomerates. Collision frequency determines the rate of oil attachment or agglomerate growth. Long range interaction forces between particles can affect these rates by changing collision efficiency, defined as the fraction of collisions which actually lead to adhesion. Adhesion following collision also determines the integrity of the resulting agglomerate.

Classical coagulation theory (Overbeek, 1952) indicates that the frequency b_{ij} of collisions between dispersed species i and j can be expressed by

$$b_{ij} = K_{ij} n_i n_j \quad 5.1$$

where n_i and n_j are the respective number concentrations and K_{ij} is a rate constant which depends on the nature of the relative motion responsible for collisions to occur. The rate constant can be generalized (Hogg 1981) as

$$K_{ij} = K_m x_i^m p_{ij} \quad 5.2$$

where x_i is the particle size for species i , p_{ij} depends on the collision mechanism and the relative size of the interacting particles; the exponent m and the constant K_m depend only on the collision mechanism. In the context of oil agglomeration, the primary collision mechanisms are Brownian motion ($m = 0$) and mechanical agitation ($m = 3$). For Brownian coagulation, the parameters in Equation 5.2 are given by:

$$m = 0$$

$$K_0 = 2 kT/3\mu$$

$$p_{ij} = (2 + x_i/x_j + x_j/x_i)$$

and, for agitated systems:

$$m = 3$$

$$K_3 = \bar{G} / 6$$

$$p_{ij} = (1 + x_j/x_i)^3.$$

In the above, k is Boltzmann's constant, T is absolute temperature, μ is fluid viscosity and \bar{G} is mean shear rate. For vigorously agitated, stirred-tank systems, the latter can be estimated (Camp and Stein 1943) from

$$\bar{G} \approx \sqrt{\frac{P}{\mu V}} \quad 5.3$$

where P is the power input to the tank and V is the tank volume. For agitation at high Reynolds Number ($>10^4$) in a standard cylindrical tank, P is given by (Rushton et al., 1950):

$$P \approx 6\rho_f N^3 D^5 \quad 5.4$$

where ρ_f is the fluid density, N is the rotational speed and D is the impeller diameter.

The relative importance of collisions due to Brownian motion and agitation can be evaluated by considering the ratio of the appropriate rate constants for particles of the same size. By appropriate substitutions into Equation 5.2, the ratio can be expressed as

$$Q = \frac{\bar{G} \mu x^3}{2 kT} \quad 5.5$$

For 1 μm particles in water at ambient temperature, Q is greater than unity for shear rates larger than about 10 sec^{-1} . Since oil agglomeration typically involves substantially higher shear rates, it follows that shear is the dominant collision mechanism for these systems under all reasonable conditions.

5.3. Disruption/Breakage Processes

Emulsification of oil involves the breakdown of large droplets into smaller units. Agglomerates of fine coal are also subject to breakage in a turbulent environment. Droplet breakage during emulsification has been discussed in Chapter 3. A similar approach can be used in the analysis of agglomerate breakage (Hogg 1994) by assuming that breakage occurs when the hydrodynamically induced shear stresses exceed the strength of the agglomerate. According to Rumpf (1961), the effective binding force in a porous, spherical agglomerate of diameter d built up from individual particles of size x can be estimated from

$$F_B = \frac{\pi d^2 (1 - \epsilon) F}{4 \epsilon x^2} \quad 5.6$$

where ϵ is the agglomerate porosity and F is the adhesional force between individual particles.

It is generally observed (Vold, 1963; Sutherland, 1967; Weitz and Huang, 1984; Klimpel and Hogg, 1991) that flocs exhibit a self-similar, fractal structure such that

$$1 - \epsilon \approx \left(\frac{x}{d}\right) \quad 5.7$$

If the principal binding force between individual particles is of the van der Waals-London dispersion type,

$$F \approx \frac{Ax}{24H^2} \quad 5.8$$

where A is the Hamaker constant (Hamaker, 1937) and H is the effective separation between particles in the agglomerate. Combination of Equations 5.6, 5.7 and 5.8 leads to

$$F_B \approx \frac{\pi dA}{96H^2} \quad 5.9$$

for relatively large agglomerates ($d \gg x$).

Procedures for estimating the hydrodynamic force acting on agglomerates in an agitated suspension have been developed (Thomas, 1984; Tomi and Bagster 1978) based on velocity fluctuations in locally isotropic turbulence. The effective force is generally recognized to depend on the size of the agglomerate relative to the Kolmogorov turbulence micro-scale λ_o , defined by:

$$\lambda_o = \left(\frac{\mu^3}{\rho_f^2 e_o} \right)^{1/4} \quad 5.10$$

where μ and ρ_f are respectively the viscosity and density of the fluid medium and e_o is the effective rate of energy dissipation (power input per unit volume) in the agitated fluid.

For agglomerates larger than the micro-scale, the hydrodynamic force can be estimated from:

$$F_H \sim \rho_f e_o^{2/3} d^{8/3} \quad 5.11$$

Equations 5.9 and 5.11 reveal that, whereas the binding force increases more or less linearly with agglomerate size, the disruptive, hydrodynamic forces increase with the 8/3 power of size. It follows that breakage becomes increasingly likely as agglomerate size increases. It has been shown (Parker et al. 1972) that, for typical flocculation systems, the binding forces generally dominate for agglomerates smaller than about 30-50 μm . At the very high shear rates typically used in oil agglomeration, this could be reduced to 10 μm or less.

5.4 Agglomerate Formation and Growth

In simple coagulation processes where adhesion between particles results from van der Waals forces or polymer bridging, flocs grow through a sequence of binary

collisions. Hogg (1992) has shown that the mean agglomerate size \bar{x} in an agitated system increases with time according to

$$\bar{x} = \bar{x}_0 e^{4\bar{G}\phi t/3\pi} \quad 5.12$$

where \bar{x}_0 is the initial particle size and ϕ is the volume fraction of solids in suspension. For the typical concentrations, shear rates etc., encountered in oil agglomeration, Equation 5.12 predicts extremely rapid growth with agglomerate size reaching many times the initial size in a matter of seconds.

As noted above, Equation 5.9 and 5.11 predict that the relative strength of agglomerates should decrease with increasing size. It is to be expected then, that breakage rates should increase as agglomerates grow to larger sizes. Eventually, agglomerate size should approach a limiting value at which the growth and breakage rates are equal. Combination of agglomeration and size reduction models has been used to formulate a simplified model for simultaneous agglomerate growth and breakage (Hogg et al., 1990). In this formulation, the change in mean agglomerate size with time in an agitated suspension is expressed by

$$\frac{d\bar{x}}{dt} = K_a \bar{x} - K_b \bar{x}^{1+\alpha} \quad 5.13$$

where K_a is an overall growth rate constant, K_b is a breakage rate constant and the exponent α reflects the size dependence of the breakage process. For conventional size reduction (grinding) processes, α has a value close to unity. The solution to Equation 5.13 can be written:

$$\bar{x} = \bar{x}_0 \left[\frac{K_b \bar{x}_0^\alpha}{K_a} + \left(1 - \frac{K_b \bar{x}_0^\alpha}{K_a} \right) e^{-K_a t} \right]^{-1/\alpha} \quad 5.14$$

Equation 5.14 has been shown fit experimental data from simple flocculation systems (Maffei, 1989; Hogg et al., 1990). An example, showing the effects of increased adhesion efficiency on the initial growth rate and limiting size, is given in Figure 5.1.

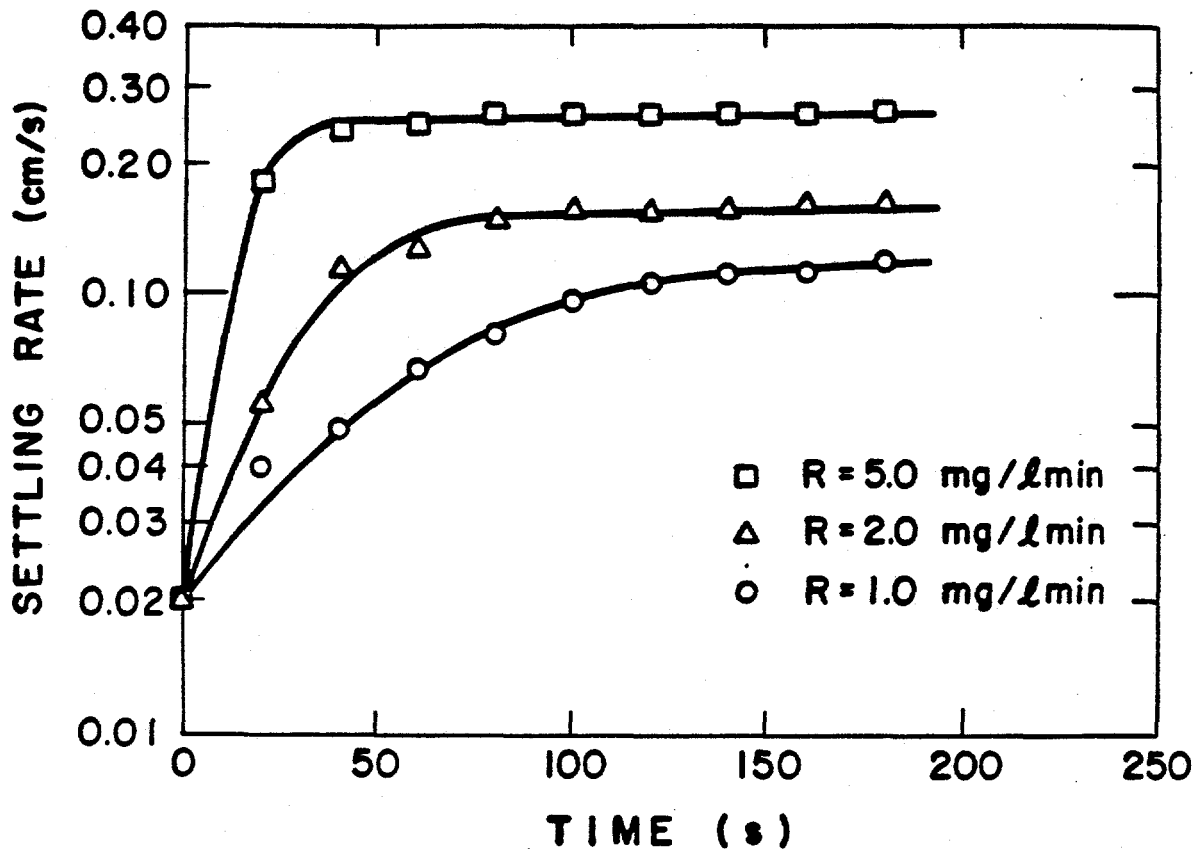


Figure 5.1. Agglomerate growth in simple flocculation systems showing the effect of enhanced adhesion efficiency (as determined by the rate of flocculant addition R) on settling rate (a measure of floc size). (After Maffei, 1989).

5.5 Experimental

5.5.1 Materials

A 10 kg batch of a sample of coal from the Pittsburgh Seam was ground to nominal sizes of -40 and -20 μm using the following procedure:

1. The entire batch was passed through a Holmes pulverizer.
2. The pulverized coal was classified at the specified size using a Donaldson Acucut classifier.
3. The oversize coal was passed again through the pulverizer and reclassified.
4. This process was repeated until essentially all of the coal was reduced to -40 or -20 μm as required.

The fine coal samples were stored under argon in 500 g sealed bags and designated P40 and P20 respectively. The particle size distributions are shown in Figures 5.2 and 5.3.

The dry grinding/air classification procedure is very convenient for sample preparation in the laboratory since it permits the use of air classification, the preparation of sufficient material for a complete series of tests and obviates the need for storage of wet coal. In practical (i.e., commercial) applications, however, the coal would normally be ground wet.

A drawback of the dry grinding and storage procedure is that dispersion of the coal in water becomes a critical first step in the evaluation of the agglomeration process. Because of the natural hydrophobicity of the coal, pre-wetting of the material is especially important and, in order to preserve the hydrophobic character, no surfactants or wetting agents can be used except when their use is actually specified. An important consequence of the hydrophobic nature of coal is that the presence of even very small quantities of air can promote agglomeration of the particles. For studies of the growth of agglomerates following oil addition, therefore, it is vital to ensure that the coal is thoroughly pre-wetted and dispersed.

A standardized procedure has been developed for wetting and dispersion of the coal. The sample of dry coal is first wetted by means of a water spray from a wash bottle. When wetting appears, visually, to be complete, more water is added until the

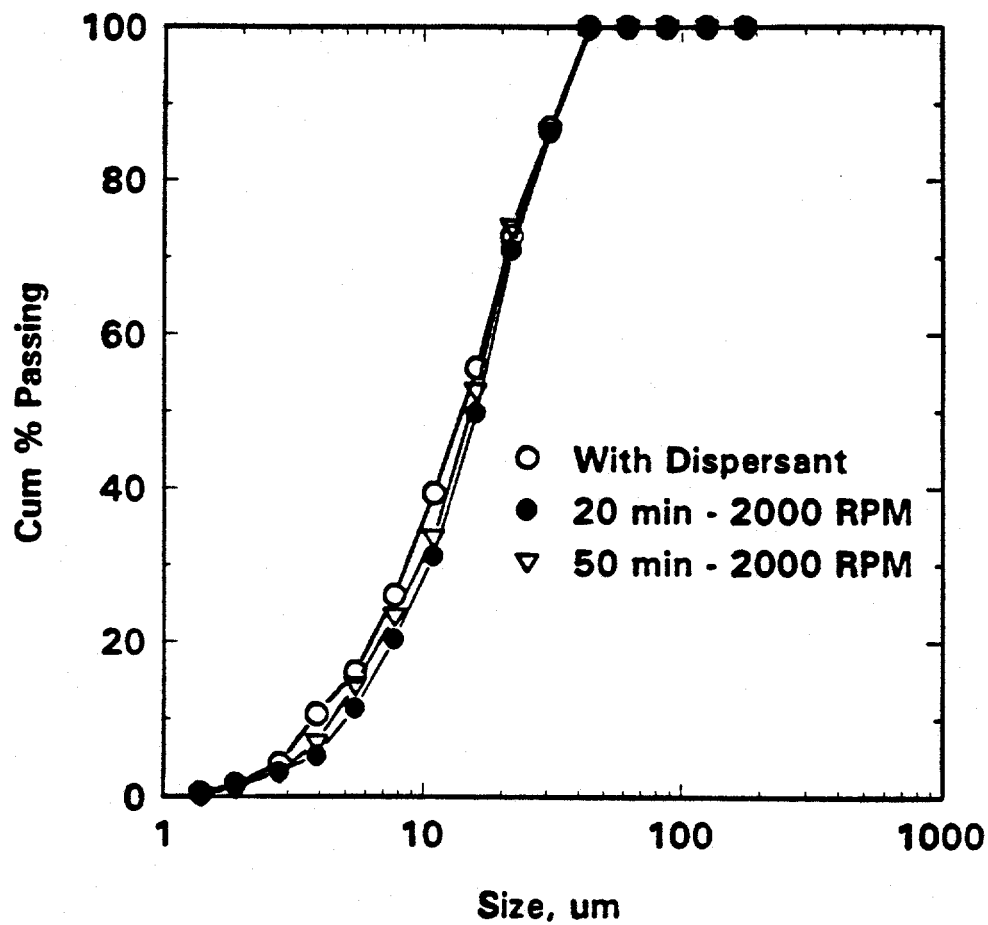


Figure 5.2. Size distribution of P40 coal sample showing comparison of results obtained using wetting and dispersing agents with those using the standard reagent-free procedure.

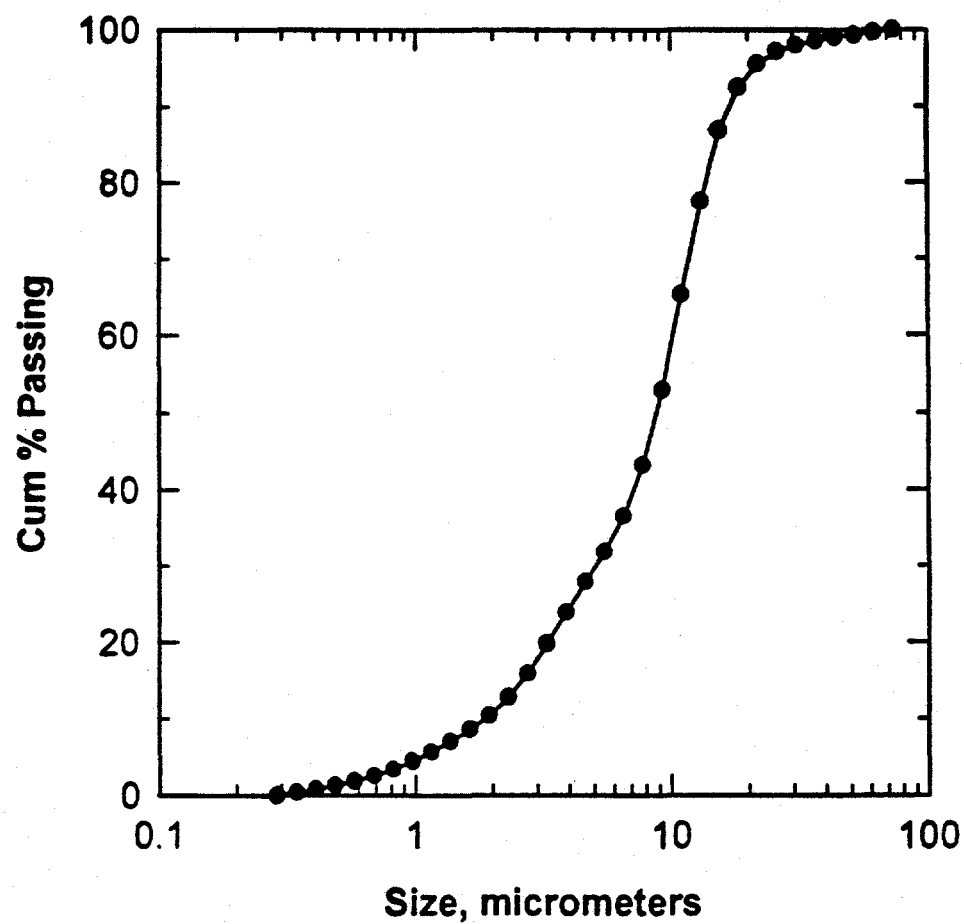


Figure 5.3. Particle size distribution for P20 coal.

desired solids concentration (normally 1% by weight) is achieved. The resulting suspension is then agitated for 20 minutes at 2000 rpm in a standard, 1.5-liter tank. The effectiveness and reproducibility of the wetting-dispersion procedure are evaluated by particle size analysis (Microtrac) on samples taken directly from the tank and subjected only to the required dilution. The measured size distribution is compared to the standard result obtained using wetting agents and dispersants. An example of such a comparison is given in Figure 5.2. The close agreement among the curves indicates that the procedure is adequate and there is no significant agglomeration of the dispersed coal particles.

5.5.2 Procedure

A systematic investigation of the kinetics of agglomerate growth has been carried out. Experiments were conducted in a 1.5 liter standard mixing tank of the type discussed in Chapter 3 and illustrated in Figure 3. 2. The procedure used was to agitate 1200 ml of the coal slurry at the desired solids concentration (usually 1% by weight at the selected speed for 10 minutes to ensure complete wetting and dispersion. The appropriate amount of oil (corresponding to 1 weight percent of the coal present in most cases) was added rapidly (over about a 2 second period) to initiate agglomeration. Samples were taken using a 6 mm diameter, open glass tube immediately prior to oil addition and at appropriate time intervals thereafter. Particle/agglomerate size distributions were measured by laser light scattering/diffraction (Microtrac Standard Range Analyzer in earlier tests Microtrac X-100 in later test-work). Special precautions were taken to minimize changes in agglomerate size distribution during analysis.

5.5.3 Results

Some typical results, showing the evolution of the agglomerate size distribution with time following oil addition, are given in Figure 5.4. Generally, it can be seen that the size distributions undergo relatively parallel shifts with time while their general shape remains largely unaltered. This indicates that the changes can be characterized using a

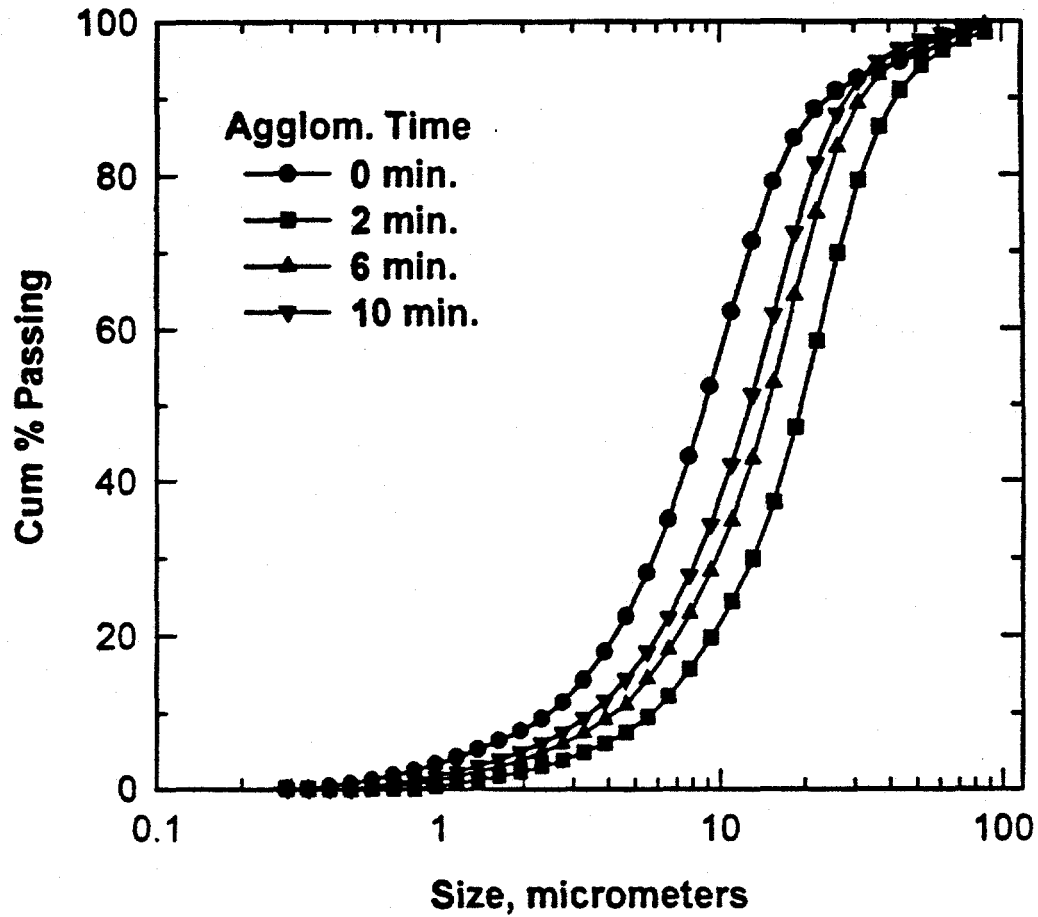


Figure 5.4. Typical agglomerate size distributions observed following oil addition to P20 coal.

single size parameter such as the volume median size x_{50} . An example of the time dependence of the median size is given in Figure 5.5.

The growth curves consistently show an initial period of rapid growth up to a maximum size, followed by one of decreasing size. In the context of the growth/breakage model, this behavior suggests a direct time dependence of either the growth or the breakage rate (or both). Growth rates could decrease through a reduction in the collision adhesion efficiency while breakage rates could increase due to a reduction in agglomerate strength.

It is clear that oil agglomeration is considerably more complicated than simple coagulation. In this case, collisions occur between particles or small agglomerates and oil droplets as well as between particles. Furthermore, because of the high shear rates, simple agglomeration will be severely limited by agglomerate breakage. The frequency of particle-droplet collisions can be estimated using Equations 5.1 and 5.2 with appropriate values for the concentrations, sizes, shear rate, etc. Calculations based on this approach reveal that large oil droplets become completely coated by solid particles almost instantaneously. Agglomeration then proceeds by association of these particle-coated oil droplets. The agglomerate growth rate can be predicted using Equation 5.12 with \bar{x}_0 representing the initial droplet size and ϕ representing the fractional oil concentration. The occurrence of such agglomerates has been observed directly by high-speed motion analysis (Polat and Chander 1994).

The association of particle-coated oil droplets produces large, open-structured agglomerates, which quickly reach a limiting size at which growth and breakage rates are equal. At the same time, partial coalescence of the agglomerate can occur such that the "pores" in the agglomerate become water droplets entrapped in the oil-filled agglomerate matrix. The existence of such water-in-oil-in-water emulsions in the presence of fine coal was demonstrated by Hsu (1987). For the agglomeration systems investigated in this program, the ratio of oil to coal is very small (typically 0.01 by weight or about 0.019 by volume). Thus, the coated droplets formed after oil addition must exist in the presence of "free", dispersed coal particles or small, essentially oil-free agglomerates. As the agglomerated oil droplets grow in the highly turbulent environment they are subjected to

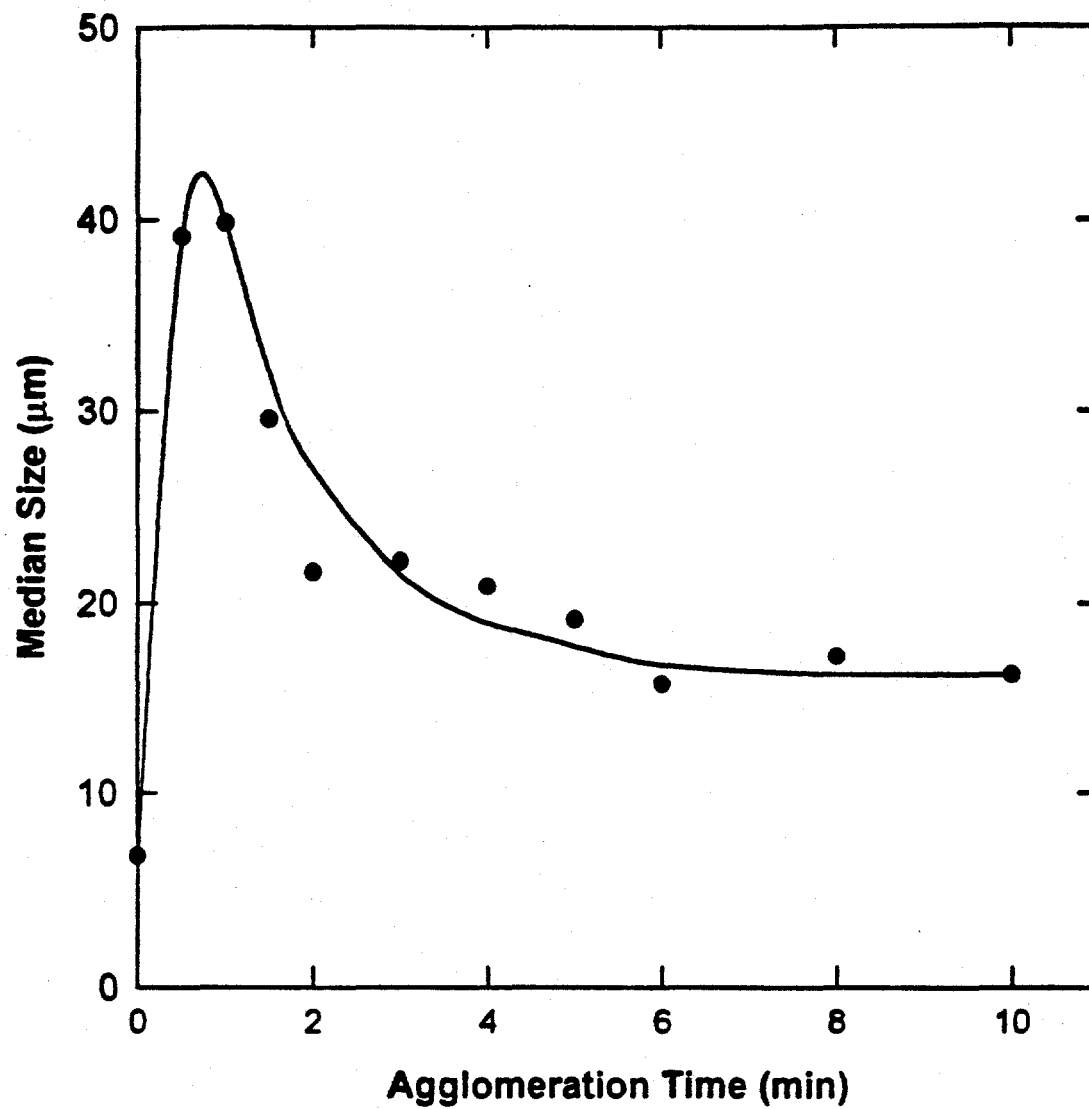


Figure 5.5. Typical agglomerate growth curve.

breakage at increasing rates. The maximum in the growth curve probably corresponds to a dynamic equilibrium between growth and breakage of these agglomerates.

Each breakage event can be expected to expose fresh oil surface which will allow additional coal particles to be incorporated. The resulting decrease in the oil to coal ratio in the agglomerates should, in turn, affect subsequent rates of growth and breakage. Growth rates should decrease due to reduced "stickiness" of the agglomerate surfaces. The effect on breakage rates may be more complex due to changes in the nature of the binding forces.

In the early stages of agglomerate development it is reasonable to assume that particle-coated oil droplets gradually incorporate additional particles until they become completely saturated. In this state, the agglomerates are held together by capillary bonding; their strength should reach a maximum level which can be estimated from (Rumpf 1961):

$$\sigma_c = \frac{6(1-\varepsilon)\gamma_{ow}}{\varepsilon X} \quad 5.15$$

where γ_{ow} is the oil-water interfacial tension. Even with close packing of the particles in the agglomerates ($\varepsilon \sim 0.5$) each would have to contain about 50% oil by volume. With an overall oil to coal ratio of less than 2% by volume, such saturated agglomerates could include only about 2% of the total coal present.

The addition of further coal to the agglomerates leads to an unsaturated condition in which water-filled pores are formed in the structure. The presence of such pores reduces the agglomerate strength substantially. Eventually, the agglomerates should approach a condition of so-called *pendular bonding* with the particles connected through very small pendular rings at the points of contact. The strength of such agglomerates is given by (Rumpf 1961; Hogg, 1989):

$$\sigma_p = \frac{\pi(1-\varepsilon)\gamma_{ow}(1-f/2)}{\varepsilon X} \quad 5.16$$

where f is the ratio of the diameter of the pendular ring to the diameter of the solid particle. Rumpf (1961) showed that for agglomerated spheres, the strength of the

pendular bond is typically about 2 to 4 times less than that of the capillary bond. The strength reduction may, in fact, be substantially more for irregular particles.

It is postulated that the maximum agglomerate size seen in Figure 5.5 corresponds to the saturation, capillary-bonding condition. As these agglomerates are transformed into the pendular state, breakage rates increase due to reduced strength. The result is a decrease in the median agglomerate size towards a final condition of dynamic equilibrium between growth and breakage of pendular-bonded agglomerates.

Further insight into the complex processes involved in agglomerate development can be obtained by re-evaluation of the complete size distributions at different stages in the process. The general pattern appears to be consistent for results obtained under a variety of conditions but can be seen most clearly at high oil concentrations and low agitation speeds. An example is given in Figure 5.6. It is postulated that the initial stage of agglomeration involves the formation of a multimodal distribution consisting of some dispersed fines together with a hierarchy of agglomerates of different size. As the process continues, these coalesce into a narrow distribution of relatively large agglomerates corresponding to the maximum in the median size. With further agitation, the multimodal distribution re-emerges, due to breakage of the large agglomerates. Finally, the smaller agglomerates recombine to form a stable, relatively narrow distribution of agglomerates which are somewhat smaller and probably denser than those present at the maximum in the growth curve. Qualitative confirmation of this pattern has been obtained by direct, microscopic examination of the agglomerates.

The general model described above is consistent with our observations on both fine (P40) and ultrafine (P20) coal. Preliminary testing with the P40 coal using direct oil addition showed, on average, the typical trend. However, the results were widely scattered with variations in median agglomerate size of up to 50%, especially in the region close to the maximum in the growth curve. Based on extensive replicate testing it was concluded that these variations were generally real and not simply due to experimental error. With direct oil addition, the initial stage of the process involves a combination of oil emulsification, coal-oil attachment and agglomerate growth. Because

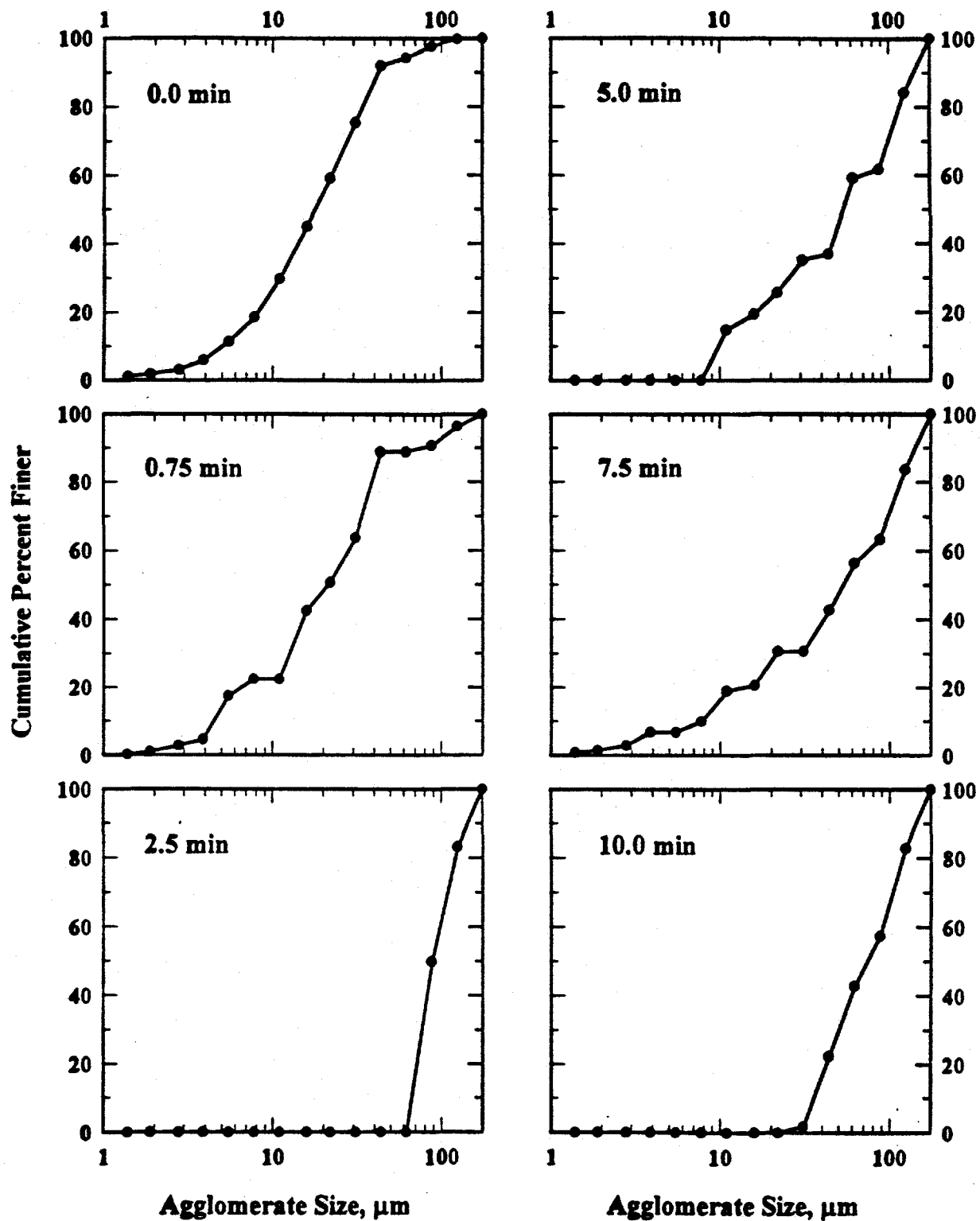


Figure 5.6. Development of the agglomerate size distribution for 5% oil (dodecane) addition to P40 coal at 1500 rpm.

of the statistical nature of these processes and the low oil and coal concentrations involved, the outcome was highly variable, especially over short time periods.

In order to improve test reproducibility and provide greater and more consistent control over the agglomeration process, subsequent tests were performed using pre-emulsified oil. For this purpose, a Waring blender was used to emulsify a 15% dodecane/distilled water mixture which was then added in appropriate amounts, to the coal-water slurry. Studies of this emulsification process indicated that the median droplet size decreased progressively with blending time even after 40 minutes of blending. In order to ensure a consistent droplet size in the emulsion added to the coal slurry, a procedure was adopted in which each agglomeration test was carried out with freshly prepared emulsion. For the 30 ml blending vessel used in these tests, a blending time of 3 sec, giving a median droplet size of about 27 μm , was adopted as a standard pre-emulsification procedure.

Agglomeration tests using the pre-emulsified oil indicated that, at low oil concentration (0.1%), pre-emulsification leads to an increase in the initial rate of agglomerate growth. At higher concentration (0.5%), the initial rate is essentially unchanged but subsequent growth becomes less erratic with the pre-emulsified oil. The long-time behavior of the agglomerates does not appear to be affected by pre-emulsification.

The effects of agitation speed during agglomeration of P40 coal are illustrated in Figure 5.7. The general trend is in accordance with the growth/breakage model described above. Increasing agitation speed increases the initial growth rate, as would be expected for growth by shear-induced collisions. At the same time, breakage rates also increase with speed, as evidenced by the reduced, long-time median size at the higher agitation speeds. The maximum size attained appears to increase slightly with speed, perhaps indicating a somewhat greater effect on growth than on breakage, at least over the range of speeds studied.

The effects of the amount of oil added are also shown in Figure 5.7. For the most part, it seems that higher oil concentrations have little effect on the initial growth period but produce larger agglomerates in the later stages of the process. This may be due to

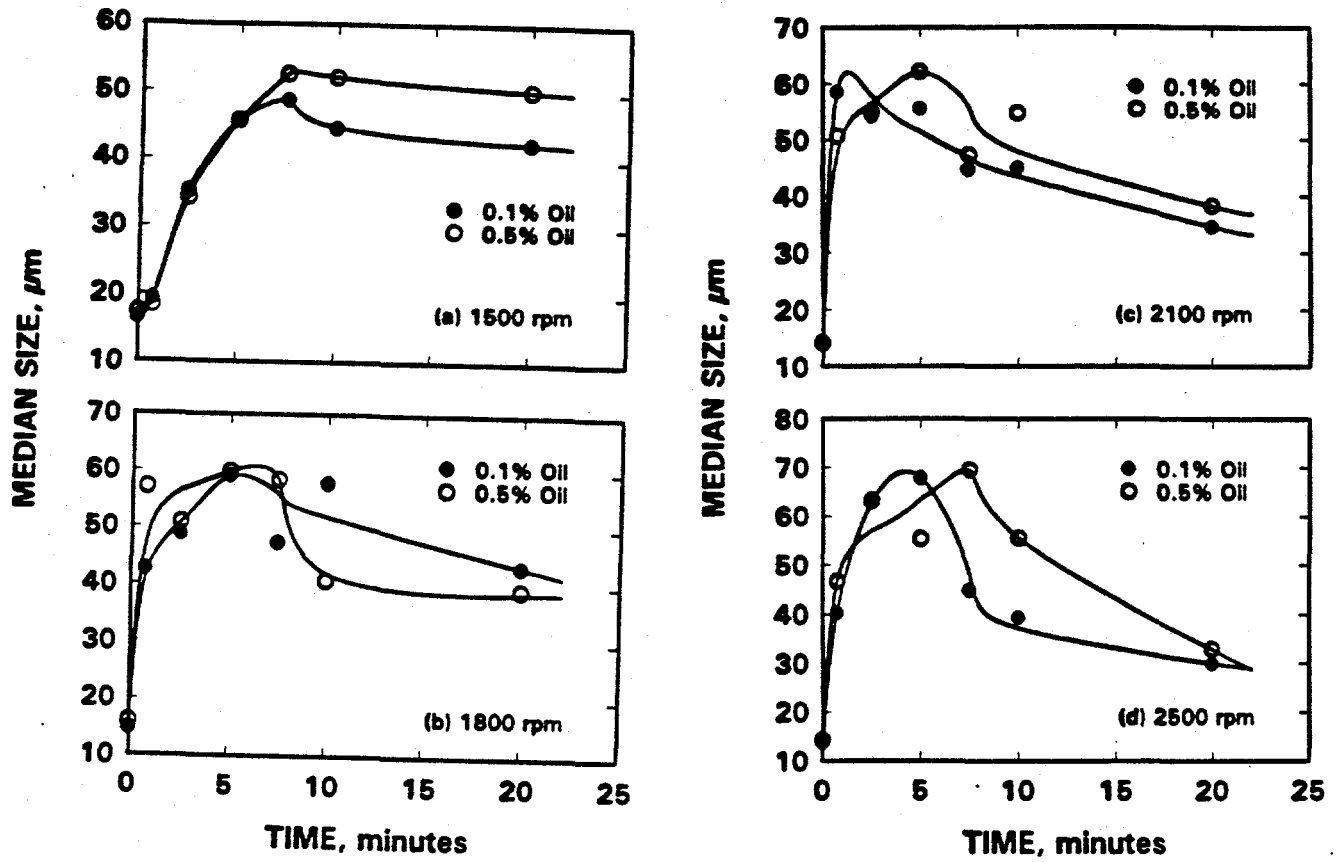


Figure 5.7. Effect of agitation speed and oil addition level on agglomerate formation and growth (P40 coal).

reduced breakage rates or enhanced reagglomeration rates or a combination of the two. The latter trend appears to be reversed at the intermediate speed of 1800 rpm. The reasons for this are not entirely clear but may reflect the complexities of the redistribution of oil during long-time development of the agglomerates.

The effects of surfactant (Pluronic L-64) addition on the agglomeration process have also been investigated. A series of experiments was carried out at an agitation speed of 1500 rpm in the presence of 0.1 weight percent dodecane with respect to the coal. In these tests, surfactant was added to the standard mixing tank 30 seconds prior to the addition of emulsified oil. Enough surfactant was added to a one weight percent coal slurry to achieve the desired final concentration. 30 seconds later, 0.1 ml of a 15.0% by volume dodecane/distilled water emulsion was added. Samples were taken and measured in the Microtrac SRA. The effects of surfactant concentration on agglomerate growth in this system are shown in Figure 5.8. Agglomerate size increases with increasing surfactant concentration up to a maximum at 10^{-6} M. At higher concentrations, it appears that the surfactant begins to act as a wetting agent reducing the extent of agglomeration. Agglomerate formation seems to be eliminated entirely at a surfactant concentration of 10^{-5} M. These results correspond well with the contact angle studies reported in Chapter 4. Further experiments, in which the surfactant was added in the oil emulsification step were somewhat inconclusive due to foaming problems during pre-emulsification. However, there may be potential advantages to the use of split surfactant addition in which some is used to aid in pre-emulsification of the oil and the remainder added to the coal slurry. This approach was not evaluated in this project.

Agglomerate growth for the finer, P20, coal was found to follow the same general pattern as the coarser, P40 material. However, the effects of process variables such as agitation speed and surfactant addition were substantially less pronounced. Some examples can be seen in Figures 5.9 and 5.10; the growth curves are essentially the same in each case. It appears that different mechanisms control the growth and breakage processes in the coarser and finer coals. Ultimately, development of the agglomerate size distribution must depend on the relative rates of growth and breakage. These seem to be controlled by hydrodynamic factors and by oil droplet size for the P40 coal, but not for

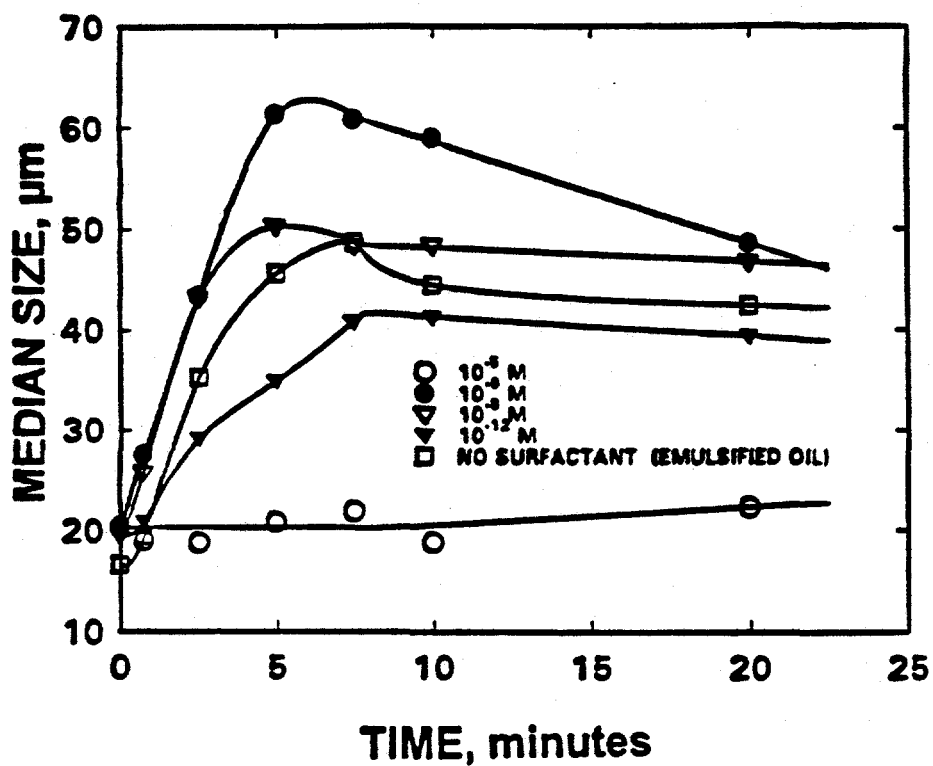


Figure 5.8. Effect of surfactant concentration (Pluronic L-64) on agglomerate formation and growth for P40 coal with pre-emulsified oil. (Surfactant added prior to pre-emulsified oil).

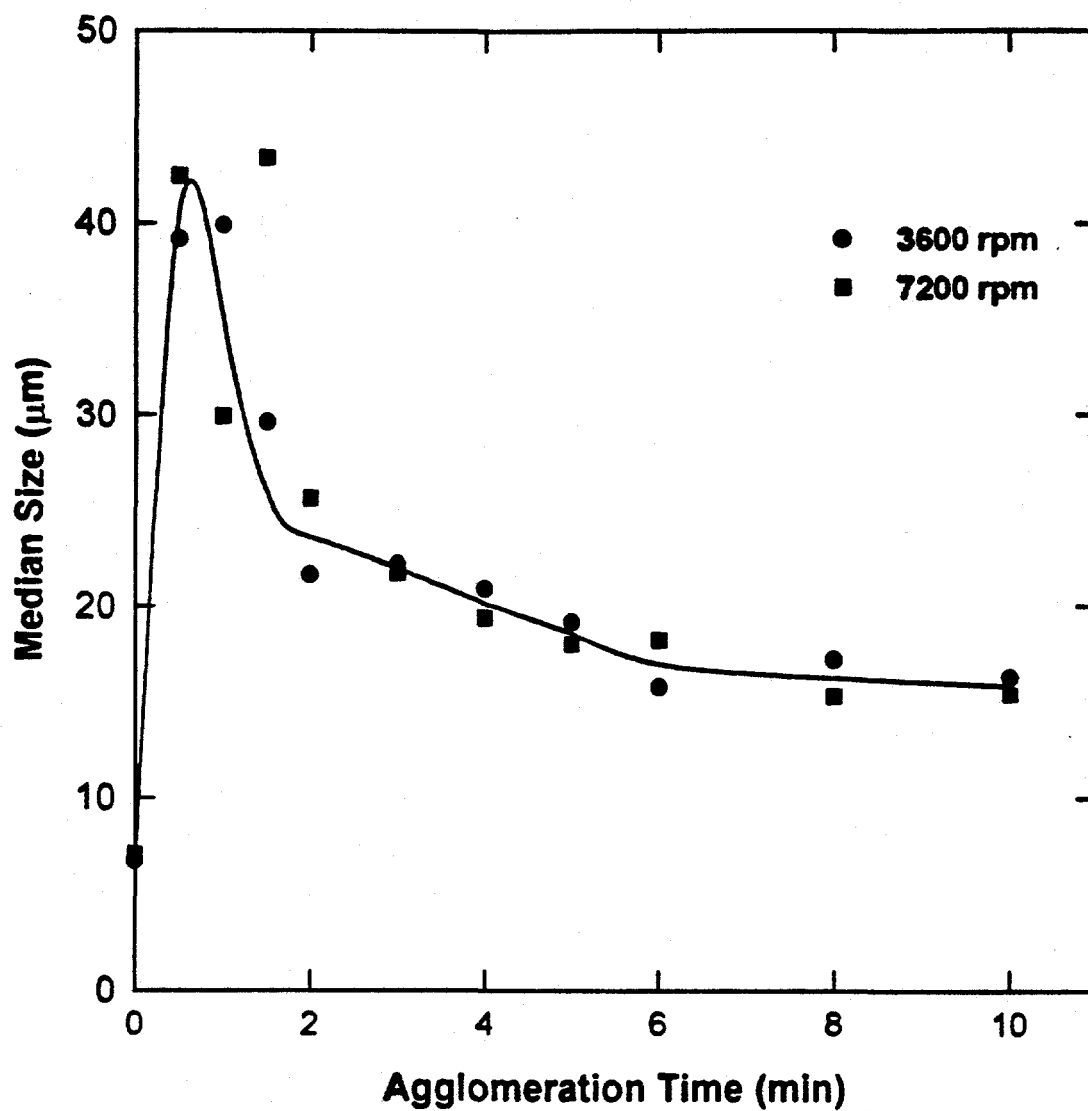


Figure 5.9. Effect of agitation speed on agglomerate development for P20 coal.

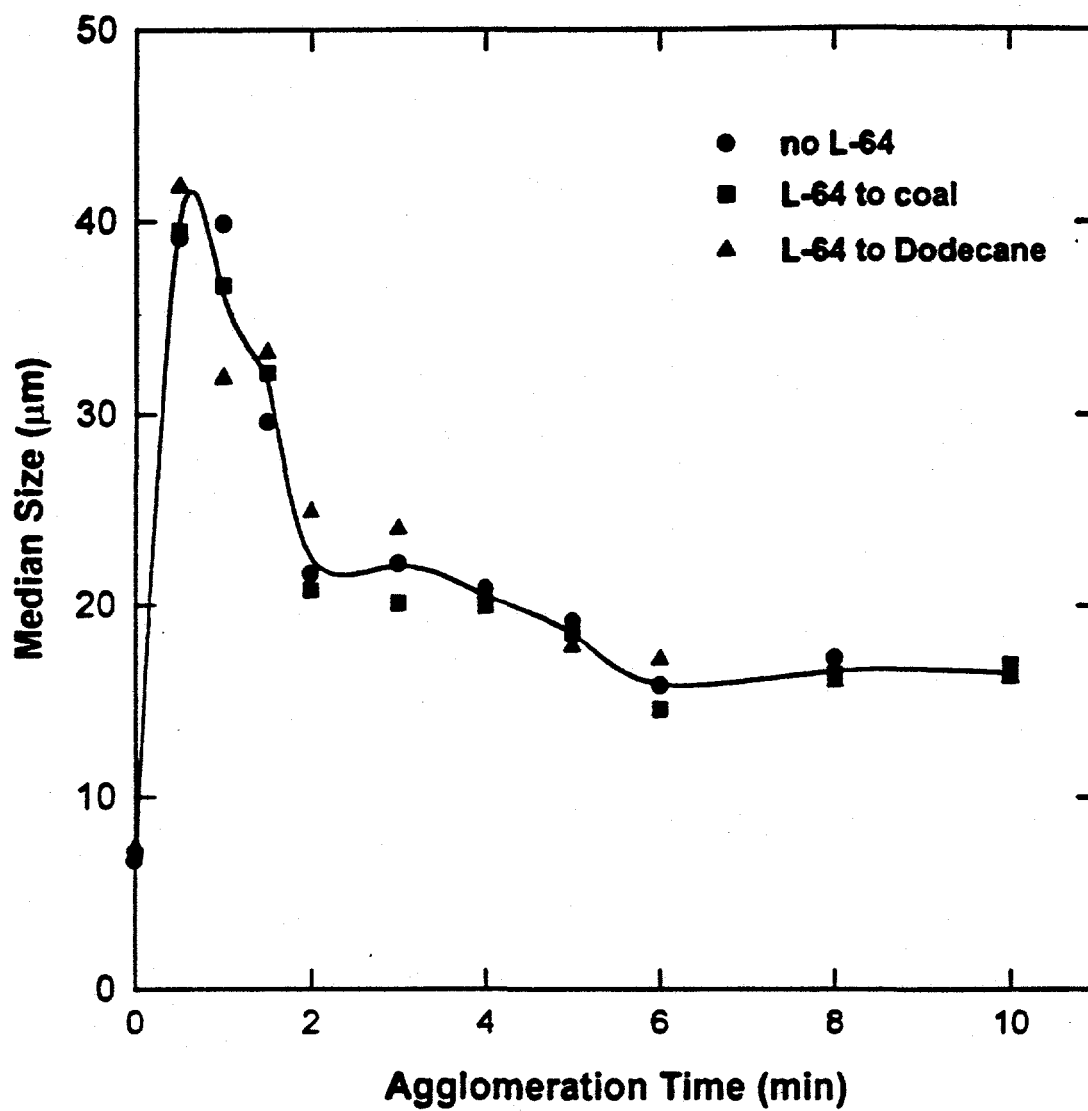


Figure 5.10. Effect of surfactant addition on agglomeration of P20 coal at 3600 rpm.

the P20. It is possible that, for the finer material, the mobility of oil within the agglomerates is substantially reduced and becomes the rate-controlling factor. Growth and breakage events occur with high frequency but their relative rates change slowly as oil is redistributed in and among the agglomerates.

5.6 Conclusions

Agglomeration of fine coal in the presence of oil is a complex process which involves numerous steps - sometimes sequential, often concurrent.

- Emulsification of the oil is a basic first step. With direct oil addition to the coal slurry, emulsification must take place in the presence of fine coal particles. The result is rather erratic agglomeration with poor experimental reproducibility. Pre-emulsification provides substantially improved control over the agglomeration process.
- Agglomeration consistently follows a pattern of rapid initial growth to a maximum size followed by a slow decrease in the median size and an approach to some, long-time, limiting size.
- Agglomerate development is controlled by growth and breakage in the turbulent environment.
- Growth rates are probably controlled by the effectiveness of adhesion between colliding particles/agglomerates, i.e., by contact "stickiness".
- Breakage rates appear to vary according to agglomerate strength which itself changes due to redistribution of oil in the agglomerates.
- Oil redistribution can occur as a result of breakage and reagglomeration or by internal, capillary flow. It is postulated that the former mechanism dominates in the case of $-40 \mu\text{m}$ coal while the latter becomes the controlling factor at finer sizes (i.e. $-20 \mu\text{m}$).
- Surfactant additions can affect agglomeration. For the coarser coal studied ($-40 \mu\text{m}$) agglomerate growth appears to be maximum at a surfactant concentration corresponding to a maximum in the coal-water-air contact

angle. The surfactants studied seemed to have little or no effect on agglomeration at finer sizes ($-20 \mu\text{m}$).

Chapter 6

AGGLOMERATE FLOTATION

6.1 Introduction

The problems in flotation of fine coal and those of selective flocculation and spherical agglomeration were discussed in previous chapters. Selective agglomeration offers considerable potential for deep cleaning of coal but many problems in obtaining the required selectivity with acceptable recovery of combustible remain. In froth flotation, selectivity is substantially reduced at fine sizes due, primarily, to overloading of the froth phase which leads to excessive carryover of water and entrained mineral matter. Selective flocculation, on the other hand, can provide good selectivity at low levels of oil addition but the agglomerates tend to be too fragile for separation by the screening methods normally used. The addition of larger amounts of oil, as in spherical agglomeration can yield large, strong agglomerates which are easily separated by screening, but the selectivity is reduced and reagent costs can become excessive.

A hybrid process - Micro-agglomerate flotation - which is a combination of oil-agglomeration and froth flotation was studied in this investigation to determine the critical variables that determine the process response. The basic concept is to use small quantities of oil to promote the formation of dense micro-agglomerates with minimal entrapment of water and mineral particles and to use froth flotation to separate these micro-agglomerates from the water/dispersed-mineral phase. Since the floating units are relatively large agglomerates (30-50 μm in size) rather than fine coal particles (1-10 μm) the problems of froth overload and water/mineral carryover should be significantly alleviated. This method has considerable potential for the practical deep cleaning of coal on a commercial scale. We believe it should be possible to achieve both high selectivity and high yield at reasonable cost. The process requires only conventional, off-the-shelf equipment and reagent usage (oil, surfactants, etc.) should be small. There are, however, complications. The process involves at least five phases: two or more solids (coal and mineral), two liquids (oil and water) and one gas (air). It is demonstrated in this study

that precise control over the chemistry of the liquid phases, and agitation conditions is required to ensure high selectivity and obtain reasonably large recovery. The highly sensitive nature of the process emerges from the fact that both kinetics as well as thermodynamic factors are critical in determining the overall system response.

6.2. Background Discussion

Spherical or oil agglomeration has been used commercially to clean coal for many years. The so-called Trent process was used at several commercial installations in the early decades of this century, and was found to work better than flotation for -300 mesh coal (Ralston, 1922). However, its use had to be discontinued due to high process costs (Mehrotra et al., 1983). A reduction in the oil consumption from about 30% (oil:coal) in the Trent process was achieved in the Convertol process which used only ~3 to 10% oil (Lemke, 1954; Brisse and McMorris, 1958). Further developments in oil agglomeration occurred in the early 1960's at the National Research Council of Canada where the emphasis was on the use of a combination of agitator cells for the production of compact, spherical pellets (Capes and Darcovich, 1984). A similar pelletizing separator which combines the effect of several agitating vessels into a single unit was developed by Shell (Zuiderweg, et al., 1968). Relatively high ash and moisture contents of the pellets together with high oil requirements have prevented this process from becoming a success. Conventional applications of oil agglomeration have generally been based on the separation, by size, of agglomerated coal from dispersed mineral particles. This approach requires large, strong agglomerates which infers high oil usage and consequent loss of selectivity and high reagent costs. An additional problem is that the agglomerates tend to have high moisture content and, because of their integrity, are not amenable to simple, mechanical dewatering. Agglomeration at low levels of oil addition can give excellent selectivity but the agglomerates tend to be small and not strong enough to withstand separation by size.

Froth flotation is commercially practiced to clean approximately - 28 mesh coal using fuel oil as the collector. The quantity of oil usually increases as the rank decreases;

ranging from ~1 lb/ton for high rank coals to about 5-35 lb/ton for sub-bituminous coals (Aplan et al., 1987). Grinding to fine sizes is needed to achieve the desired liberation for deep cleaning of coal, but the efficiency of flotation separation decreases as the particle size becomes small, especially for particles < 10 mm. In the past, different approaches have been used to float fine particles. Yoon and Luttrell (1986), employed fine bubbles to increase the rate of flotation of fine particles. Although the recovery is higher when fine bubbles are used, the grade is often poor because of the large amount of water carryover into the froth phase. This is the reason for the necessity to use wash water in column flotation cells. An alternative approach to increase the rate of flotation is to aggregate the fine particle as was discussed by Fuerstenau, Chander and Abouzeid (1979).

A general requirement for the use of selective agglomeration for the deep cleaning of fine coal is the production of agglomerates which are sufficiently large for effective separation from the dispersed phases (refuse) and have high density - to minimize the inclusion of water and dispersed mineral particles. In recent years, there has been extensive research into the size and structure of agglomerates formed by coagulation/flocculation of fine particles from liquid dispersion. Theoretical analyses and simulations (Vold 1963; Sutherland 1967; Weitz and Huang 1984) and experimental studies (Medalia 1967; Koglin 1977; Klimpel, Dirican and Hogg, 1986) consistently indicate that there is an inverse relationship between agglomerate size and agglomerate density. Studies in our laboratories (Klimpel and Hogg, 1986; 1991) have shown that the relationship is essentially independent of the mechanisms of agglomerate formation, the binding forces in the agglomerates and the conditions of agglomerate growth. As a general rule, the density of an agglomerate is determined primarily by its size relative to that of the particles from which it is formed. In the agglomeration of particles in the 1 to 10 mm size range, however, we have shown (Klimpel and Hogg, 1986; 1991) that agitation of the suspension during agglomerate growth promotes the development of dense micro-agglomerates of size up to about 50 mm. Further agglomeration leads to more open structures which follow the general size-density relationships but are built up from the dense micro-agglomerates rather than from primary particles. To our

knowledge, such studies have not been carried out on oil-agglomerated coal, but the consistency of the results obtained for a very broad variety of systems (carbon black in air, minerals in water with polymer flocculants, etc.,) strongly support the proposition that such relationships should indeed be valid for coal-water-oil systems.

The key problem in previous attempts to use this approach has been the difficulty of producing agglomerates relatively free of ash. The polymeric reagents often used in efforts to selectively flocculate coal (Venkatadri, et al., 1989; Attia and Yu, 1988) tend to produce large, low density flocs which generally entrain large quantities of mineral matter. A substantial increase in ash and sulfur with agglomerate size was observed by Lai, et. al. 1989). The objective of this research was to make use of oil and surfactants to produce dense, micro-agglomerates of high grade. Such aggregates have a higher rate of flotation because of their larger size (30-50 mm) and enhanced hydrophobicity. The latter can be readily attained by proper use of oil with and without reagents. The success of such a flotation scheme depends upon the ability to float the micro-aggregates as independent units so as to prevent entrainment of mineral matter. The increased rate of flotation of such aggregates reduces water carryover with a resultant increase in selectivity. The suggested approach appears to be applicable to flotation in conventional cells or in columns because the aggregate size is never large enough to have an adverse effect.

The use of flotation to separate selectively aggregated fine coal particles from mineral matter using flotation was preferred over other separation methods because the agglomerates produced are in the size range of 30-50 mm. In this size range other methods of separation such as screening or sedimentation are not very effective. It was pointed out in a previous section that the rate of flotation of ultrafine particles can be increased by aggregation of the particles. To prevent entrainment of mineral matter, such agglomerates would have to be floated as individual units rather than flocs of micro-agglomerates. Standard procedures for flotation testing were used to determine the floatability of micro-agglomerates. If necessary, the floated material can be further cleaned in a second stage of flotation. Alternatively, column flotation cells which are known to be more effective in cleaner operations can be used. The type of reagents

needed and their concentrations depend on coal rank and the type of impurities present in the coal. The data on floatability of coals of various rank are already available in our laboratories. Studies have been carried out to determine the affect of micro-agglomerate size and structure on the kinetics of flotation. Our objective was to establish general criteria for increasing the rate of flotation so as to minimize water carry-over at the same time preventing the flotation of clean coal as a slug which inherently leads to high entrapment of mineral matter.

6.3 Agglomerate Flotation Studies

6.3.1 Flotation of P40 Coal Sample

Agglomerate flotation studies were conducted after growing the agglomerates at various speeds and times by the procedure discussed in Chapter 5. In one series of tests, the agglomeration was done at speeds of 1500, 2500, 3500, and 4500 RPM, 10^{-6} M Pluronic L-64 concentration, and at 0.01% dodecane (based on the amount of coal). The droplet size was 11 μm at the time of emulsion addition to the agglomeration vessel. No frother was used for these tests. Froth samples were taken for 0-20 seconds, 20-40 seconds, 40-60 seconds, 1-2 minutes, and 2-4 minutes. The tailings were also collected and analyzed. The percent recovery of combustible material versus the cumulative percent ash for the samples conditioned at 2500 and 3500 RPM are shown Figures 6.1 and 6.2, respectively. One may conclude from these results that the flotation performance improved with increase in agitation speed.

The effect of agglomeration time and speed on A_{80} , the ash corresponding to 80% recovery of combustible matter, is presented in Figure 6.3. With increase in agitator speed the ash content decreased and the effect of agglomeration time was small in this series of tests. The ash content was lower when MIBC frother was used, as can be seen by comparing the results in Figures 6.3 and 6.4

The minimum in ash content after 2.5 minutes of agglomeration time shows rejection of some mineral matter upon agitation. The minimum at 2.5 minutes corresponds to the downward slope of the agglomeration growth curve or the

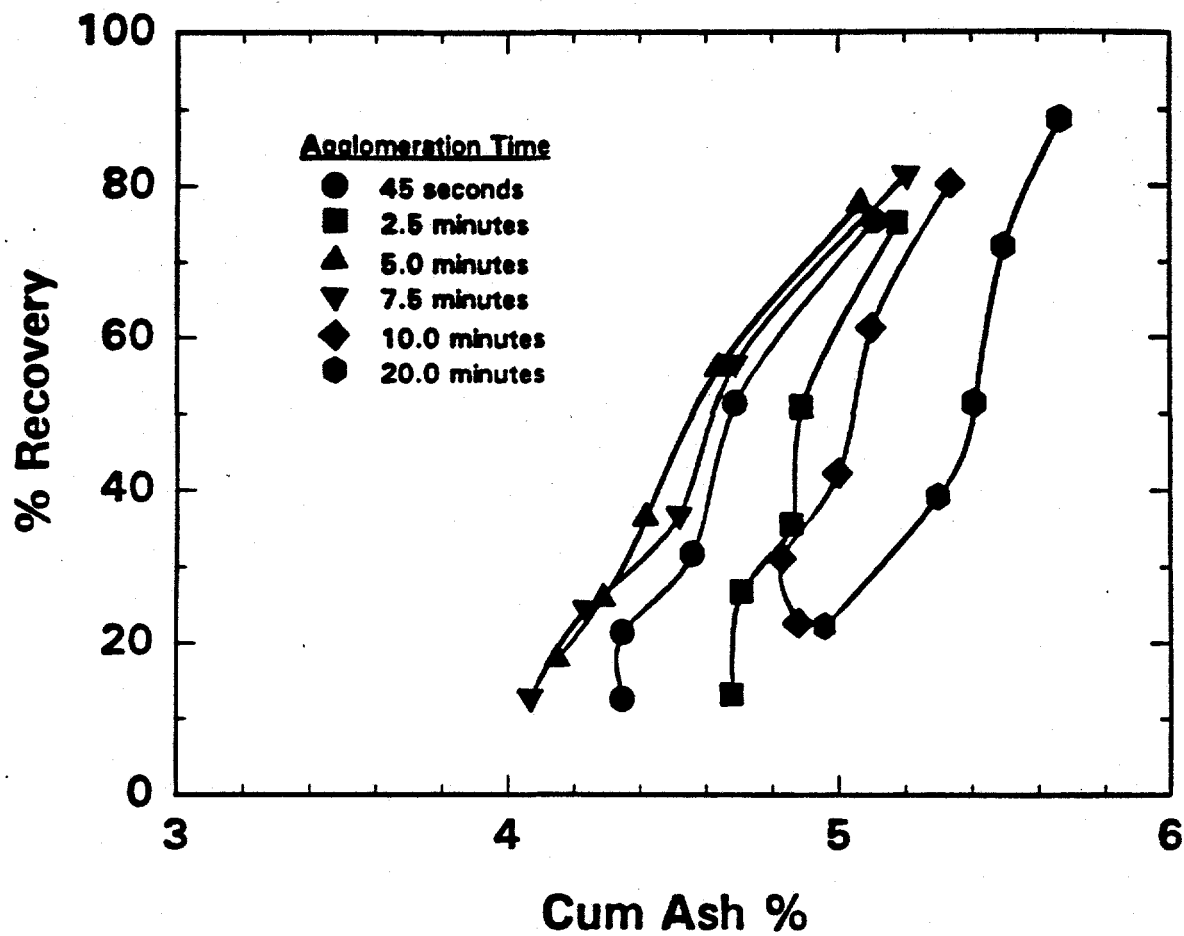


Figure 6.1. Recovery vs. cumulative ash for flotation of P40 coal preagglomerated at various times. Agitator speed during agglomeration was 2500 rpm.

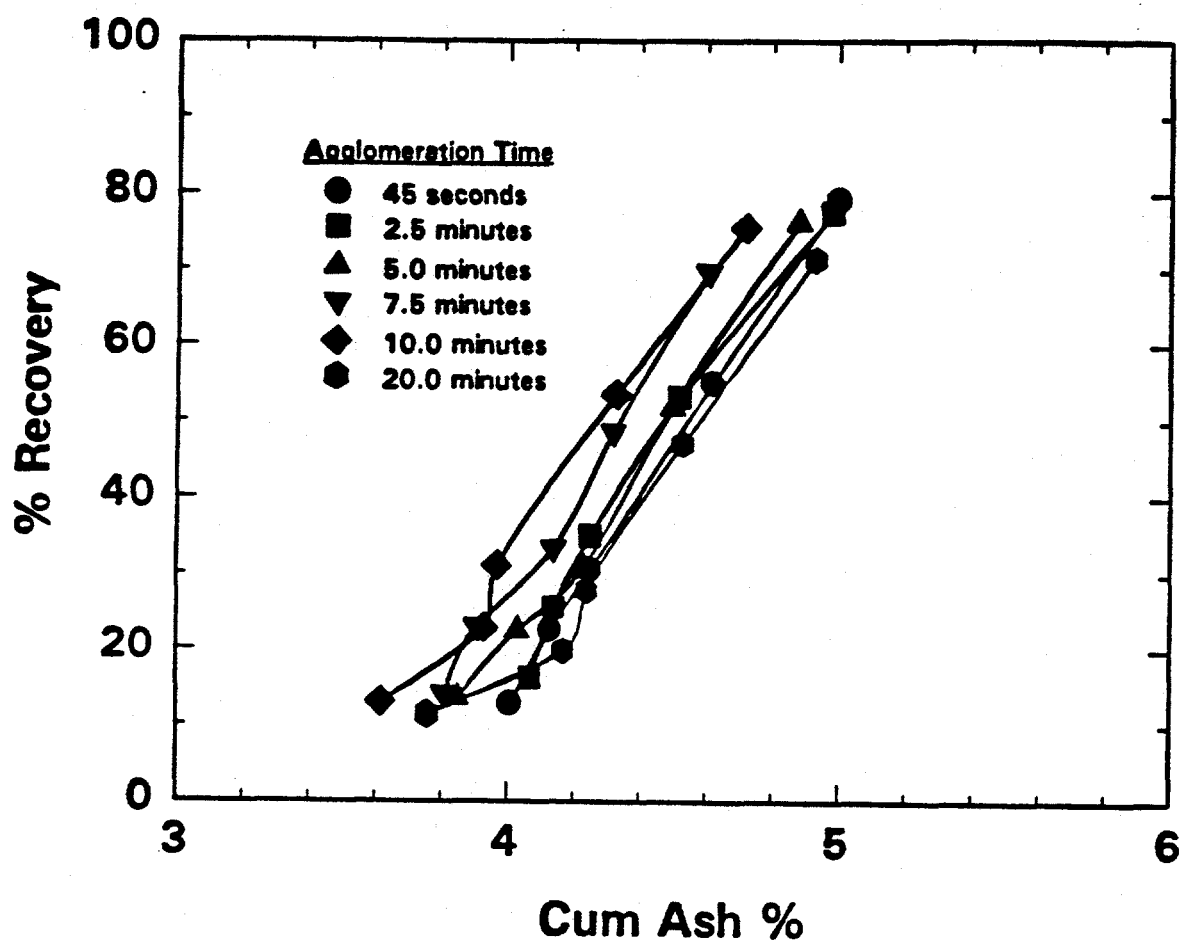


Figure 6.2. Recovery vs. cumulative ash for flotation of P40 coal preagglomerated at various times. Agitator speed during agglomeration was 3500 rpm.

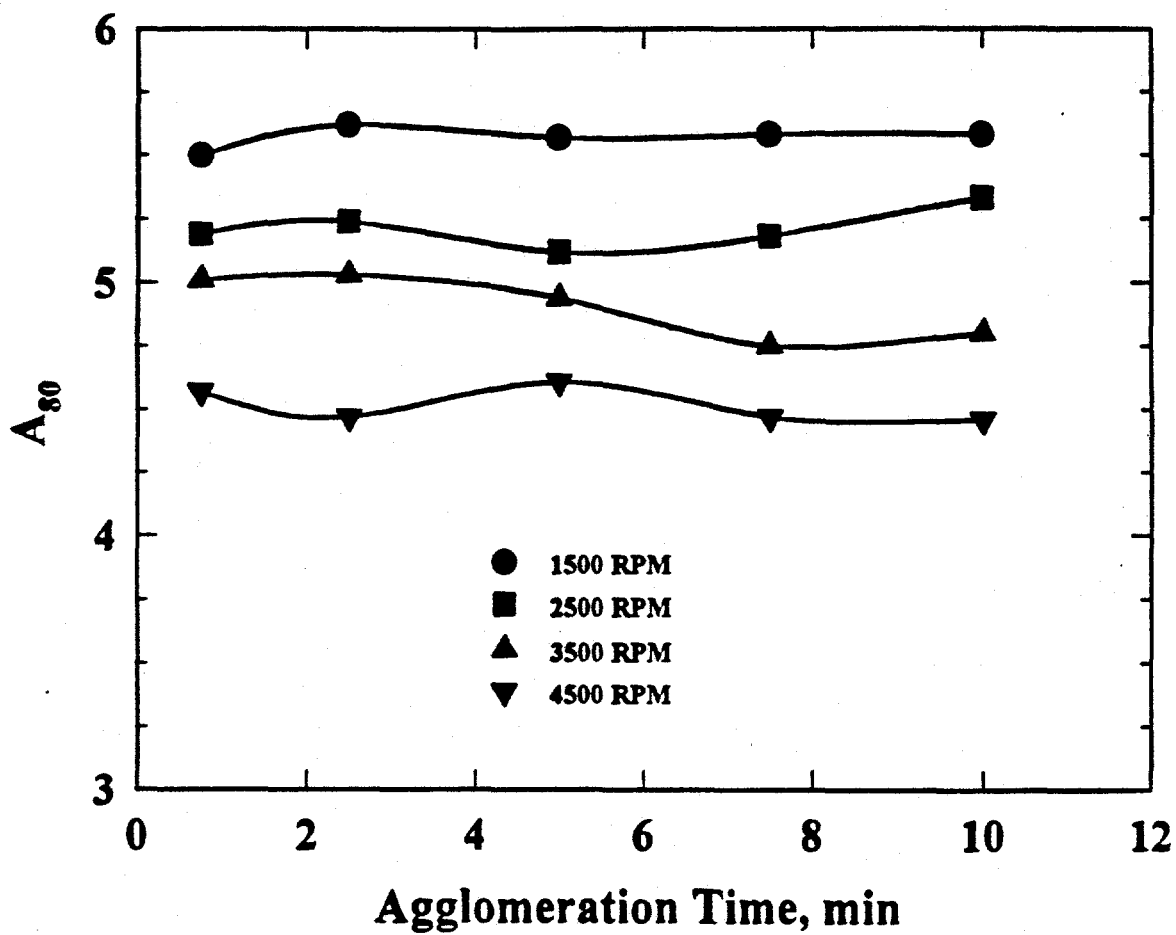


Figure 6.3. Effects of agglomeration time and agitation speed on cumulative ash percent A_{80} recovery by flotation in the absence of frother. (P40 coal)

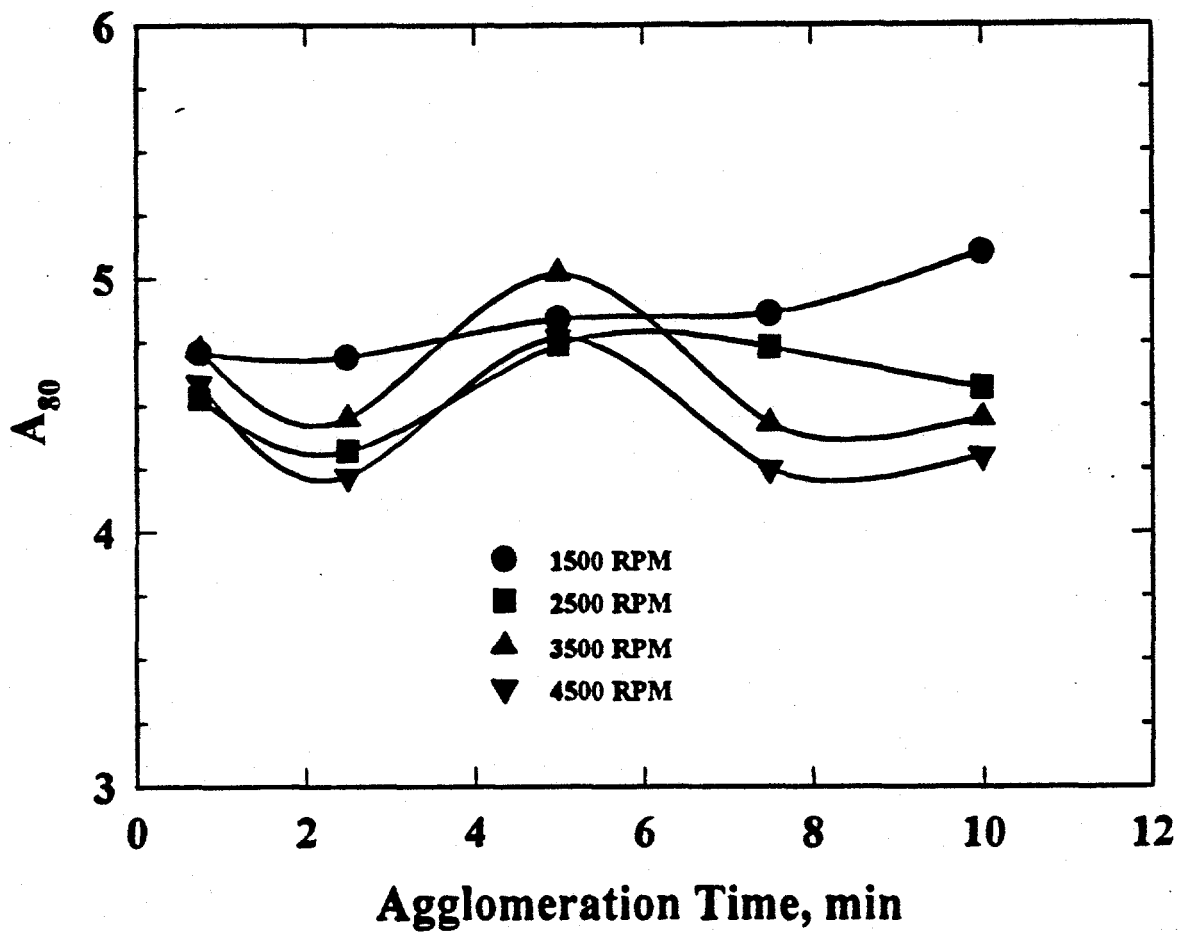


Figure 6.4. Effects of agglomeration time and agitation speed on cumulative ash percent A_{80} at 80% recovery by flotation with 50 μm MIBD as frother. (P40 coal)

deflocculation zone. This is in agreement with findings in the literature (Lapidot and Mellgren, 1968). In their studies, the best grade of ilmenite was obtained during this deflocculation zone. The effect of physical variables (agglomeration time, agitation speed) and chemical variables (frother and surfactant concentration) became quite complex as can be seen by comparing the results in Figures 6.4 and 6.5. It appears that surfactant addition aids in ash rejection for lower agitation speeds in the agglomeration stage. The effect seems to disappear at higher speeds, suggesting that the surfactant may be assisting in oil dispersion. This is consistent with the hypothesis that addition of surfactant with oil promotes its emulsification. The effect of various variables could not be fully explained, however. The flotation performance became very sensitive to various variables in an unpredictable manner. The reasons became evident only after additional tests were performed with an ultra-fine coal with a nominal size of $-20\mu\text{m}$ (referred to as the P20 Coal). The results are discussed in a later section.

The results discussed in previous paragraphs show that surfactant addition was beneficial at low agitation speed but had little effect at higher speeds. The effect was generally attributed to enhancement of the emulsification process at low agitation speeds. To further investigate the effect of agitation speed, additional tests were performed with and without surfactant addition and the results, expressed as ash content at 85% recovery of coal (A_{85}), are presented in Table 6.1. It is clear from the results that the surfactant addition affects selectivity, but in a rather complicated fashion. Some clarification is offered in Figure 6.6 in which a comparison of selectivity is made with and without surfactant addition. If the surfactant had no effect, the points would fall on or at least close to the diagonal line. Points above and to the left of the line indicate detrimental effects of surfactant; points below and to the right show beneficial effects. Obviously both kinds of effects occur depending on agitation speed and agglomeration time. These tests were performed at a fixed amount of the surfactant in the system, which in itself is an additional variable. Somewhat different patterns emerge for different speeds. Surfactant is largely detrimental at 4500 rpm but beneficial at 2500 and 7800 rpm, depending on time. The effect of agglomeration time is significant, though complex, at speeds of 2500 and 4500

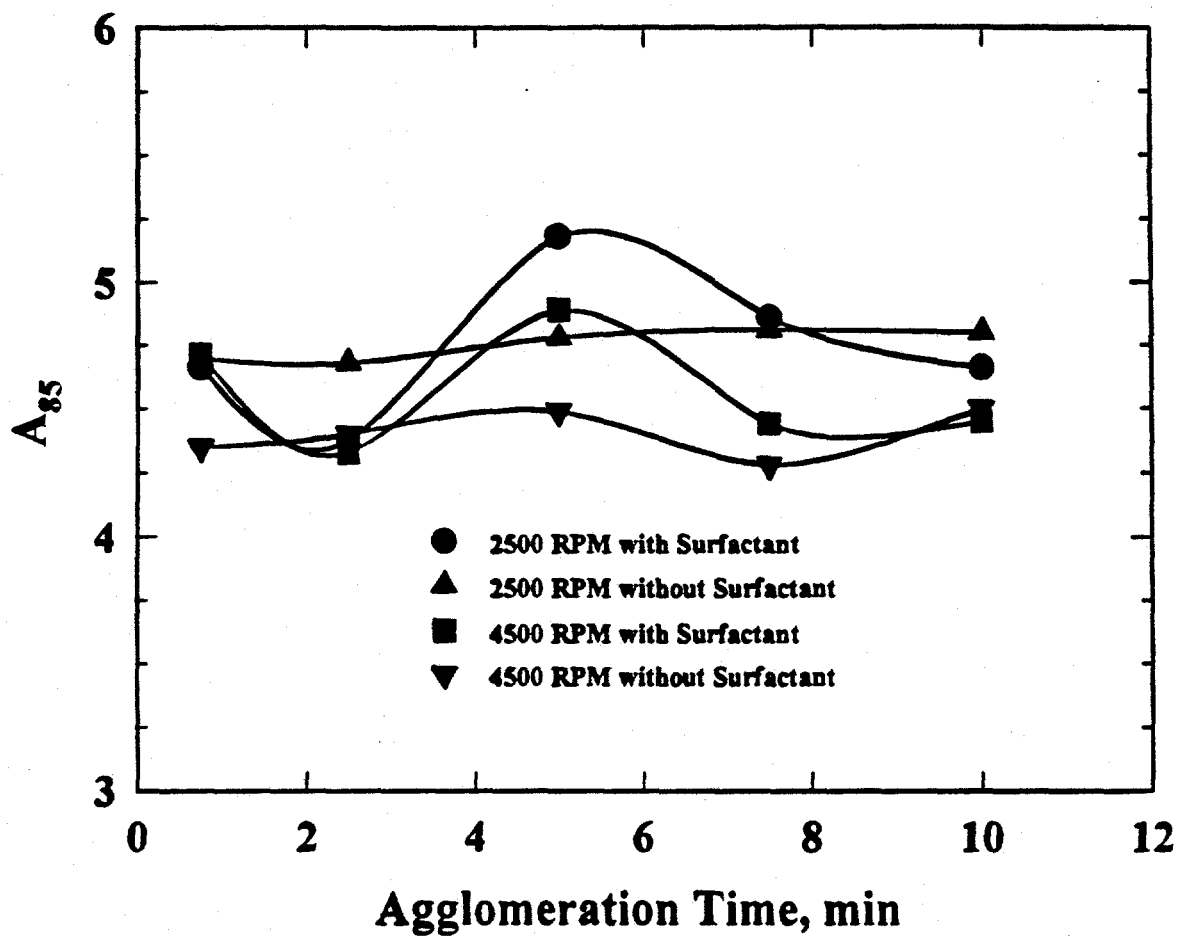


Figure 6.5. Effect of surfactant addition (Pluronic L-64) on ash rejection in coal flotation following preagglomeration for different times and agitation speeds. (P40 coal)

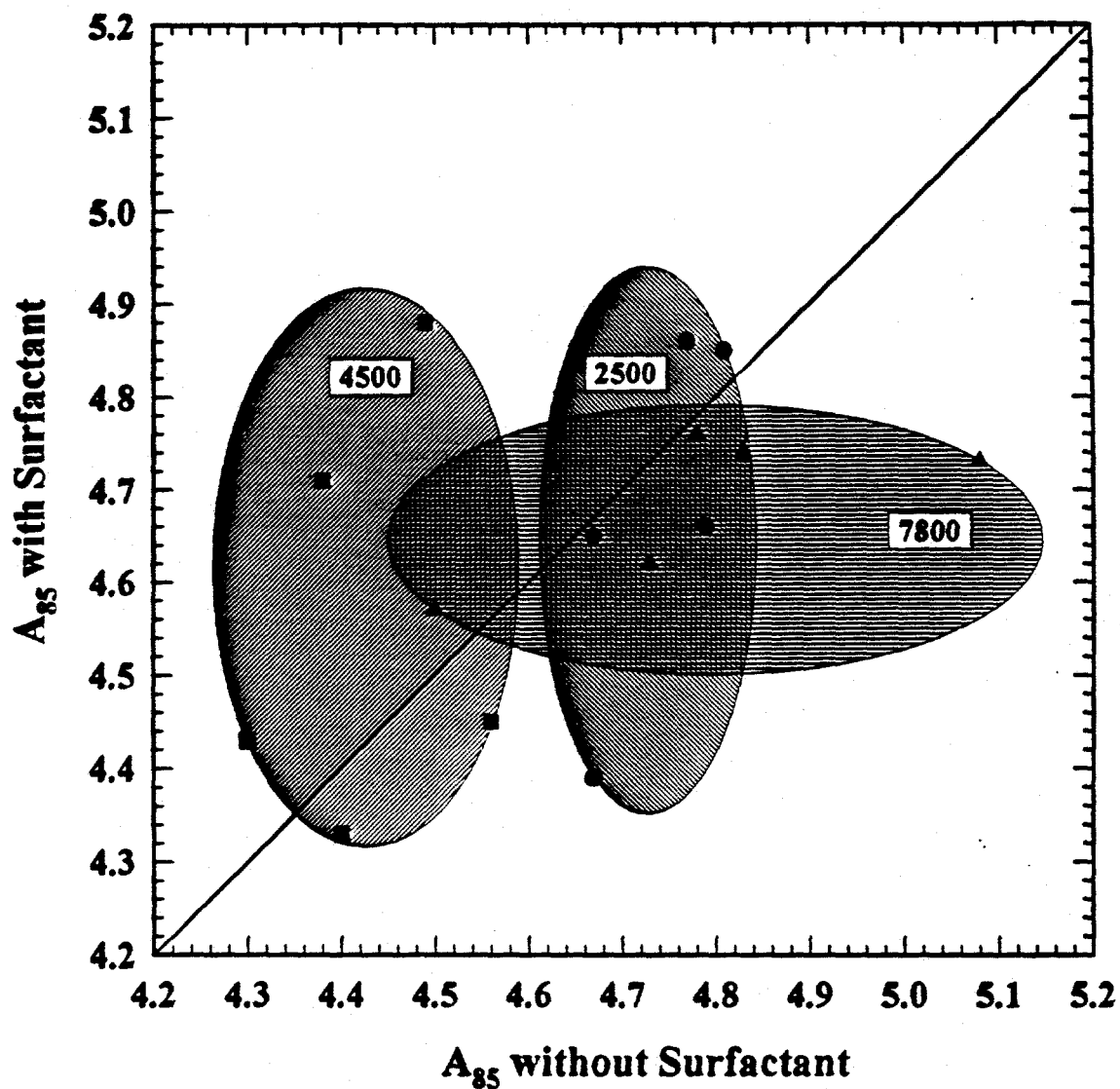


Figure 6.6. Effect of surfactant addition (10^{-6} M Pluronic 64) on the selectivity of flotation after preagglomeration at different speeds.

Table 6.1. Effect of agglomeration conditions on flotation selectivity expressed as product ash content at 85% coal recovery.

Agitator Speed (RPM)	Agglomeration Time	Product Ash at 85% Recovery, A_{85} (%)	
		without Surfactant	with Surfactant
2500	45 sec.	4.67	4.65
	2.5 min.	4.67	4.39
	5.0 min.	4.77	4.86
	7.5 min.	4.81	4.85
	10.0 min.	4.79	4.66
4500	45 sec.	4.38	4.71
	2.5 min.	4.40	4.33
	5.0 min.	4.49	4.88
	7.5 min.	4.30	4.43
	10.0 min.	4.56	4.45
7800	15 sec.	5.08	4.73
	30 sec.	4.78	4.76
	45 sec.	4.83	4.74
	2.5 min.	4.73	4.62
	5.0 min.	4.50	4.57

rpm, but relatively little at 7800 rpm. On the other hand, with no added surfactant, there are only small time effects at 2500 and 4500 rpm but quite significant effects at 7800 rpm.

Based on these results, it is apparent that the role of surfactant in the selectivity of agglomerate flotation encompasses more than just facilitating emulsification. Other factors such as contact angle modification must also come into play.

6.3.2 Flotation of P20 Coal

To further test the hypothesis presented in previous sections a second series of agglomerate flotation tests was performed using ultrafine coal with a nominal particle size of $-20\mu\text{m}$, designated as P20 Coal sample.

The amount of dodecane required to achieve the desired aggregation was higher for this coal. As a result the amount of dodecane was increased to 1% for the P20 sample, which is an order of magnitude greater than that used for the P40 coal sample.

The effect of agglomeration time on the combustible matter recovery versus ash curves is presented in Figure 6.7 for agglomeration at 3600 rpm and in Figure 6.8 for 7200 rpm. These tests were performed in the absence of the surfactant and at somewhat higher speeds because of smaller size of particles and larger quantity of oil used. Although the agglomerate growth curves for these two speeds were similar, as discussed in Chapter 5, significant differences were observed in the flotation performance, especially at the agglomeration time of 3 minutes, which was chosen on the basis of the performance of P40 coal sample. The ash content was more for the larger speed at comparable recoveries. On the basis of these results one may conclude that the droplet size does play an important role in flotation performance. Very fine droplets could be detrimental because they promote formation of large aggregates that entrap water and associated mineral matter. Upon continued agitation, the agglomerate size and structure changes that eventually affects flotation response.

The effect of surfactant is presented in Figures 6.9 and 6.10. The results in Figure 6.9 correspond to the addition of surfactant to the dodecane phase prior to emulsification. This procedure favors the role of the reagent as an emulsifier. When these results are compared with the results in Figure 6.7, it can be seen that production of finer droplets increased pick-up of mineral matter, especially at short times. The recovery versus ash curves were identical at agglomeration times of 10 minutes.

In comparison, when the reagent was added to the coal slurry prior to addition of dodecane, the effect on flotation was quite different as can be seen from the results in Figures 6.7 and 6.10. At the reagent concentration used in this series of tests, the reagent acts as a wetting agent, reducing hydrophobicity or the value of the contact angle. As a result the ash content was high and the recovery was low at the short agglomeration time of 3 minutes. Upon continued agitation, the flotation performance improved, however. The efficiency of separation after 10 minutes of agglomeration was better in the presence of the reagent when compared to that in its absence.

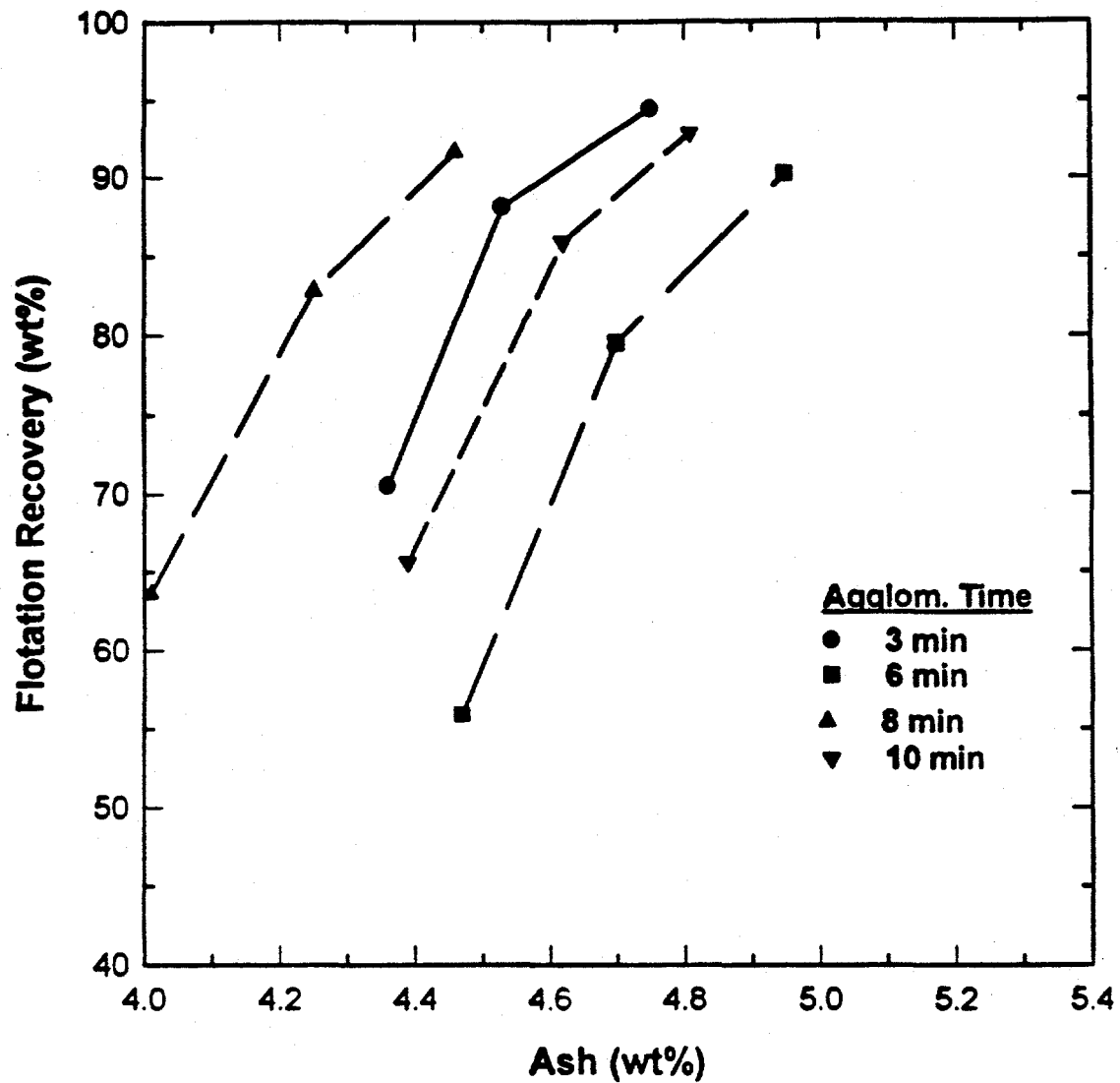


Figure 6.7. Recovery-residual ash content curves for flotation of P20 coal after agglomeration with wt % dodecane at 3600 rpm.

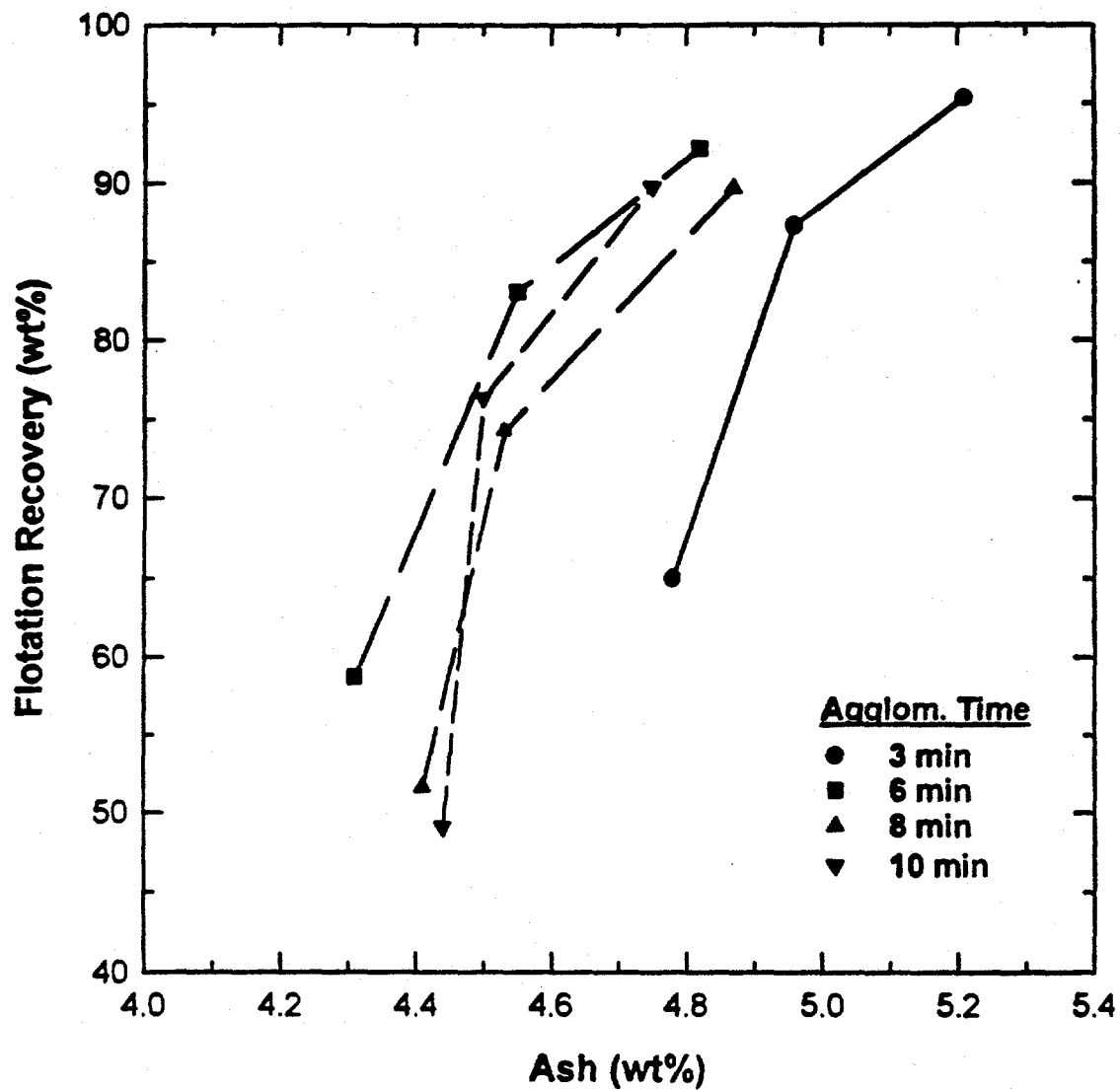


Figure 6.8. Recovery-residual ash content curves for flotation of P20 coal after agglomeration with wt % dodecane at 7200 rpm.

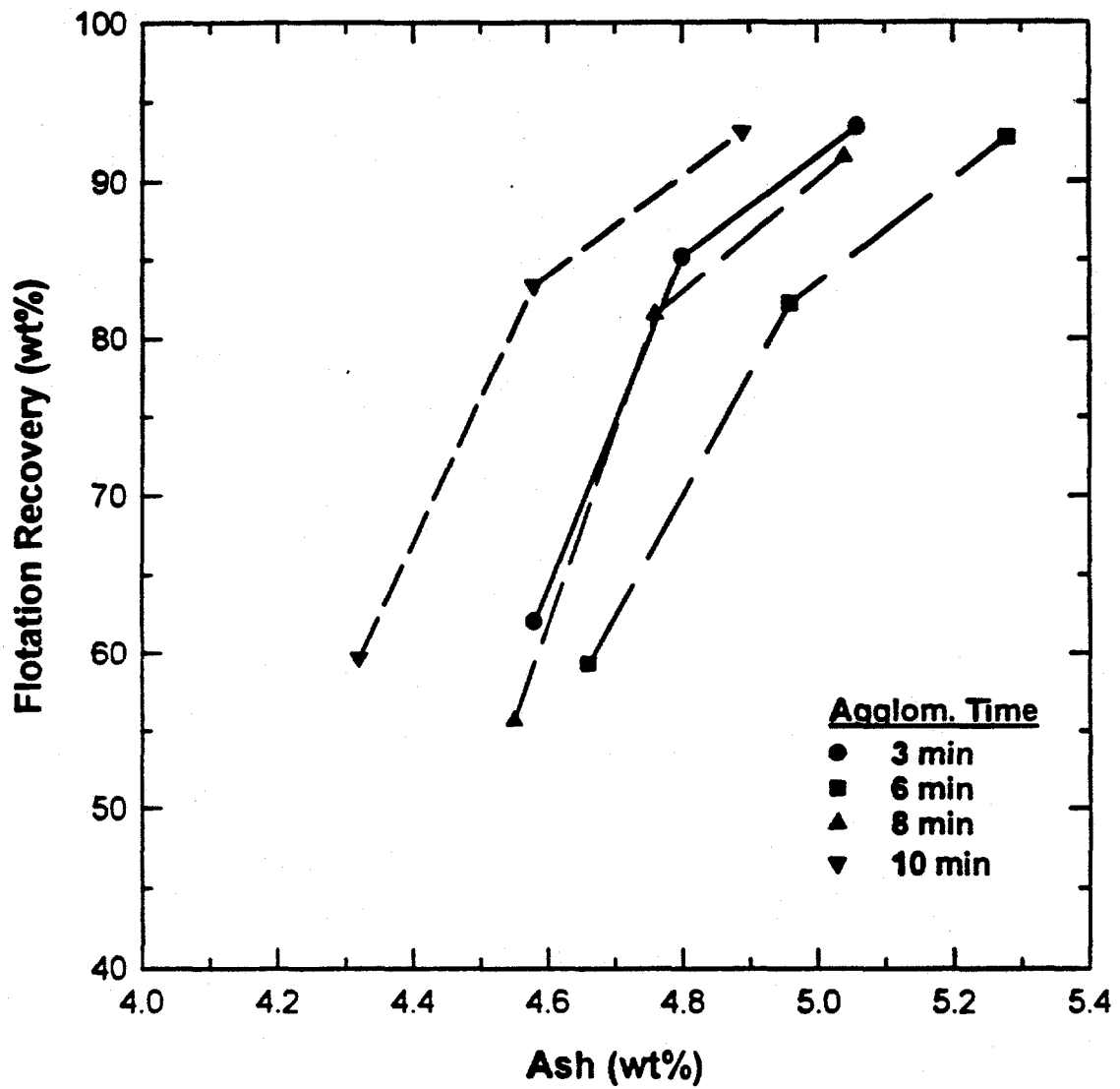


Figure 6.9. Recovery-residual ash content curves for flotation of P20 coal after agglomeration at 3600 rpm with wt % dodecane pre-emulsified in the presence of L-64 surfactant.

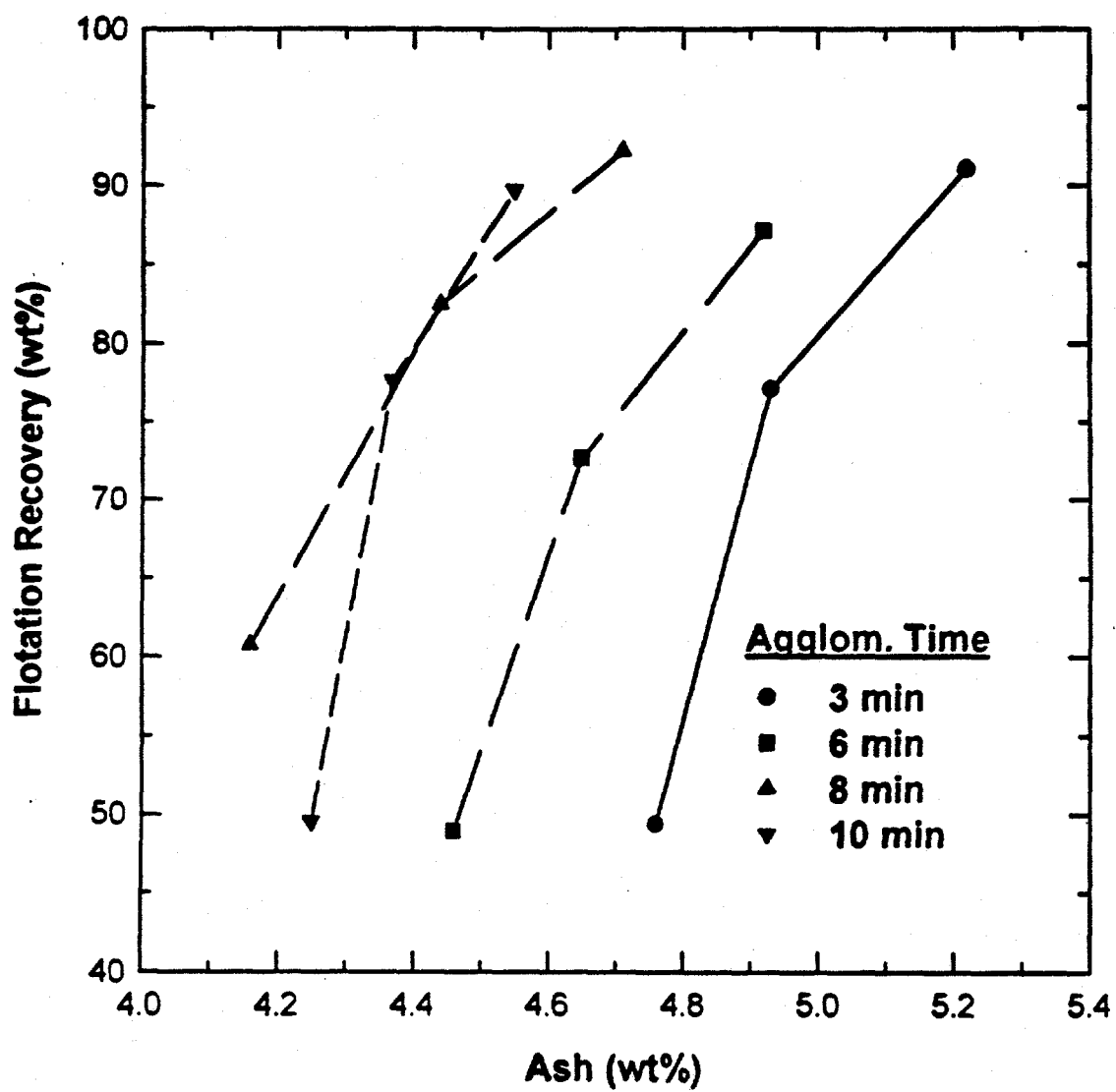


Figure 6.10 Recovery-residual ash content curves for flotation of P20 coal after agglomeration at 3600 rpm with wt % dodecane. L-64 added to the coal slurry, prior to the addition of (mechanically) pre-emulsified oil.

6.4 Conclusions

Formation of micro-agglomerates and their flotation is a very complex process in which both physical and chemical variables play significant roles. The overall process response is a result of many sub-processes involving particle dispersion, droplet formation, agglomerate growth, agglomerate breakage and flotation. Based on the results of studies presented in this and previous chapters, the following conclusions were made:

- Agglomeration is the critical stage of the process which determines the overall performance. The efficiency of separation, that is ability to clean coal depends on preferential agglomeration of coal during the growth period. Although some degree of emulsification is essential to promote selective formation of agglomerates, too much agglomeration, that is formation of very small droplets, could be detrimental.
- Although the issue of phase inversion was not specifically investigated in this study, sufficient evidence exists to suggest the phase inversion from oil/water to water/oil emulsion, which is favored by the presence of hydrophobic coal particles at the interface, promotes rejection of mineral matter and enhances the overall flotation separation.
- If the conditions exist that favor the formation of large and strong agglomerates, the entrapped mineral matter cannot be rejected by continued agitation. Such a condition is analogous to flotation of partially liberated particles and the selectivity is generally poor.

The overall results of this investigation demonstrate the general viability of the micro-agglomerate flotation process for the deep cleaning of fine coal. Because of the numerous variables involved, appropriate operating conditions tend to be system specific. However, some important guidelines have emerged. In particular, it is clear that the agglomerate growth step is critical and must be controlled so as to ensure that separation is carried out in the descending region of the growth curve. Pre-emulsification of the oil also appears to be a necessary condition. Mechanical pre-emulsification may be adequate in many cases, but the use of appropriate surfactant additions can serve to reduce aging affects which could arise in applications. Since surfactants also affect agglomerate

growth and flotation rate through modification of hydrophobicity, process design may require extensive testing to evaluate the appropriate balance among the different affects.

REFERENCES

- Adamson, A.W., 1990, "Physical Chemistry of Surfaces", Fifth edition, John Wiley & Sons, Inc., New York, NY.
- Almgren, M., Bahadur, P., Jansson, M., Brown, P.L.W. and Bahadur, P., 1992, Journal of Colloid and Interfacial Science., Vol. 151, pp. 157.
- Alexandridis, P., Athanassiou, A., Fukuda, S. and Hatton, T.A., 1994, "Surface Activity of Poly (ethylene Oxide)-Block-Poly (propylene Oxide)-Block-Poly (ethylene Oxide) Copolymers," Langmuir, Vol. 10, pp. 2604-2612.
- Alexandridis, P. and Hatton, T.A., 1995, "Poly (ethylene oxide)-Poly (propylene oxide)-Poly (ethylene oxide) Block Co-polymer Surfactants in Aqueous and at Interfaces: Thermodynamics, Structure, Dynamics, and Modeling, Colloids and Surfaces A: Physicochemical Engineering Aspects, Vol. 96, pp. 1-46.
- Anderson, R.A., 1972, Pharm. Acta. Helv., Vol. 47, pp. 304.
- Aplan, F. F., Chander, S. and Arnold, B. J., 1986, "Reagents Used in Coal Preparation," Chemical Reagents in the Mineral Processing Industries, Eds., D. Malhotra and W. F. Riggs, SME, Littleton, CO, pp. 271-279.
- Arai, K., Konno, M., Matunga, Y. and Satio, S., 1977, "Effect of Dispersed Phase Viscosity on the Maximum Stable Drop Size for Break-up in Turbulent Flow," Journal of Chemical Engineering of Japan, Vol. 10, pp. 325-330.
- Attia, Y. A. and Yu, S., 1988, "Feasibility of Separation of Coal Floccs by Column Flotation," Column Flotation, ed. K. V. S. Sastry, SME, Littleton, CO, pp. 249-254.
- Baker, J.A. and Berg, J.C., 1988, "Precipitation-Redissolution Phenomena in Sulfonate-AlCl₃ Solutions," Langmuir, Vol. 5, pp. 1055-1061.
- Baker, J.A., Pearson, R.A and Berg, J.C., 1989, "Influence of Particle Curvature on Polymer Adsorption Layer Thickness," Langmuir, Vol. 5, pp. 339-342.
- BASF-Wyandotte, 1986, "Pluronic Surfactants, BASF Chemical Catalog.
- Becher, P. and McCann, M.J., 1991, "The Process of Emulsification: Computer Model", Langmuir, Vol. 7, pp. 1325-1331.
- Bell, W.E., 1959, "Effect of Micellar Behavior on Adsorption Characteristics of two Surfactants," Journal of Physical Chemistry, Vol. 63, pp. 299-300.

- Bonner, C. M. and Aplan, F. F., 1993, "The Influence of Reagent Dosage on the Floatability of Pyrite During Coal Flotation," Separation Science and Technology, Vol. 28, pp. 747-764.
- Brisse, A. M. and McNorris, Jr., W. L., 1958, "Convertol Process," Min. Eng., Feb: 258-261.
- Camp, T.R. and Stein, P.C., 1943, "Velocity Gradients and Internal Work in Fluid Motion," J. Boston Soc. Civ. Engrs., Vol. 30, p. 219.
- Capes, C. E. and Darcovich, K., 1984, "A Survey of Oil Agglomeration in Wet Fine Coal Processing," Powder Technology Vol. 40, pp. 43-52.
- Chander, S., Mohal, B.R. and Aplan, F.F., 1987, "Wetting Behavior of Coal in the Presence of Some Non-ionic Surfactants", Colloids and Surfaces, Vol. 26, pp. 205-216.
- Chander, S., and Polat, M., 1995, "Coal Flotation Kinetics: Interaction Between Physical and Chemical Variables," Mineral Processing - Recent Advances and Future Trends, Eds., S.P. Mehrotra and R. Shekhar, Allied Publishers, New Delhi, pp. 616-631.
- Coulaloglou, C.A. and Tavlarides, L.L., 1976, "Drop Size Distributions and Coalescence Frequencies of Liquid-Liquid Dispersions in Flow Vessels. AIChE. J., Vol. 22, pp. 289-297.
- Coulaloglou, C. A. and Tavlarides, L.L., 1977, "Description of Interaction Processes in Agitated Liquid-Liquid Dispersions," Chemical Engineering Science, Vol. 32, pp. 1289-1297.
- Dwiggins, C.W., Bolen, R. J. Jr. and Dunning, H.N., 1960, "Ultracentrifugal Determination of the Micellar Character of Non-ionic Detergent Solutions," Journal of Physical Chemistry, Vol. 64, pp. 1175-1178.
- Faers, M.A. and Luckham, P.F, 1994, "Rheology of Polyethylene Oxide-Polypropylene Oxide Block Copolymers Stabilized Lattices and Emulsions"; Colloids and Surfaces, A: Physicochemical and Engineering Aspects, Vol. 86, pp. 317-327
- Fuerstenau, D. W., Chander S., and Abouzeid, A. M., 1979, "The Recovery of Fine Particles by Physical Separation Methods," in Beneficiation of Mineral Fines, eds. P. Somasundaran and N. Arbiter, National Science Foundation, p. 59.
- Gao, Z. and Eisenberg, A., 1993, "A model of Micellization for Block Co-polymers in Solutions," Macromolecules, Vol. 26, pp. 7353-7360.

- Glasgow, L.A. and Hsu, J.P., 1985, "Characterization of Turbulence-Induced Aggregate Breakage," in Flocculation Sedimentation & Consolidation, Eds. Brij M. Moudgil, P. Somasundaran, Engineering Foundation, New York, pp. 191-203.
- Gutierrez-Rodriguez, J.A., Purcell Jr. and Aplan, F.F., 1984, "Estimating the Hydrophobicity and Floatability of Coal," Colloids and Surfaces, Vol. 12, pp. 1-25.
- Hamaker, H.C., 1937, "The London-van der Waals Attraction Between Spherical Particles," Physica, Vol. 4, p. 1058.
- Hecht, E. and Hoffmann, H., 1994, "Interaction of ABA Block Copolymers with Ionic Surfactants in Aqueous Solutions"; Langmuir, Vol. 10, pp. 86-91.
- Heydegger, H.R. and Dunning, H.N., 1959, "A Radiotracer Study of Adsorption of an Ethylene Oxide-Propylene Oxide Condensate on Quartz Powders," Journal of Physical Chemistry, Vol. 63, pp. 1613-1616.
- Hiemenz, P.C., 1986, "Principles of Colloid and Surface Chemistry", 2nd edition. Marcel Dekker, Inc. New York, NY.
- Hinze, J.O., 1955, "Fundamentals of the Hydrodynamic Mechanism of Splitting up in Dispersion Process", AIChE, Vol. 1, pp. 289-295.
- Hogg, R., 1981, "Modeling of Porous Agglomerate Formation and Growth," Proceedings, 3rd International Symposium on Agglomeration, Nurnburg West Germany.
- Hogg, R., 1989, "Role of Colloid and Interface in Agglomeration," Proceedings, 5th International Symposium on Agglomeration, The Institution of Chemical Engineers, Rugby, Warwickshire, England, pp. 483-4931
- Hogg, R., 1992, "Agglomeration Models for Process Design and Control," Powder Technology, Vol. 69, pp. 69-76.
- Hogg, R., 1994, "Hydrodynamic Effects in Flocculation and Dispersion of Fine-Particle Suspensions," in Dispersion and Aggregation: Fundamentals and Applications, eds., B.M. Mondgil and P. Somasundaran, Engineering Foundation, NY, pp. 21-31.
- Hogg, R., Maffei, A.C., and Ray, D.T., 1990, "Modeling of Flocculation Processes for Dewatering System Control," in Control 90, Eds. R.K. Rajamani and J.A. Herbst, SME, Littleton, CO., pp. 29-34.
- Holland, F.A. and Chapman, F.S. 1966, "Liquid Mixing and Processing in Stirred Tanks, Reinhold Publishing, New York, NY.
- Hsu, T-C., 1987, "Liquid-Liquid Separation of Ultrafine Coal," M.S. Thesis, The Pennsylvania State University.

- Hsu, T-C., and Chander, S., 1988, "Interfacial and Colloidal Effects in Liquid-Liquid Separation of Ultrafine Coal", Interfacial Phenomena In Biotechnology and Materials Processing, Ed. by Y. A. Attia, B. M. Moudgil and S. Chander, Elsevier Science Publishers B. V., Amsterdam, pp. 399-411.
- Kayes, J.B. and Rawlings, D.A., 1979, "Adsorption Characteristics of Certain Polyethylene-Polypropylene Block Co-polymers on Polystyrene Latex," Colloid and Polymer Science, Vol. 257, pp. 612-629.
- Kilmann, E., Maier, H. and Baker, J.A., 1988, "Hydrodynamic Layer Thickness of Various Adsorbed Polymers on Precipitated Silica and Polystyrene Latex," Colloids and Surfaces, Vol. 31, pp. 51-66.
- Klimpel, R. C., Dirican, C. and Hogg, R., 1986, "Measurement of Agglomerate Density in Flocculated Fine-Particle Suspensions," Particulate Science and Technology, Vol. 4, pp. 45-59.
- Klimpel, R. C. and Hogg, R., 1986, "Effects of Flocculation Conditions on Agglomerate Structure," J. Colloid Interface Sci., Vol. 113, pp. 121-131.
- Klimpel, R.C. and Hogg, R., 1991, "Evaluation of Floc Structures," Colloid and Surfaces, Vol. 55, pp. 279-288.
- Koglin, B., 1977, "Assessment of the Degree of Agglomeration in Suspension," Powder Technol., Vol. 17, pp. 219-227.
- Kolmogorov, A.N., 1949, Doklady Akad. Nauk SSSR, Vol. 66, pp. 825 .
- Konno, M., Arai, K. and Saito, S., 1982, "The Effect of Stabilizer on Coalescence of Dispersed Drops in Suspension Polymerization of Styrene," Journal of Chemical Engineering of Japan, Vol. 15, pp. 131-135.
- Koshy, A., Das, T.R. and Kumar, R., 1988, "Effect of Surfactants on Drop Breakage in Turbulent Liquid Dispersions", Chemical Engineering Science, Vol. 43, No. 3. pp. 649-654.
- Lachaise, L., Mendiboure, C, Dicharry, C., Marion, G., Bourrel, M., Cheneviere, P. and Salager, J.L., 1995, "A Simulation of Emulsification by Turbulent Stirring," Colloids and Surfaces A: Physicochemical and Engineering Aspects, Vol. 94, pp. 189-195.
- Lagisetty, J.S., Das, P. K., Kumar, R. and Gandhi, K. S., 1986, "Breakage of Viscous and Non-Newtonian Drops in Stirred Dispersions," Chemical Engineering Science, Vol. 41, pp. 65-72.

Lai, R.W., Gray, M.L., Richardson, A.G. and Chiang, S.H., 1989, "Size Reduction and Selective Agglomeration of Coal: Technical Feasibility of Cleaning Pittsburgh Seam Coal With Isooctane," Advances in Coal and Mineral Processing Using Flotation, Eds. S. Chander and R.R. Klimpel, SME, Littleton, CO, pp. 120-129.

Lai, R.W.M. and Fuerstenau, D.W., 1968, "Liquid-Liquid Extraction of Ultrafine Particles", Transactions of AIME, Society of Mining Engineers., Vol. 241, pp. 549-556.

Lapidot, M. and Mellgren, O., 1968, "Conditioning and Flotation of Ilmenite Ore," Trans. IMM, Sec. C, 77, pp. 149-165.

Lemke, K., 1954, "The Cleaning and Dewatering of Slurries by the Convertol Process," Proc. Second International Coal Preparation Congress, Essen, Paper AIV2.

Maffei, A.C., 1989, "Scale-up of Flocculation Processes," M.S. Thesis, The Pennsylvania State University.

Malmsten, M., Linse, P. and Cosgrove, T., 1992, "Adsorption of PEO-PPO-PEO Block Co-polymers at Silica," Macromolecules, Vol. 25, pp. 2474-2481.

Mankowich, A.M., 1954, Journal of Physical Chemistry, 58:1028.

Medalia, A. I., 1967, "Morphology of Aggregates," J. Colloid Interface Sci., Vol. 24, p. 393.

Mehrotra, V.P., Sastry, K.V.S. and Morey, B.W., 1983, "Review of Oil Agglomeration Techniques for Processing of Fine Coals," International Journal of Mineral Processing, Vol. 11, pp. 175-201.

Mellgren, O. and Shergold, H.L., 1966, "Method for Recovering Ultrafine Mineral Particles by Extraction with Organic Phase," Trans. Instn. Min. Metall., London, Vol. 75, pp. C267-C268

Miano, F., Bailey, A., Luckham, P.F. and Tadros, Th.F., 1992, "Adsorption of Poly (Ethylene Oxide)-Poly (Propylene Oxide) ABA Block Co-polymers on Carbon Black and the Rheology of the Resulting Dispersions," Colloids and Surfaces, Vol. 68, pp. 9-16.

Mlynek, Y. and Resnick, W., 1972, "Drop Sizes in an Agitated Liquid-Liquid System," AICHE Journal, Vol 18, pp. 122-127.

Mohal, B.R., 1988, "Enhancement of the Wettability of Coal Powders Using Surfactants," Ph.D. Thesis, The Pennsylvania State University.

Myers, D., 1988, "Surfactant Science and Technology", Second Edition, VCH Publishers, New York, NY.

Narsimhan, G., Ramkrishna, D. and Gupta, J.P., 1980, "Analysis of Drop Size Distributions in Lean Liquid-Liquid Dispersions," AICHE Journal, Vol. 26, No. 6, pp. 991-1000.

Nevolin, F.V., Tipisova, T.G., Polyakova, V.A. and Semenova, A.M., 1963, Maslob-Zhir. Prm., Vol. 29, pp. 23.

Nikolov, A.D. and Wasan, D.T., 1989, "Ordered Micelle Structuring in Thin Films Formed from Anionic Surfactant Solutions", Journal of Colloid and Interface Science, Vol. 133, pp. 1-12.

Nishikawa, M., Mori, F., Kayama, T. and S. Nishioka, 1990, "Drop Size Distribution in a Liquid-Liquid Phase Mixing Vessel, Journal of Chemical Engineering of Japan, Vol. 24, No. 1, pp. 88-94.

Olson, T.J. and Aplan, F.F., 1987, "The Effect of Frothing and Collecting Agents on the Flotation of Coal Pyrite and Locked Particles in a Coal Flotation System", Processing and Utilization of High Sulfur Coals, II, Editors, Y.P. Chugh and R.D. Caudle, Elsevier, Amsterdam, pp. 71-82.

Overbeek, J.Th.G., 1952, "Kinetics of Flocculation," in Colloid Science I, H.R. Kruyt, Ed., Elsevier, Amsterdam.

Pandya, K., Bahadur, P., Nagar, T.N. and Bahadur, A., 1993, "Micellar and Solubilizing Behavior of Pluronic L-64 in Water"; Coll. And Surfaces, A: Physicochemical and Engineering Aspects, Vol. 70, pp. 219-227.

Parker, D.S., Kaufman, W.J. and Jenkins, D., 1972, "Floc Breakup in Turbulent Flocculation Processes," J. Sanitary Engineering Div. ASCE, pp. 79-99.

Polat, M. and Chander, S., 1994, "Kinetics of Emulsification in the Presence of Fine Particles", Dispersion and Aggregation: Fundamentals and Applications, Ed. B.M. Moudgil and P. Somasundaran, Engineering Foundation, New York, NY. pp. 515-536.

Prasad, K.N., Luong, T.T., Florence, A.T., Paris, J., Vaution, C., Seiller, M. and Puisieux, F., 1979, Colloid and Interface Science, Vol. 69, pp. 225.

Raghavan, S. and Fuerstenau, D. W., 1975, "On the Wettability and Flotation Concentration of Submicron Hematite Particles with Octylhydroxamate as Collector," American Institute Chemical Engineers Symposium Series, Vol. 71, No. 150, p.59.

Ralston, O. C., 1922, "Comparison of Froth with the Trent Process," Coal Age, Vol. 22, pp. 911-914.

Reddy, N.K., Fordham, P.J., Attwood, D. and Booth, C., 1990, Journal of Chemical Society, Faraday Trans., Vol. 86, pp. 1569.

Rosen, M.J., 1988, "Surfactants and Interfacial Phenomena", Second edition, John Wiley & Sons, Inc., New York, NY.

Ross, S. and Olivier, J.P., 1959, "A New Method for Determination of Critical Micelle Concentrations of Un-ionized Association Colloids in Aqueous Solutions," Journal of Physical Chemistry, Vol. 63, pp. 671-1674.

Rumpf, H., 1961, "The Strength of Granules and Agglomerates," in Agglomeration, W.A. Knepper, Ed., Interscience, NY.

Rushton, J.H., Cotich, E.W., and Everett, H.J., 1950, "Power Characteristics of Mixing Impellers," Chem. Eng. Prog., Vol. 46, p. 467.

Saski, W. and Shah, S.G., 1965, "Availability of Drugs in the Presence of Surface Active Agents I: Critical Micelle Concentrations of Some Oxyethylene Oxypropylene Polymers"; J. Pharmac. Sci., Vol. 54, No. 1, pp. 71-75.

Schmolka, I.R. and Raymond, A.J., 1965, "Micelle Formation of Polyoxyethylene-Polyoxypropylene Surfactants"; J. Am. Oil Chem. Soc., Vol. 42, pp. 1088-1091.

Schick, M., 1967, "Nonionic Surfactants", Marcel & Dekker, Inc., New York, NY.

Schmolka, I.R., 1967, In M.J. Schick (Editor), Nonionic Surfactants, Marcel Dekker, Inc., NY pp. 300-371.

Shinnar, R., 1961, "On the Behavior of Liquid Dispersions in Mixing Vessels," Fluid Mechanics, Vol. 10, pp. 259-275.

Sprow, F. B., 1967, "Distribution of Drop Sizes Produced in Turbulent Liquid-Liquid dispersion. Chemical Engineering Science, Vol. 22, pp. 435-442

Sutherland, D.N., 1967, "A Theoretical Model of Floc Structure," J. Colloid and Interface Science, Vol. 25, pp. 373-380.

Tadros, Th.F., and Vincent, B., 1980, "Influence of Temperature and Electrolytes on the Adsorption of Poly (Ethylene oxide)- Poly (propylene Oxide) Block Co-polymer on Polystyrene Latex and on the Stability of the Polymer Coated Particles," Journal of Physical Chemistry, Vol. 84, pp. 1575-1580.

Tattersson, G.B., 1991, "Fluid Mixing and Gas Dispersion in Agitated Tanks," McGraw-Hill, Inc, New York, NY.

Thomas, D.G., 1964, "Turbulent Disruption of Floccs in Small Particle Size Suspensions," AICHE Journal, Vol. 10, pp.517-523.

Tiberg, F., Malmsten, M., Linse, P. and Lindman, B., 1991, "Kinetic and Equilibrium Aspects of Block Co-polymer Adsorption," Langmuir, Vol. 7, pp. 2723-2730.

Tjaberinga, W.J., Boon, A. and Chesters, A.K., 1993, "Model Experiments and Numerical Simulations on Emulsification under Turbulent Conditions," Chemical Engineering Science, Vol. 48, No. 2, pp. 285-293.

Tomi, D.T. and Bagster, D.F., 1978, "The Behavior of Aggregates in Stirred Vessels, Part I - Theoretical Considerations of the Effects of Agitation, Part II - An Experimental Study of the Flocculation of Galena in a Stirred Tank," Trans. IChemE, Vol. 56, pp. 1-19.

Venkatadri, R., Markuszewski, R. and Wheelock, T.D., 1989, "Flocculation of Coal and Mineral Particles With a Polyanionic Biopolymer," Coal Preparation, Vol. 6, pp. 207-225.

Vold, M.J., 1963, "Computer Simulation of Floc Formation in a Colloidal Suspension," J. Colloid and Interface Science, Vol. 18, pp. 684-695.

Walstra, P., 1983, "In Encyclopedia of Emulsion Technology: Becher, P., Ed.; Vol. 1, Marcel Dekker, Inc.: New York and Basel, Vol. 1, Chapter 2.

Wanka, G., Hoffman, H. and Ulbricht, W., 1990, "The Aggregation Behavior of Poly-(Oxyethylene)-Poly (Oxypropylene)-Poly (Oxyethylene)-Block Co-polymers in Aqueous Solution, Colloid and Polymer Science, Vol. 268, pp. 101-117.

Weitz, D.A. and Huang, J.S. 1984, "Self-similar Structures and the Kinetics of Aggregation of Gold Colloids," in Kinetics of Aggregation and Gelation, F. Family and D.P. Landau, Eds., North Holland, Amsterdam.

Yarab, R.R., Abdul-Baset, Z., Given, P.H., 1979, "Hydroxyl Content of Coal: New Data and Statistical Analysis", Geochimica et Cosmochimica Acta, 43:281-287.

Yoon, R. H. and Luttrell, G. H., 1986, "The Effect of Bubble Size on Fine Coal Flotation," Coal Preparation, Vol. 2, pp. 179-192.

Zambrana, G. Z., Medina, R.T., Gutierrez, G.B., and Vargas, R.R., 1974, "Recovery of Minus Ten Micron Cassiterite by Liquid-Liquid Extraction," International J. Mineral Processing, No. 1, pp. 335-345.

Zhou, Z. and Chu, B., 1988, "Light-Scattering Study on the Association Behavior of triblock Polymers of Ethylene Oxide and Propylene Oxide in Aqueous Solution"; Journal of Colloid and Interface Science, Vol. 126, No. 1, pp. 171-180.

Zuiderweg, F.J., and van Lookeren Campagen, M., 1979, "Pelletizing of Soot in Waste Water of Oil Gasification Plants - The Shell Pelletizing Separator," The Chemical Engineer (London), Vol. 220, pp CE223-CE227.